

Aprotic Lithium Based Oxygen Battery Built in
Hybrid Electrolytes Design

September 2020

DENG HAN

Aprotic Lithium Based Oxygen Battery Built in
Hybrid Electrolytes Design

Graduate School of Systems and Information Engineering
University of Tsukuba

September 2020

DENG HAN

ABSTRACT

With the consumption of the irreversible fossil fuels and the growing concern for environmental issues, human society has been more and more aware of the importance of using sustainable energy. As a result, the energy storage system gains increasing attention as it's a necessity for the green energy like solar energy and wind energy. The successful commercialization of lithium ion batteries (LIBs) boost the market of small electrical devices, but face with challenges when it comes to application for the large electrical devices, like electric vehicles (EVs). There is urgent need for reversible battery systems with higher energy density.

Among the candidates for the next generation batteries, the lithium oxygen (Li-O₂) battery stands out for it can potentially store and deliver extremely high specific capacity at a low cost. Li-O₂ battery works with the oxygen from the air as the cathode active material and lithium metal as the anode active material. However, there are many problems in this new battery system. In the cathode, the accumulation of discharge product Li₂O₂ would block the cathode, leading to an early discharge ending. The direct contact of Li₂O₂ with the porous carbon, which is a common material for oxygen cathode, would cause parasitic reaction. The electrolyte for Li-O₂ battery is vulnerable to the super oxide species, an intermediated species during oxygen reduction reaction, which make it suffer from irreversible decomposition as well. For the anode side, the successful application of lithium metal anode has been long challenged by the low Coulombic Efficiency and dendrite growth problems.

The issues concerning these challenges are always not independent, and an overall consideration is needed to improve the battery performance. At present, the RM strategy seems an effective choice for lowering the overpotential and stabilizing the cathode and electrolyte during cycling. But the direct application of them would lead to so-called crossover effect and affect the anode. On the other hand, alternatives for lithium metal in Li-O₂ battery would face with a major challenge that they cannot suit well to the Li-O₂ battery electrolyte.

In this dissertation, we propose a hybrid electrolyte battery design for the lithium based oxygen battery. By separating the cathode and anode into two systems, the potential of each side could be fully realized. The electrolyte optimization strategies and separator fabrication are also discussed. Our work is mainly focusing on improving the performance of lithium based oxygen battery in several aspects, including cycling stability, rate performance with safety and its practical potential.

Firstly, we aim at the cycling stability problem of the Li-ion oxygen battery based on Si anodes. We fabricate a Li⁺ form Nafion membrane to work as a separator in the battery to divide the cathode and anode systems separately and build a hybrid electrolyte battery so that both electrodes can work in their suitable electrolytes. As a result, the cycling stability is largely increased compared with a normal type Li-O₂ battery. The SEI of Si anodes in different electrolytes are also investigated to clarify their relation to the cycling performance.

Secondly, we focus on the rate performance and safety for the lithium based oxygen battery by introducing an organic liquid anode. A metal organic frameworks (MOFs) based membrane is applied to bridge the organic liquid anode and oxygen cathode by conducting Li ions while simultaneously separating the liquid anode at the anode side and RMs at the cathode side. Consequently, superior rate performance and cycling durability are achieved in this design. And we firstly study SEI-like layer of the organic liquid anode.

Thirdly, we also make a practical test for the hybrid electrolyte design for the pouch-type Li-O₂ battery. We aim at the oxygen transport problem when scaling up the cell to the pouch-type cell, and address it by introducing a per-fluorinated chemical in to the cathode electrolyte to improve the oxygen solubility. Consequently, the output energy density of the hybrid electrolyte cell is obviously improved compared with a normal one, proving the large practical potential of Li-O₂ battery with this structure.

We hope our results would contribute to the development of the Li-O₂ battery with high energy density, superior power performance, long durability and improved safety for the next generation energy storage devices.

Table of Contents

ABSTRACT	I
Table of Contents	III
List of Figures	VI
List of Table	XI
List of Abbreviation	XII
Chapter 1. General Introduction	1
1.1 Growing Demands for Energy Storage Systems	1
1.2 Lithium Ion Battery.....	2
1.2.1 Success and Bottleneck of Lithium Ion Battery	2
1.2.2 Working Mechanism of Lithium Ion Battery	3
1.3 Lithium Oxygen Battery	5
1.3.1 Types of Lithium Oxygen Battery Based on Configurations.....	5
1.3.2 Working Mechanism of Lithium Oxygen Battery	7
1.4 Current Challenges for Lithium Oxygen Battery.....	9
1.4.1 Complicated Problems within Oxygen Cathode and Electrolyte	9
1.4.2 Li Metal Challenge	12
1.5 Target and Outline of This Dissertation	13
1.5.1 Research Motivation	13
1.5.2 Target	14
1.5.3 Outline.....	16
Chapter 2. Hybrid Electrolyte Design for Silicon Alloy Anode Based Lithium Ion Oxygen Battery	18
2.1 Introduction.....	18
2.2 Experimental Section	20
2.2.1 Preparation of the Narion@PTFE Membrane	20

2.2.2 Permeation Test.....	21
2.2.3 Preparation of KB Cathodes and Si anodes	21
2.2.4 Cell Assembly	22
2.2.5 Cell Assembly	22
2.3 Results and Discussions	23
2.3.1 Lithiated Nafion Membrane for Hybrid Electrolyte Design.....	23
2.3.2 Fabrication of Silicon Alloy Anode Based Lithium Ion Oxygen Battery	27
2.3.3 Characterization on Oxygen Cathode during Discharge/Charge	29
2.3.4 Cycling Performances of Oxygen Batteries with Different Configurations.....	31
2.3.5 Characterizations on Silicon Anodes after Cycling	32
2.4 Conclusions.....	35
Chapter 3. Hybrid Electrolyte Design for Organic Liquid Anode based Oxygen Battery.....	36
3.1 Introduction.....	36
3.2 Experimental Section	38
3.2.1 Preparation of biphenyl-Li complex (Bp-Li) liquid anode	38
3.2.2 Preparation of zeolitic imidazolate frameworks (ZIF7) particles	39
3.2.3 Water reaction test.....	39
3.2.4 Preparation of ZIF7 membrane	39
3.2.5 Permeation test.....	40
3.2.6 Conductivity measurements	40
3.2.7 Cathode preparation	41
3.2.8 Cell assembly	41
3.2.9 Electrochemical measurements.....	42
3.2.10 Characterizations.....	42
3.3 Results and Discussions	43
3.3.1 Biphenyl based Organic Liquid	43

3.3.2 Metal Organic Frameworks based Membrane for Hybrid Electrolyte Design	45
3.3.3 Rate and Cycling Performance	48
3.3.4 Characterization of Liquid Anode/Membrane Interface	50
3.4 Conclusions.....	55
Chapter 4. A Practical Lithium Oxygen Cell Based on Hybrid Electrolyte Design	56
4.1 Introduction.....	56
4.2 Experimental Section	58
4.2.1 Preparation of cathodes for Li-O ₂ cells	58
4.2.2 Preparation of metal organic frameworks (MOFs) based separator	58
4.2.3 Preparation of electrolytes	58
4.2.4 Fabrication of coin type Li-O ₂ cells	59
4.2.5 Fabrication of pouch type Li-O ₂ cells	59
4.2.6 Electrochemical measurements.....	60
4.2.7 Characterizations.....	60
4.3 Results and Discussions	60
4.3.1 Perfluoro Solvents for Oxygen Solubility Improvement	60
4.3.2 Pouch-type Cell Fabrication	63
4.3.3 Discharging Energy Density	65
4.3.4 Cycling Performance	68
4.4 Conclusions.....	70
Chapter 5. General Conclusions and Perspectives	71
5.1 General Conclusions	71
5.2 Perspectives.....	73
Acknowledgement.....	76
References.....	78

List of Figures

Figure 1.1 What will be the energy storage device for EVs like LIBs for portable electric devices?	3
Figure 1.2 Schematic illustration of the state-of-art LIB. LMO is short for lithium metal oxide, and the metal could be transition metal element like cobalt, manganese, nickel and aluminum. Figure reproduced from ref 12, American Chemical Society.	4
Figure 1.3 Schematic illustration of two main types of Li-O ₂ battery based on the electrolyte the oxygen cathode works in. Figure reproduced from ref 19, American Chemical Society.	6
Figure 1.4 Two pathways during ORR process in a Li-O ₂ battery. Figure reproduced from ref 27, Springer Nature.....	8
Figure 1.5 Schematic diagram of the major performance obstacles for Li-O ₂ battery: a) large OER overpotential, b) limited capacity and c) poor cycle performance. Figure reproduced from ref 36, Elsevier B.V.	9
Figure 1.6 Exploratory reactions of superoxide at the oxygen cathode with various components. Figure reproduced from ref 37, American Chemical Society.	10
Figure 1.7 Schematics of cathode reactions on discharge and charge in the presence of two typical RMs, DBBQ and TEMPO. Figure reproduced from ref 46, Springer Nature.	11
Figure 1.8 Effective results of RMs in lowering the overpotential for the Li-O ₂ battery. Figure reproduced from ref 27, Springer Nature.	11
Figure 1.9 Obstacles that have long bothered the development of lithium metal anode. Reproduced from Ref. 50 with permission from The Royal Society of Chemistry.....	12
Figure 1.10 Schematic outline for research pathway in this dissertation.....	17
Figure 2.1 Schematic illustration of different electrolytes for Si Based Li-Ion O ₂	

Batteries.	19
Figure 2.2 a) Cross-sectional SEM image and b) upside SEM image of the Nafion@PTFE membrane.	23
Figure 2.3 FT-IR spectrum of the Nafion@PTFE membrane.....	24
Figure 2.4 a) Schematic illustration of the permeation test. b) Images of the devices during permeation experiment.	24
Figure 2.5 FT-IR spectrum of the permeation test. a) 1 M G4 with RMs vs 1 M EC/DEC and b) 1 M G4 with RMs vs 5 M EC/DEC. c) Raman spectrum of 1 M and 5 M LiTFSI-EC/DEC electrolytes with pure EC/DEC solvents.	25
Figure 2.6 a) the images of permeation test: 5M carbonate based anode electrolyte Celgard separator 1M G4 cathode electrolyte with RMs. b) FT-IR spectrum of electrolytes extracted during the permeation experiment within certain times.	26
Figure 2.7 Proposed structure of hybrid electrolyte design Li-ion O ₂ battery, achieved by a Nafion@PTFE membrane, with dual RMs in the cathode electrolyte and the high concentration carbonate based anode electrolyte.....	27
Figure 2.8 a) SEM images of the pristine Si anode. b) XRD patterns of pristine Si anode (black), Li-Si anode lithiated in 5M EC/DEC (red) and 1M G4 (blue). (c) The delithiation capacity of Li-Si anode in 5M EC/DEC (red) electrolyte and 1M G4 (blue) electrolyte.....	28
Figure 2.9 Electrochemical profile of hybrid electrolyte design Li-ion O ₂ battery and normal type Li-ion O ₂ battery at a current of 200 mA·g ⁻¹	29
Figure 2.10 XRD patterns of the cathodes at different states.	30
Figure 2.11 SEM images of the cathodes at different states.	30
Figure 2.12 Electrochemical performance of Li-ion O ₂ batteries with a) G4 based electrolyte, b) Nafion separated G4-based electrolyte, and c) hybrid electrolyte design. d) Terminal voltages of different cells with cycles.	31

- Figure 2.13** SEM images of lithiated Si anodes a) before and b) after 12 cycles in the Nafion-separated G4-based electrolyte. SEM images of lithiated Si anodes before c) and after d) 50 cycles in the hybrid electrolyte Li-ion O₂ cells.33
- Figure 2.14** a,c) C 1s spectrum and (b, d) F 1s spectrum of Si anodes in the Nafion separated G4-based cell and the hybrid electrolyte design cell after cycling.34
- Figure 3.1** Schematic illustration of the cell structure for the electrochemical test of the Bp-Li liquid anode41
- Figure 3.2** Properties of the Bp-Li liquid anode. a) Preparation of the Bp-Li liquid anode. b) Reaction of Bp-Li anode with water.43
- Figure 3.3** a) Measurements of conductivity of Bp-Li liquid anode through EIS methods. The calculated total conductivity $1.11 \times 10^{-2} \text{ S} \cdot \text{cm}^{-1}$ for 1 M Bp-Li liquid anode, and $1.36 \times 10^{-2} \text{ S} \cdot \text{cm}^{-1}$ for the 2 M Bp-Li liquid anode. b) Potential-current plots obtained from voltmeter ammeter method. The electrical conductivity of 2M Bp-Li anode is calculated as $1.24 \times 10^{-2} \text{ S} \cdot \text{cm}^{-1}$44
- Figure 3.4** a) Schematic illustration of the difference between the previous reports of biphenyl-Na/K liquid anode with solid state electrolytes (SSEs) and this study of biphenyl-Li liquid anode with a ZIF7 membrane separator. The proposed function of the ZIF7 membrane in three aspects is also displayed. b) The cross-side SEM images of the ZIF7 membrane. Inset: the digital image of the ZIF7 membrane.46
- Figure 3.5** a) Digital images of the permeation device in the beginning (black) and after 7 days (orange). b) FT-IR spectrum of the electrolyte samples extracted from the G4 side at different time.47
- Figure 3.6** The schematic illustration of the organic oxygen battery with Bp-Li liquid anode, dual RM assisted KB cathode and ZIF7 membrane as a separator.48
- Figure 3.7** a) The electrochemical profiles of the dual RM assisted oxygen cathode and Bp-Li liquid anode half cells. b) Rate performances of the fabricated Li based organic oxygen batteries.49

Figure 3.8 Cycling performance of the Li based organic oxygen batteries within 100 cycles.....	50
Figure 3.9 The cross-side and upside SEM images of the ZIF7 membranE. The interfaces of ZIF7 membrane facing cathode side (yellow) and anode side (red) exhibit different morphologies after cycling. The pristine morphology (blue) of ZIF7 membrane is also displayed to be compared with.	51
Figure 3.10 a) The FT-IR spectrum of ZIF7 membranes before and after cycles. b) The XRD patterns of the ZIF7 membrane before and after electrochemical cycles in the organic O ₂ battery.....	51
Figure 3.11 XPS C 1s, F 1s and Zn 2p spectrum of the ZIF7/Bp-Li interface after cycles.	52
Figure 3.12 a) The electrochemical profiles of the organic oxygen batteries with a PVDF based ZIF7 membrane. b) The cross-side SEM images, c) FT-IR spectrum and d) XPS F1s spectrum of the PVDF based ZIF7 membrane after cycles.....	53
Figure 3.13 The schematic illustration of the formation of SEI-like ZIF7/Bp-Li interface.....	54
Figure 4.1 a) Discharge load curves of coin type Li-O ₂ cells in various condition at 0.1 mA·cm ⁻² . b) Discharge load curves of DBBQ contained coin type Li-O ₂ cells with and without HFE at different current densities.	61
Figure 4.2 Oxygen cathodes in various electrolytes after discharging.	61
Figure 4.3 CV curves of KB cathode under Ar and oxygen atmosphere at various scanning rates in the electrolyte of a) only DBBQ and b) DBBQ and HFE.....	62
Figure 4.4 a) Schematic illustration of the pouch type Li-O ₂ cells with oxygen windows at the cell side in a hybrid electrolyte design. b) Digital image of the fabricated pouch type Li-O ₂ cells.	63
Figure 4.5 Discharge load curves of pouch type Li-O ₂ battery in a hybrid electrolyte	

design with a) DBBQ only and b) DBBQ and HFE contained cathode electrolyte. ...65

Figure 4.6 XRD patterns of the cathodes in the pouch type Li-O₂ cells with two kinds of cathode electrolyte respectively.....67

Figure 4.7 Cycling tests of pouch type Li-O₂ cells in hybrid electrolyte design with dual RMs and HFE in the cathode electrolyte. The fixed capacity is a) 40 mAh and b) 60 mAh respectively.68

Figure 5.1 Schematic illustration of the potential of hybrid electrolyte design for the energy storage devices.73

List of Table

Table 4.1 Cell parameters of the pouch type Li-O₂ cells with two kinds of cathode electrolyte respectively.67

List of Abbreviation

Abbreviation	Definition
EVs	Electric Vehicles
LIB	Lithium Ion Battery
SSEs	Solid State Electrolytes
ORR	Oxygen Reduction Reaction
ORR	Oxygen Evolution Reaction
RMs	Redox Mediators
SEI	Solid Electrolyte Interface
DME	1,2-Dimethoxyethane
DBBQ	2,5-di-tert-butyl-1,4-benzoquinone
TDPA	Tris[4-(diethylamino)phenyl]amine
ZIF7	Zeolitic Imidazolate Frameworks
Bp-Li	Biphenyl-Li Complex
HFE	Per Fluorinated Chemical
TEMPO	2,2,6,6-tetramethylpiperidinyloxy

Chapter 1. General Introduction

1.1 Growing Demands for Energy Storage Systems

The modern world is built on the usage of the fossil fuels. Its massive application could be dated back to the First Industrial Revolution, and ever since then it has deeply influence the modernization of the global society. On the one hand, human beings are getting to realize that the fossil fuels are non-renewable energy, on the other hand, burning of fossil fuels would always lead to release of greenhouse gas, resulting in the global warmth problem. Searching for alternative energy sources has become a task for the total society.¹ As renewable energy, solar energy, wind energy and tidal energy have been long developed during the decades.² However, their massive application is limited by the discontinuous distribution nature in space and time. As a result, energy storage devices become more and more importance recently, if we want to take advantage of the green energy more efficiently and universally.³

Batteries are a kind of devices that could store energy chemically and release it electronically.⁴ They can be categorized into primary battery and secondary battery respectively. A primary battery could only be discharged once, while a secondary battery is rechargeable and can be used many times. The battery device has been experiencing a long development with a variety of types being invented, and the goal for a better battery is always to store more energy into a lighter and smaller device.

As an answer to cutting down the need for the fossil fuel, electric vehicles (EVs) are recently emerging and got policy supports from countries and organizations all over the world. In China, financial support for EVs consumers has been provided as incentives for the EVs market. Japan has promoted co-operative approach aiming to reduce 80% of greenhouse gas emissions from vehicles produced by domestic automakers to be achieved by 2050 with a combination of hybrid electric vehicles (HEVs), EVs and fuel cell electric vehicles (FCEVs). In EU, policy that encourage the public procurement of electric buses was provided in 2018.⁵ As a result, there has been a rapid growth in the EVs market during the past 10 years. The growing trend of EVs worldwide would still

continue under the shift from the fossil fuel cars to the EVs, resulting in a growing demand for the energy storage systems with high performance and durability.

1.2 Lithium Ion Battery

1.2.1 Success and Bottleneck of Lithium Ion Battery

Lithium element marks the third element in the periodic table of elements. It is the smallest, lightest and most electropositive metal atom, thus making it a suitable charge carrier to work in a high energy density battery system.⁶ The first trial to build a lithium based battery is dated back to 1970s, when lithium metal was chosen as the anode material to build a durable primary cell for small electric devices like watches and calculators.⁷ However, the application of lithium metal soon encountered obstacle when it was coupled with a reversible cathode material to build a secondary battery. The uneven plating of lithium ion on the lithium metal during the battery charging would lead to the dendrite growth, and thus resulting in the short circuit and even safety hazards sometimes. From then on, efforts, including the Nobel Prize winner Akira Yoshino's work to introduce carbon materials as anode, to search for alternatives for lithium metal has taken 20 years till the commercialization of LIBs. On the other hand, the development of the cathode materials has also experienced a lot of trials, till another Nobel Prize winner Goodenough proposed the transition metal oxide compounds with a layer structure for lithium ions to intercalate and de-intercalate, which is still the mainstream cathode material of today's LIBs.⁸

Benefitting from all these efforts in both cathode and anode for the Li-based battery, the company Sony gave birth to the first type of commercial LIBs in the beginning of 1990's.⁹ From then on, LIBs have brought a great boom in the market of portable electric devices. DAPs (digital audio players), laptops and smart phones with the rechargeable LIBs are able to make a prompt development and achieve great success. It's not hyperbolic to say that the LIBs have changed our daily life, as they enable the electronics revolution by powering the devices we find indispensable for working, studying, playing and communication.

As a successful battery in the portable electric devices, LIBs are considerably applied as the energy tank in the coming EVs revolution.¹⁰ Scientists and engineers try their best to improve the state of art LIBs based on the layer material cathode and graphite anode, in order to give them the quality in energy density, rate performance and durability to match experience that fossil fuels give to the ICE (Internal Combustion Engine) cars.¹¹ However, the improvement that can be achieved for LIBs is becoming less and less, and there is the believe that the energy density of the LIBs at the cell level could be pushed up to near $300 \text{ Wh} \cdot \text{Kg}^{-1}$. The energy density at this level cannot cover the expectation of consumers who have got used to the performance of an ICE car. Thus, there is so-called “range anxiety” for the EV driver, who is always worried that the EV would stop on the way to some place. The limitation of energy density for the LIBs marks the main reason for the poor range of EVs. And the limitation lies on the material structure and working mechanism of the LIBs, which will be discussed next.



Figure 1.1 What will be the energy storage device for EVs like LIBs for portable electric devices?

1.2.2 Working Mechanism of Lithium Ion Battery

A typical LIB works based on the intercalation/de-intercalation of lithium ions between the cathode and anode (Figure 1.2).¹² A LIB should usually be charged first, during which the lithium ion contained cathode releases lithium ions, then they transport to the anode side and intercalate into the anode. The cathode is basically LiCoO_2 , a kind of layer structure metal oxide with a high lithium working voltage of

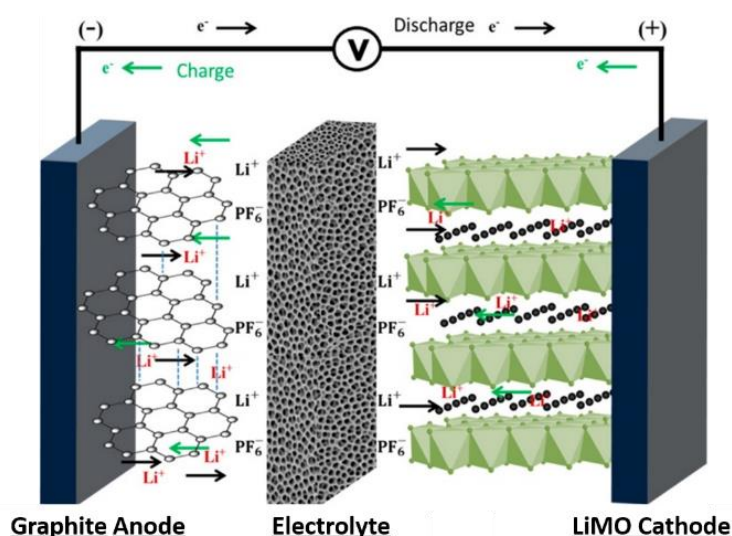


Figure 1.2 Schematic illustration of the state-of-art LIB. LMO is short for lithium metal oxide, and the metal could be transition metal element like cobalt, manganese, nickel and aluminum. Figure reproduced from ref 12, American Chemical Society.

3.5 V~4.0 V vs. Li^+/Li and a calculated theoretical specific capacity of $274 \text{ mAh}\cdot\text{g}^{-1}$ assuming 1 mole of lithium ions are extracted. Unfortunately, the de-intercalation of more than 0.5 mole lithium in 1 mole LiCoO_2 requires high potential that might lead to the electrolyte decomposition and the material itself unstable.⁷ As a result, commercial applications of LiCoO_2 is limited to a 4.2 V cut-off, which means that nearly $150 \text{ mAh}\cdot\text{g}^{-1}$ of specific capacity is practically used. To address the capacity and stability issue of LiCoO_2 , researchers concentrate their eyes back onto the LiNiO_2 , which shares the same structure with LiCoO_2 but has a higher working potential and specific capacity. It was once studied but gave up due to its instability. Researchers try to solve its problems by introducing substituted atom into the structure of LiNiO_2 , aiming at stabilizing the structure during the lithium ion de-intercalation. And this lead to the layered Ni-Mn-Co oxide (NMC) and Ni-Co-Al oxide (NCA), which are considered promising cathode materials for the EVs. However, their theoretical specific capacity, though improved compared with that of LiCoO_2 , is still limited due to the crystalline structure of the material. Other materials like olivine structure LiFeO_4 or rock salt structure LiMnO_2 , are also explored and commercialized but still suffered from the poor specific capacity.¹³

The anode materials, on the other hand, the alternative of lithium metal was finally determined to be the carbon-based anode.¹⁴ It shows a high reversibility of lithium intercalating into or de-intercalating out of the carbon material. Graphite, one of the typical carbon-based anode, shows a reversible specific capacity of $372 \text{ mAh}\cdot\text{g}^{-1}$ and a low working potential of nearly 0.1 V vs. Li^+/Li , which makes it an appropriate candidate to couple with the metal oxide cathode to build a well-performed LIB. It's also worth noting that the electrolyte also matters a lot on the reversibility of electrodes, especially for the anode. It took quite an effort for the researchers to realize that the stable cycling of graphite relies on the formation of a solid electrolyte interface (SEI) on the anode material surface.¹⁵ And the electrolyte composite plays a key role for the SEI formation. Anyhow, the successful application of the graphite anode attributes to the practical application of LIBs up to now. And trials to bring in anode with higher specific capacity are still on the way.

The lithium storage ability of both metal oxide cathode and carbon-based anode is decided by the crystalline structure of the materials. This indicates that the specific capacity of materials based on the intercalation/de-intercalation mechanism is hard to be further improved, which determines the bottle neck of the energy density of the nowadays LIBs. As a result, there rises up a call for the next generation Li-based battery systems with brand new working mechanism and promising theoretical energy density, among which is the lithium oxygen (Li-O_2) battery.

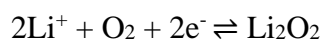
1.3 Lithium Oxygen Battery

1.3.1 Types of Lithium Oxygen Battery Based on Configurations

The scientific community studied the primary metal-air battery system dating back to 1970's, and ever since then they have realized that a battery system like this could provide plausible energy output due to the usage of air and a considerable working voltage at near 3.0 V .¹⁶ However, it's then ignored for a long period, and then regained the scientists' concentration after the first report of a rechargeable Li-O_2 battery by Abraham and Jiang in 1996.¹⁷ Later, the research interests towards this battery system

was boosted by Bruce and co-workers, who demonstrated the reversible electrochemistry based on Li_2O_2 at the cathode with a MnO_2 catalyst during discharging and charging in an organic liquid electrolyte in 2006.¹⁸ From then on, Li-O₂ battery quickly became a hot topic for the researchers trying to searching for the battery coming next after LIBs.

Up to now, Li-O₂ battery can be mainly categorized into three types regarding to the electrolyte that oxygen cathode works in.¹⁹ In the proposed battery models, all types of Li-O₂ batteries take advantage of the reversible stripping/plating of lithium metal at the anode side. The differences locate in the cathode side. In an aprotic Li-O₂ battery, the ideal electrochemistry at the cathode is based on the formation and decomposition of Li_2O_2 , the reductive product of oxygen. The cathode reaction equation could be:



The aprotic Li-O₂ battery receives the most research focus due to the fact that it shares a similar simple battery structure with the state-of-the-art LIBs.²⁰ When all the cell

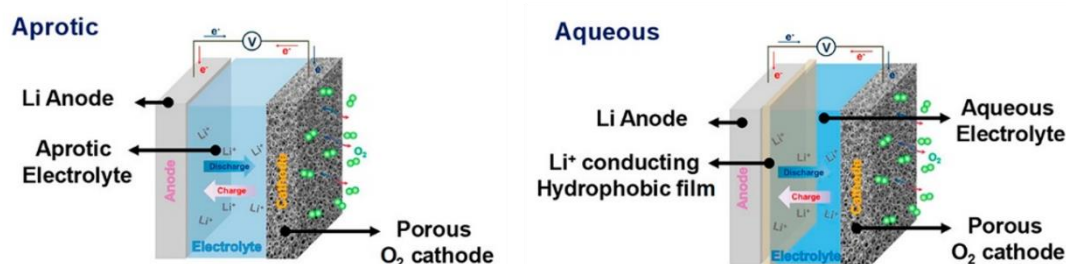


Figure 1.3 Schematic illustration of two main types of Li-O₂ battery based on the electrolyte the oxygen cathode works in. Figure reproduced from ref 19, American Chemical Society.

components including electrolyte is in solid state, then we get the all solid state Li-O₂ battery. It shares the same Li_2O_2 based electrochemistry with the aprotic Li-O₂ battery. And it's considered an ultimate battery system, as it possesses the benefits of safety of the solid state electrolytes (SSEs) and promising energy density of the oxygen based electrochemistry in the cathode. However, it will still be suffering from the poor conductivity of SSEs and we will not give further discussion on this type in this dissertation.

On the other hand, oxygen could also be reduced at the cathode in an aqueous electrolyte.²¹⁻²² In an aqueous cathode electrolyte, the reductive product of oxygen is soluble LiOH, though the electrochemical reactions differs in terms of the acidity and alkaline of the aqueous electrolyte. The cathode reaction follows equations below respectively:



The output potential of Li-O₂ battery an aqueous is higher than that of an aprotic Li-O₂ battery. Moreover, the soluble discharge product would avoid the cathode from being clogged by the discharge product, which is considered a major challenge for the aprotic Li-O₂ battery, thus achieving much higher capacity.²³ However, the lithium metal could not work in an aqueous electrolyte, which makes the solid state electrolytes necessary for the aqueous Li-O₂ battery. With the help of SSEs, the lithium metal could be protected from the reactive aqueous cathode electrolyte. From the view of the battery structure, we'd like to call it a hybrid electrolyte Li-O₂ battery. It's worth noting that some researchers categorize it by calling the battery with SSEs directly contacting to lithium metal as aqueous Li-O₂ battery and the battery with SSEs connecting to the lithium with another organic electrolyte as hybrid electrolyte.^{11, 19} No matter what, when an aqueous electrolyte is applied to the cathode, SSEs is always necessary and the battery structure becomes complicated. This makes the hybrid electrolyte Li-O₂ battery less popular compared with the aprotic Li-O₂ battery, though we think that the basic thinking to divide the cathode part and anode part separately is inspiring for building a next generation battery, which we'll discuss later.

1.3.2 Working Mechanism of Lithium Oxygen Battery

Now we focus on the aprotic Li-O₂ battery. The below mentioned Li-O₂ battery is all aprotic type if there's no specific illustration. Plenty of efforts have been paid to reveal the complicated working mechanism of the Li-O₂ battery.²⁴⁻²⁵ During the oxygen reduction reaction (ORR) process, the solubility of the intermediate product LiO₂ and

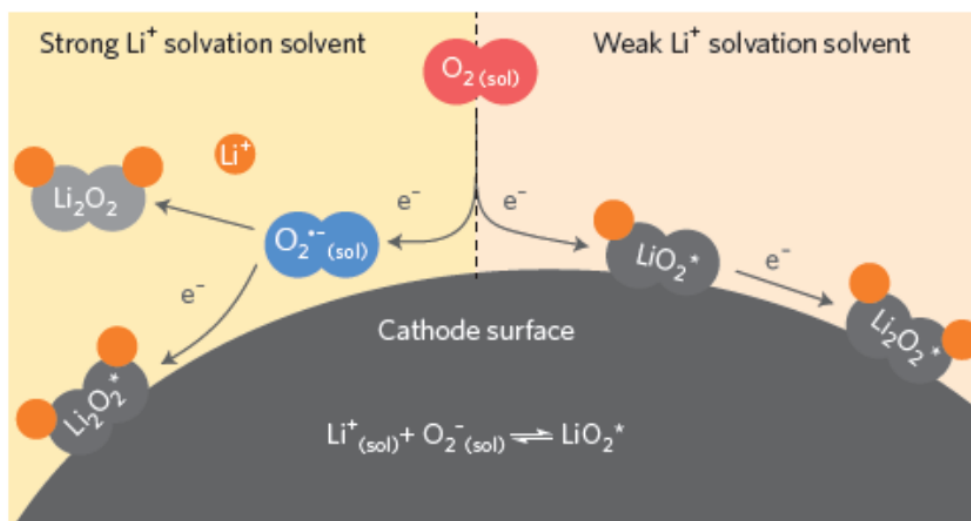


Figure 1.4 Two pathways during ORR process in a Li-O₂ battery. Figure reproduced from ref 27, Springer Nature.

the effective current density would have much influence on the growing behavior of the Li₂O₂ product. It's now well accepted that LiO₂ would firstly form during the reduction of oxygen.²⁶ Bruce et al. propose two reaction pathways of the ORR process through LiO₂ formation depending on its solubility (Figure 1.4).²⁷ There exists an equilibrium between the LiO₂ adsorbed on the cathode surface and LiO₂ dissolved into the electrolyte once it forms by the oxygen receiving an electron. The competition between the LiO₂ adsorbed or dissolved is mainly influenced by the property of electrolyte, determined by the solvents, salts and additives. The solubility of LiO₂ could be improved with a high Gutmann donor number (DN) solvent, or a salt with strong anion to solvate lithium ion, or additives with ability to solvate lithium ion or even superoxide. As a result, LiO₂ tends to dissolving in the electrolyte, which is then further reduced or disproportionate to Li₂O₂. This is called a solution pathway, which leads to large Li₂O₂ particles, high discharge capacity but poor reversibility due to low contact. For the electrolyte that cannot promote the LiO₂ dissolution, LiO₂ is preferable to adsorb on the cathode surface, which accepts another electron to form Li₂O₂. This is called a surface pathway. In this way, the contact between the Li₂O₂ and the cathode is better, but the discharge capacity is poor as the cathode surface is quickly covered by formed Li₂O₂

film. Also, at high current density, the Li_2O_2 tends to be film-like, resulting high overpotential and poor capacity.²⁸⁻²⁹

During oxygen evolution reaction (OER), the high overpotential always remains a bothering problem. It comes from two aspects, one is that Li_2O_2 itself is a poor electronic and ionic conductor,³⁰ but more important one is that the parasitic products are hard to be decomposed during charging process.³¹⁻³² Some theoretical calculations have shown that Li_2O_2 could be oxidized at some facets with low overpotential,³³ which is in accordance with the experiments conducted on a cathode pre-loaded with commercial Li_2O_2 .³⁴ However, for the electrochemically formed Li_2O_2 , the overpotential quickly increases after the OER process begins, during which Li-deficient component would present. The oxidation of these Li-deficient components is believed to be facile, but the remained parasitic products would require a high potential to decompose them.³⁴⁻³⁵ The origins of parasitic products could be decomposition both of the cathode materials or electrolytes, which quite challenges the performance of the $\text{Li}-\text{O}_2$ battery.

1.4 Current Challenges for Lithium Oxygen Battery

1.4.1 Complicated Problems within Oxygen Cathode and Electrolyte

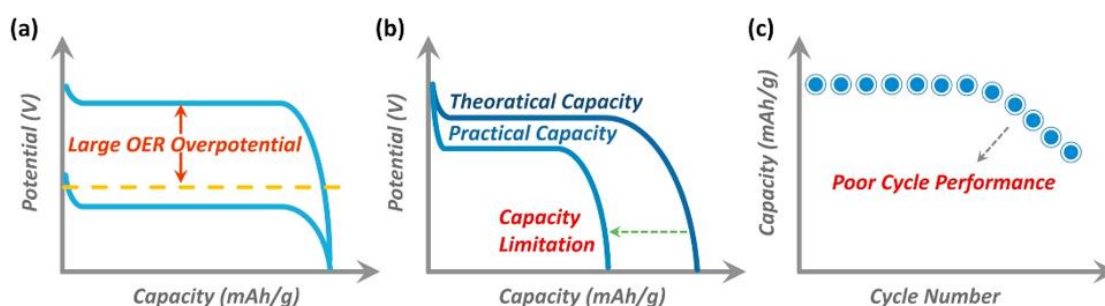


Figure 1.5 Schematic diagram of the major performance obstacles for $\text{Li}-\text{O}_2$ battery: a) large OER overpotential, b) limited capacity and c) poor cycle performance. Figure reproduced from ref 36, Elsevier B.V.

There are several challenges that should be overcome for the practical application of $\text{Li}-\text{O}_2$ battery. It always suffers from the low practical discharging capacity, large OER

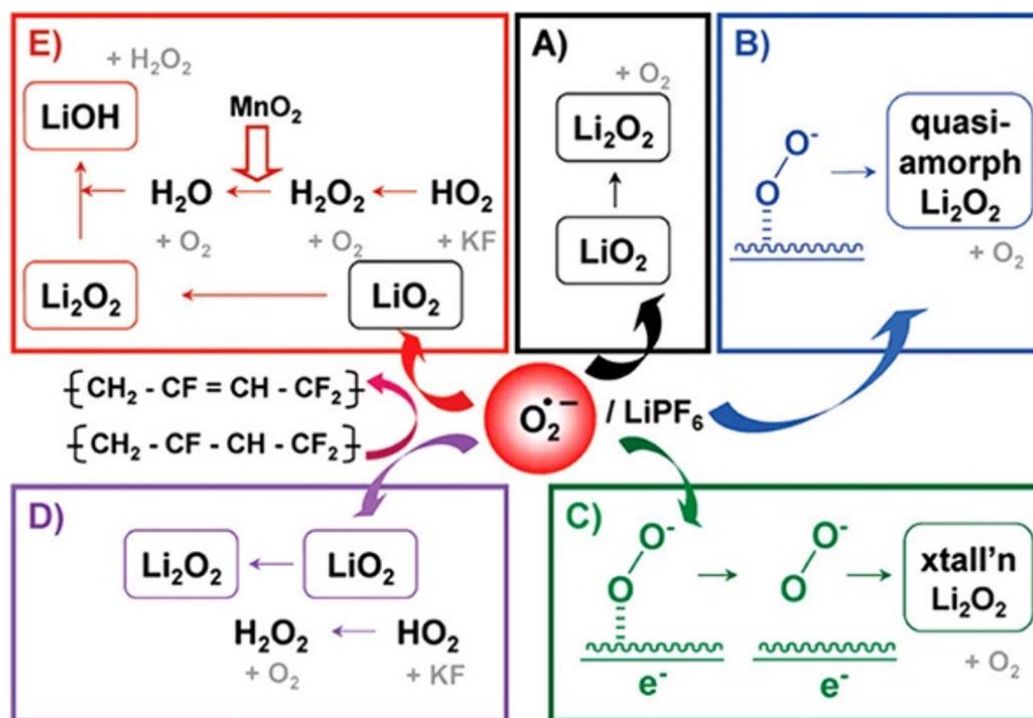


Figure 1.6 Exploratory reactions of superoxide at the oxygen cathode with various components. Figure reproduced from ref 37, American Chemical Society.

overpotential and poor cycling stability (Figure 1.5).³⁶ Though each component of the battery takes part of the responsibility, the most focused reasons are within the cathode and electrolyte. The ORR intermediate, superoxide species, is proved to be very reactive (Figure 1.6).³⁷ Both the electrolyte and cathode are found to be vulnerable to it. This leads to the formation and aggradation of parasitic products, and they in turn push up the OER overpotential, making the electrolytes and cathode materials easier to decompose. Moreover, their aggradation together with the continuous decomposition of cathode material and electrolyte would finally lead to poor durability of the Li-O₂ battery.

Two kinds of strategies have been proposed to address the problems. Inspired by the successful experiences from the fuel cell, researchers develop a lot of catalysts, based on noble metal,³⁸ transition metal,³⁹ special carbon materials⁴⁰ and their composites,⁴¹⁻⁴² with kinds of well-designed structures as the cathode materials.⁴³⁻⁴⁴ This is mainly aiming at the catalytic ability of the cathode during formation and decomposition of Li₂O₂. Moreover, the metal based materials are found more stable compared with a

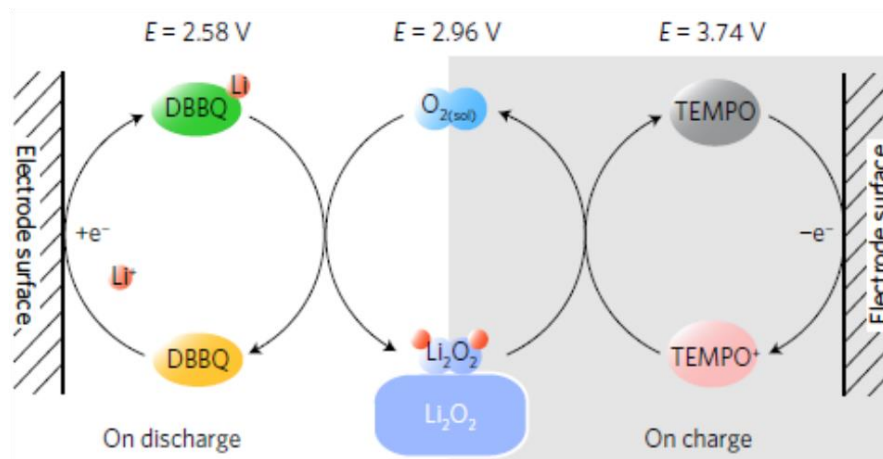


Figure 1.7 Schematics of cathode reactions on discharge and charge in the presence of two typical RMs, DBBQ and TEMPO. Figure reproduced from ref 46, Springer Nature.

typical carbon based cathode. Another strategy is focusing on the optimization of electrolyte. As is mentioned above, loose contact between Li_2O_2 particle and the cathode is always accompanied if one is trying to gain large discharging capacity, while the loose contact would no doubt lead to high OER overpotential and poor Coulombic Efficiency (CE). Redox mediators (RMs) are proposed to address these controversial problems.⁴⁵ RMs are a kind of electrolyte additive. They act as a charge carrier between the cathode and reactants in the electrolyte (Figure 1.7).⁴⁶ They benefits the

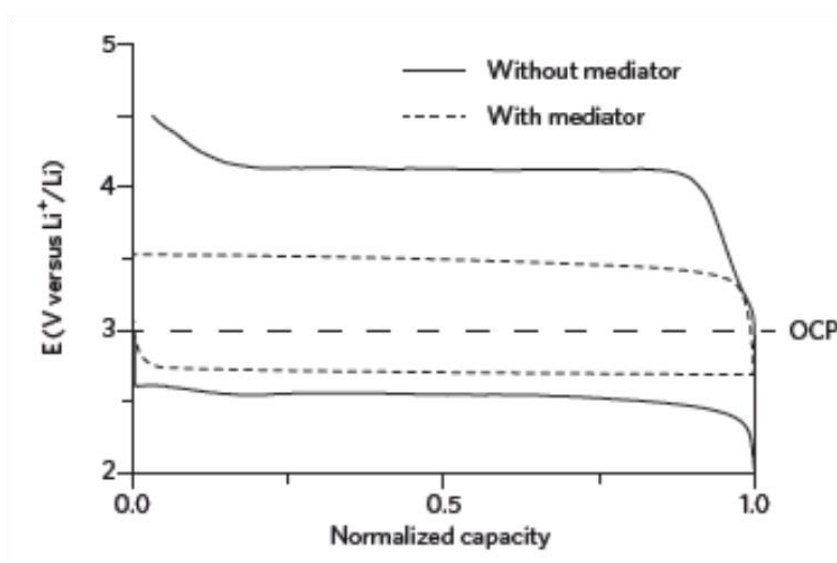


Figure 1.8 Effective results of RMs in lowering the overpotential for the $\text{Li}-\text{O}_2$ battery. Figure reproduced from ref 27, Springer Nature.

electrochemistry process mainly in two aspects: firstly, the battery would display the working potential of RMs, thus the overpotential could be well controlled with the special chosen RMs. And this effect is especially obvious in OER process (Figure 1.8); secondly, the reduced or oxidized RMs are mobile and reactive to facilitate the formation or decomposition of Li_2O_2 . The concept of RMs is promoted to reduce the overpotential of OER process in the beginning, and then expanded to the ORR process.⁴⁷⁻⁴⁹ By being reduced firstly during ORR, certain additives could avoid the formation of reactive superoxide, while remaining the large discharge capacity. And the application of different RMs for ORR and OER processes respectively, with the name dual RM strategy, has been proved a strong method to address the cathode and electrolyte related problems for Li-O₂ battery.

1.4.2 Li Metal Challenge

As the so-called “Holy Grail” anode material, lithium metal has the lowest working potential (-3.04 V vs. Li^+/Li) and the highest specific capacity ($3860 \text{ mAh} \cdot \text{g}^{-1}$).⁵⁰ At the present research scale, the application of lithium metal for the Li-O₂ battery seem to have no problems as the researches are almost conducted in small coin cells. However, the challenges for the lithium metal anode have been still remaining ever since its first trial in 1970’s, and we should never ignore them if we ever aim at the practical

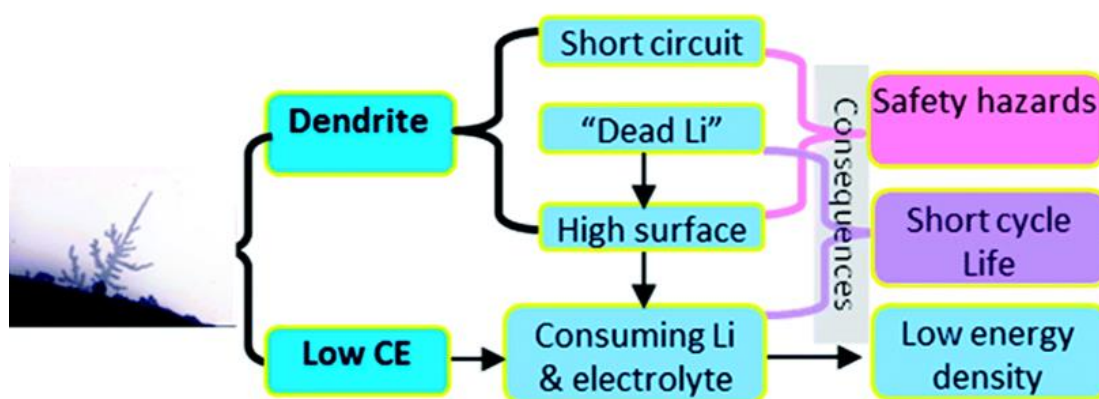


Figure 1.9 Obstacles that have long bothered the development of lithium metal anode.

Reproduced from Ref. 50 with permission from The Royal Society of Chemistry.

application of Li-O₂ battery.⁷ The low utilization and dendrite growth problems are the two major challenges that keep it from the commercial use. The low utilization would lead to poor reversibility and decreased energy density, while the dendrite growth would sometimes pierce through the separator and result in short circuit, which could turn into severe safety hazards.⁵¹

By now, varieties of strategies have been proposed to address the lithium metal related problems.⁵² As is the same with the graphite anode, the SEI also plays an important roles for lithium metal anode.⁵³ Researchers optimize the SEI formation by adjusting the electrolyte solvent composition, including kinds of solvents, salts and additives.⁵⁴⁻⁵⁵ To prevent the dendrite piercing, variety of separators with mechanical strength and ability to regulate the lithium ion plating are developed.⁵⁶⁻⁵⁷ Besides, designing frameworks to work as a host for lithium metal is considered a strategy to improve the performance of lithium metal.⁵⁸⁻⁵⁹ However, there hasn't been a decisive strategy that could totally address the lithium metal challenges in the practical scale. Therefore, it should also be considered to search for alternatives of lithium metal for the oxygen cathode.

1.5 Target and Outline of This Dissertation

1.5.1 Research Motivation

Li-O₂ battery potentially possesses the ability to drive EVs with long range, if the ideal of collaborative usage of the endless oxygen from outer atmosphere at the cathode and the ultimate anode, lithium metal, could be achieved. However, many challenges still remain for this battery system, which is still at its infant stage. The durability, power property and practical application are among the most annoying challenges that bother the development of Li-O₂ battery. The issues concerning these challenges are always not independent, and an overall consideration is needed to improve the battery performance.

At present, the RM strategy seems an effective choice for lowering the overpotential and stabilizing the cathode and electrolyte during cycling.⁶⁰ However, as RMs are

mobile in the electrolyte, their reactive state has the possibility to crossover to the anode side, and react with the lithium metal. This would in turn affect the function of not only the RMs but also the lithium metal anode.⁶¹⁻⁶² Researchers propose to solve this problem by fabricating some functional separators,⁶³ which is able to stop the RM molecules crossover but has no influence on lithium ion transporting.

The lithium metal problem is still challenging up to now. As a result, there are some research trials studying the performance of other high specific anode materials coupled with the oxygen cathode.⁶⁴⁻⁶⁷ However, the results always turn out to be disappointing. The major reason is that the incompetence of the anode material with the electrolyte, which is mainly designed for the oxygen cathode. The mismatch results in a poor SEI for the anode material, which breaks and regenerates repeatedly during the cycling, making the anode material unstable and quick to fail.

From an overall point of view, both cathode and anode need unique electrolytes to exhibit their best performances. As we mentioned in Chapter 1.3.1, the idea of the hybrid electrolyte Li-O₂ battery, to divide the cathode and anode in different electrolytes for their own better performances, could be inspiring. This gives us the motivation, to build a hybrid electrolyte structure for the aprotic lithium based oxygen battery and see how it works for the oxygen cathode and anode materials besides lithium metal. Meanwhile, to achieve the battery structure the separators could be a key component. Although SSEs are usually chosen in the aqueous Li-O₂ battery, we are very interested in other functional separators to build the structure more efficiently and simply. We believe this could open up a new gate for the research of lithium based oxygen battery.

1.5.2 Target

In this dissertation, we'd like to take advantage of the hybrid electrolyte design for the aprotic Li-O₂ battery, in order to improve its performance in several aspects, including cycling stability, rate performance, battery safety and its practical potential. Cycling stability, safe and high rate performance, and practical capability are important factors for researchers to judge a battery system, especially when it's considered as the

potential power tank for large electric devices like EVs. The cycling performance determines the functional life for the battery, and thus the durability performance of EVs. As the battery package is hard to be replaced once the car is fabricated, it's a key factor that affects the using experience of EVs. Also, the rate performance directly determines the power ability for EVs. For a high performance EV, higher output power is always demanded so that more complex circumstances could be dealt with. But for the battery system, high rate always means high safety risk. Thus how to realize a better rate performance with ensured safety is also a challenging topic. Finally, the practical potential should not be ignored for any battery systems. It represents the real potential for a battery system with so many claimed benefits in the research. For the oxygen battery whose most attractive property is the extremely high specific capacity, the cycling stability, rate and safety property and the practical capability are the most important factors that could affect its real application in EVs. Herein, taking advantages of hybrid electrolyte design, we aim at these targets in each chapter described below:

Firstly, we aim at solving the cycling stability problem of the Li-ion oxygen battery based on Si anodes. Si anode materials are a kind of representative alloy based anode materials with very high specific capacity.⁶⁸ Therefore, they are naturally considered for the lithium based oxygen battery, but the experimental results are always poor. By applying the hybrid electrolyte design to the Si based Li-ion oxygen battery, we expect the cycling performance of the battery could be largely improved.

Secondly, the rate performance and safety are concerned for the lithium based oxygen battery. As is always the case, battery works at a high rate could encounter a safety problem more easily, for the lithium ions are tend to plating unevenly at a high current density. We propose a new type of anode material that could function safely at a high rate, and with the help of the hybrid electrolyte design, we want to realize its function in a lithium based oxygen battery.

Lastly, we also make a practical test for the hybrid electrolyte design for the pouch-type Li-O₂ battery. Researches nowadays are almost conducted in a laboratory scale, which makes us wonder whether the potential of Li-O₂ battery could be achieved. We aim at the challenge during the scale-up of Li-O₂ battery from the coin cell level to the

pouch-type level, and try to figure it out with the hybrid electrolyte design.

1.5.3 Outline

This dissertation consists of five chapters as illustrated below:

Chapter 1 is the general introduction part. In this chapter, we firstly make a simple introduction of the daily increased need for the energy storage devices, and how LIBs achieve success in the field of portable electric devices and their struggle in the EVs. We explain this by illustrating its working mechanism, and then introduce the Li-O₂ battery considered as the promising candidate for energy storage device beyond LIB. We introduce the types of Li-O₂ battery, and the brief research progress and challenges for this battery systems. Finally, we present our motivation and method of hybrid electrolyte design aiming at address the challenges in several aspects.

Chapter 2 describes the work on the hybrid electrolyte design for Si alloy based Li-ion O₂ battery. In this chapter, we fabricate a Li⁺ form Nafion membrane to work as a separator in the battery to divide the cathode and anode systems separately. We build an ether based electrolyte with RMs for the oxygen cathode, and a carbonate based electrolyte for the Si anode to make both cathode and anode work in their suitable electrolytes. As a result, the cycling stability is largely increased compared with a normal type Li-O₂ battery. The SEI of Si anodes in different electrolytes are also investigated to clarify their relation to the cycling performance.

Chapter 3 describes the work on the hybrid electrolyte design for the organic liquid anode based oxygen battery. In this chapter, a metal organic frameworks (MOFs) based membrane is introduced to bridge the organic liquid anode and oxygen cathode by conducting Li ions while simultaneously separating the liquid anode at the anode side and RMs at the cathode side. Superior rate performance and cycling durability are achieved in this design. And we firstly study SEI-like layer of the organic liquid anode.

Chapter 4 describes the work on a practical Li-O₂ cell based on hybrid electrolyte design. We aiming at the oxygen transport problem when scaling up the cell to the pouch-type cell, and try to address it by introducing a per-fluorinated chemical in to the

cathode electrolyte to improve the oxygen solubility. And we also apply a hybrid electrolyte design to keep the anode from the influence of the cathode electrolyte species. Consequently, the output energy density of the hybrid electrolyte cell is obviously improved compared with a normal one, proving the large practical potential of Li-O₂ battery with this structure.

Chapter 5 is the general conclusions of this dissertation and our perspectives of the hybrid electrolyte design for the lithium based oxygen battery and other promising energy storage devices.

Based on the spirits of the hybrid electrolyte design to divide the cathode and anode systems respectively, we focus on the key issues for the current aprotic Li-O₂ battery. Focusing on the anode side, we begin our study with the improvement of the cycling stability for an alloy anode based oxygen battery in Chapter 2, and then further improve the rate performance with safety consideration with the help of the organic liquid anode. For the cathode side, we focus on the practical potential of the oxygen battery by build a pouch type Li-O₂ battery. With the improvement in these three key aspects benefitting from the hybrid electrolyte design, we hope that the way of Li-based oxygen battery to the EV power tank could be lighted on.

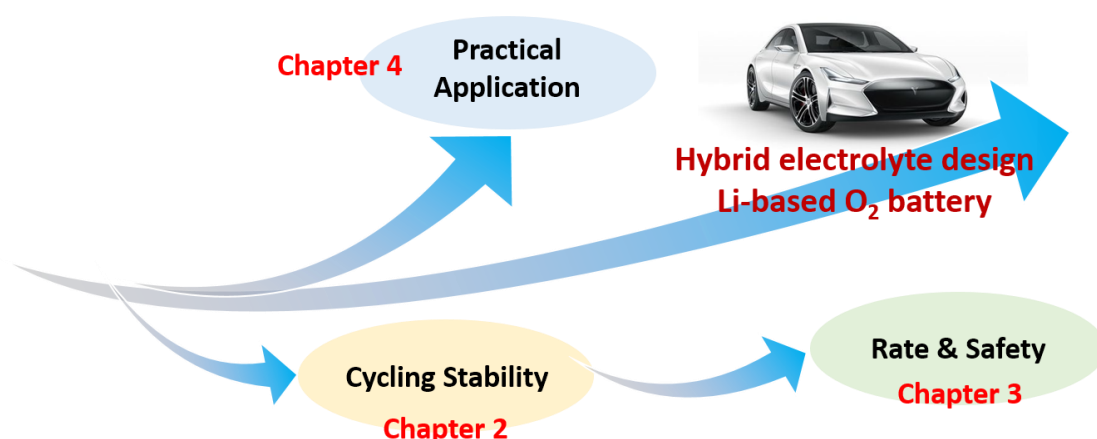


Figure 1.10 Schematic outline for research pathway in this dissertation

Chapter 2. Hybrid Electrolyte Design for Silicon Alloy Anode Based Lithium Ion Oxygen Battery

2.1 Introduction

Based on the usage of endless of oxygen from the external air and the lithium metal with high specific capacity and low working potential, Li-O₂ battery is considered to be a potential candidate for the next generation battery system, which could possibly bring a revolution to EVs.⁶⁹⁻⁷⁰ However, the battery system is still far from a practical application due to problems like high charge overpotential and poor cycling stability. Complex issues lying in the cell components would take responsibility for the unsatisfactory performance, and the consideration should be made comprehensively to improve the cathode, electrolyte and anode to a more stable and efficient level.¹¹

For the cathode of Li-O₂ battery, the insulating discharge product, Li₂O₂, would accumulate during oxygen reduction reaction (ORR) process, leading to the electrode block and poor capacity.⁷¹ In the oxygen evolution reaction (OER) process, Li₂O₂ decomposition requires a high overpotential, which would limit the round-trip efficiency of the battery and the parasitic degradation of the electrode and electrolyte. Aiming at these problems, researchers recently have proposed the redox mediator (RM) strategy to try to take place of the insufficient solid catalysts.⁷² In a typical process, the RM for ORR (RM_R) first undergoes reduction at the cathode to give RM_R⁻, then the RM_R⁻ reacts with the soluble oxygen to generate Li₂O₂.⁴⁷ In the OER process, the RM for OER (RM_E) is firstly oxidized and then RM_E⁺ in turn react with Li₂O₂ to decompose them.⁷³ By using RM_R and RM_E at the same time, the dual RM strategy frees the electrochemistry from the insulating property of Li₂O₂. However, the application of RMs would bring in drawbacks, that the soluble RMs would crossover to the anode side and react with lithium metal.⁷⁴ Therefore, the separation of the anode from the crossover reactive species is very important to get the full effect of RMs. Solid state electrolytes (SSEs) are always chosen to separate the RMs, However, SSEs are limited in practical

application, as it's hard to handle and poor in ion conductivity. Also, some polymer-modified glass fiber separators are reported to suppress the migration of the RME to the lithium metal.⁷⁵ Our group has also reported a metal organic frameworks (MOFs) based separator to retain the function of RMs, taking advantages of the pores in the MOFs structure small enough to block the RM molecular.⁶³ However, the lithium metal at the anode side, though protected from the RMs, is still struggling to be competent for Li-O₂ battery, which will be further discussed below.

The lithium metal suffers from the inherent problems like dendrite growth and low Coulombic Efficiency. In a Li-O₂ battery, lithium metal would also be affected by the soluble oxygen species. Many strategies have been proposed to work out the inherent problems of the lithium metal, but few of them is specially designed for the oxygen battery. As an alternative of lithium metal, Si anode is famous for its high theoretical

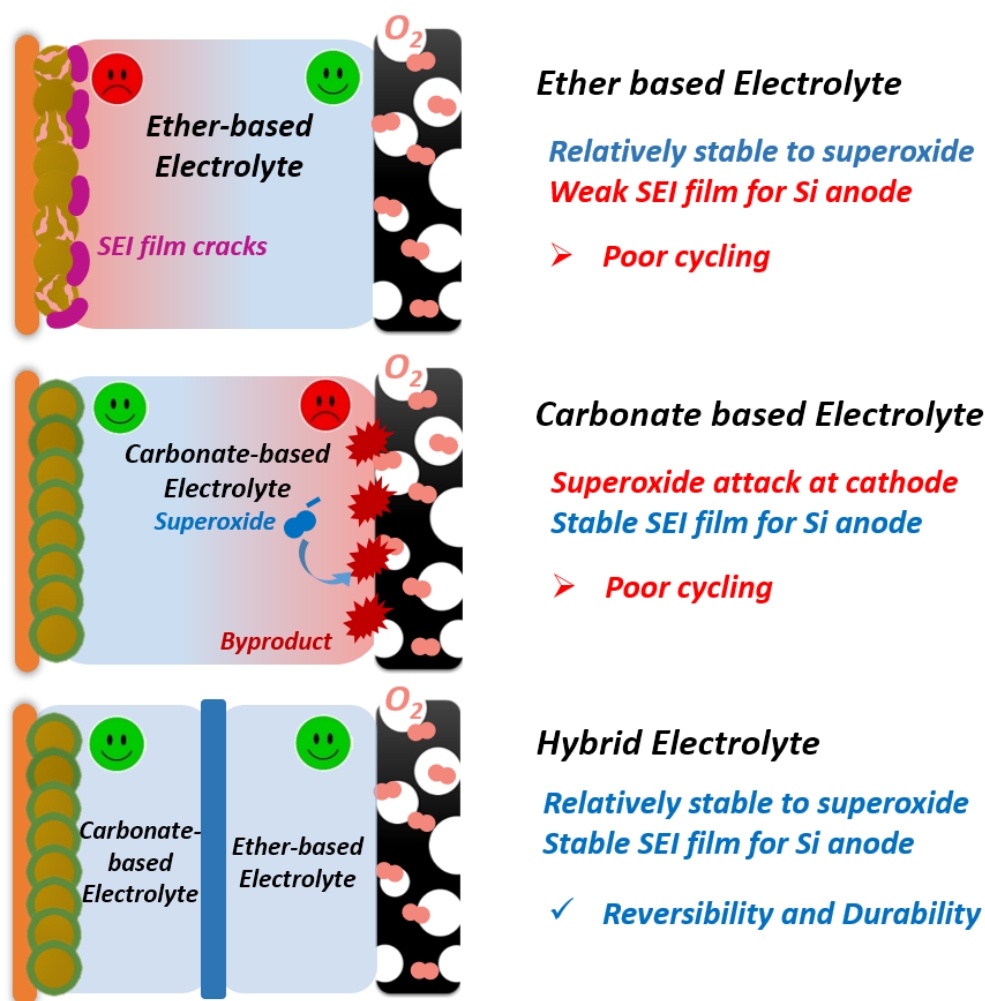


Figure 2.1 Schematic illustration of different electrolytes for Si Based Li-Ion O₂ Batteries.

specific capacity ($4200 \text{ mAh}\cdot\text{g}^{-1}$) and low working potential. However, the direct matching of Si anode with the oxygen battery always ends up in poor stability, mainly due to the compatibility of the Si anode with the ether based electrolyte commonly chosen for the oxygen cathode.^{64,76} It's reported that ethereal solvents are reactive with the Li-Si alloy materials.⁷⁷ As illustrated in Figure 2.1, ether based electrolytes are resistant to the superoxide species at the cathode side, but not beneficial to form a stable solid electrolyte interface (SEI) for the Si anode.⁷⁸ On the other hand, Si anode is more preferable in a carbonate based electrolyte with a strong SEI,⁷⁹ but the carbonate electrolyte has been proved vulnerable to the reactive superoxide species at the cathode.⁸⁰ As a result, either ether based or carbonate based electrolyte cannot build a durable Si-based Li-ion oxygen battery on their own. Nevertheless, in an overall consideration, if both ether and carbonate based electrolytes could be applied to their relative electrodes to boost their best performances, then a Li-ion oxygen battery with improved reversibility and durability can be well expected.

In this chapter, we build a hybrid electrolyte Li-ion oxygen battery by introducing the ether based cathode electrolyte with RMs and the carbonate based electrolyte for Si anode. A single ion conducting lithiated Nafion membrane is applied to bridge the two electrolyte systems, hindering the RMs crossover and limiting the solvents at their own sides. The fabricated Li-ion oxygen battery with the hybrid electrolyte design exhibits a high reversible capacity of near $18000 \text{ mAh}\cdot\text{g}^{-1}$ with low overpotential. Furthermore, thanks to the uniform SEI on the Si anode in a carbonate based electrolyte, the cycling stability of the battery is largely improved at a low anode/cathode capacity ratio and a high fixed capacity.

2.2 Experimental Section

2.2.1 Preparation of the Narion@PTFE Membrane

The method was designed according to a previous report.⁸¹ LiOH solution was used to lithiate 117 Nafion solution (Sigma-Aldrich, 5%) till pH reached 7. Then, equal volume of dimethylformamide was added and stirred for 1 h, followed by immersed

with the microporous poly(tetrafluoroethylene) (PTFE) membrane (Millipore) under vacuum dry at 60 °C for 1 h and 125 °C for another 5 h. The obtained Nafion@PTFE membrane was kept in the Ar filled glovebox before further fabrication. The membrane was cut into 16-mm pellets and immersed into pure tetraglyme (G4, 99%, Sigma-Aldrich) when the battery was assembled.

2.2.2 Permeation Test

We fabricated a home-made V-type device to conduct the permeation test.⁸² The RMs contained G4 electrolyte was kept in one tube of the device, while the carbonate based electrolyte was kept in the other one. The concentration of the G4 electrolyte was kept 1 M, and the concentration of the carbonate based electrolytes were 1 M or 5 M. The measured membrane was sandwiched by the two electrolyte-contained tubes. After certain time, 50 μ L of electrolytes were extracted out of each tubes for the Fourier-transform infrared (FT-IR) spectroscopy test, in the meanwhile digital images were taken to compare the color changes of the electrolyte showing the trace of RMs.

2.2.3 Preparation of KB Cathodes and Si anodes

The Ketjenblack (KB, EC600JD, Lion, Co. Ltd.) cathodes were fabricated by rolling the paste mixture of KB and PTFE (12% suspension) at a ratio of 85:15 and pressing it onto the carbon paper (hydrophobic) with a final mass loading of 0.15~0.20 $\text{mg}\cdot\text{cm}^{-2}$. Si anodes were prepared with alginate sodium (Wako) as the binder. In a typical way, Si powders (Alfa Aesar), the binder and super P carbon black (Timical) as conductive agent were mixed in deionized water to form a slurry.⁸³ The slurry was then casted onto a Cu foil, dried in the ambient atmosphere firstly and transferred into vacuum dry at 80 °C overnight. The mass loadings of Si anodes range from 0.5~2.0 $\text{mg}\cdot\text{cm}^{-2}$. The lithiation of Si anodes were conducted in the glovebox. Typically, the Si anodes were directly contacted with lithium metal in an ether or carbonate based electrolyte condition, under pressure and heat of 80 °C for 30 minutes. The lithiated Si anodes turned dark grey, and were washed with 1,2-Dimethoxyethane (DME) or carbonate

solvents for several time and dried under vacuum before test.

2.2.4 Cell Assembly

The cells were assembled in a glovebox filled with Ar. The G4 base electrolyte was preparing by dissolving 1 M lithium bis(trifluoromethane)sulfonimide salt (LiTFSI, Wako) in the G4 solvent. 50 mM DBBQ (Sigma-Aldrich) and 100 mM TDPA (Sigma-Aldrich) were added in the G4-based electrolyte to obtain the dual RMs G4-based electrolyte. The carbonate based electrolytes were prepared by dissolving 1 or 5 M LiTFSI salt in the ethylene carbonate and diethyl carbonate (EC/DEC with a volume ratio of 1:1). Typically, the normal type Li-ion O₂ cell was fabricated by stacking a Si anode lithiated in the G4 based electrolyte, a glassy fiber separator with a dual RM G4-based electrolyte and a KB cathode, successively. The hybrid Li-ion O₂ cell was fabricated by stacking a Si anode lithiated in the carbonate-based electrolyte, a Celgard separator with a carbonate based electrolyte, a Nafion@PTFE membrane, a glassy fiber separator with a dual RM G4 based electrolyte and a KB cathode, successively. The Li-ion O₂ cell with the Nafion separator and G4-based anode electrolyte was prepared in a similar process. In this case a Si anode lithiated in the G4-based electrolyte and a Celgard separator with the G4 based anode electrolyte were used. The prepared cells were sealed in a chamber (650 mL) and the chamber was purged with oxygen for 1 h continuously before test. The galvanostatic electrochemical tests were conducted on the system HJ1001SD8 (Hokuto Denko). In the cycling test, the specific areal capacity ratio of anode to cathode was controlled to be near 3.0 in all types of cells.

2.2.5 Cell Assembly

FT-IR measurements were conducted on an FT/IR-6200 spectrometer (JASCO Corp.). Dry KBr powders (kept under vacuum at 90 °C) were ground and pressed into a transparent pellet under vacuum with a pressure of 4.0 Mpa. The electrolyte samples from permeation tests were spread on the KBr pellet. The pellet was then quickly transferred into the IR chamber for measurement. The Raman spectra were collected

on a JASCO microscope spectrometer (NRS-1000DT). The samples were dropped on a Cu foil substrate for the test. Bruker D8 Advanced diffractometer fitted with $\text{CuK}\alpha$ X-rays ($\lambda = 1.5406 \text{ \AA}$) radiation was used for the X-ray diffraction (XRD) measurement. A home-made sample holder sealed by silicone glue with a Kapton film window was used for the test. The scanning electron microscopy (SEM) images were taken on a LEO GEMINI SUPRA 35 system. The X-ray photoelectron spectroscopy (XPS) spectrum was obtained on a PHI 5000 VersaProbe. The measured electrodes were extracted from the disassembled cell, washed with DME or carbonate solvents several times to remove the residual electrolytes, and dried in a vacuum chamber before characterization.

2.3 Results and Discussions

2.3.1 Lithiated Nafion Membrane for Hybrid Electrolyte Design

The PTFE microporous membrane-supported Li^+ -Nafion (Nafion@PTFE) membrane is prepared by drying the solution of lithiated Nafion into the microporous structure of PTFE membrane. The as prepared membrane has a thickness of near $50 \mu\text{m}$ (Figure 2.2a), with enough mechanical strength provided by the PTFE skeleton. Also,

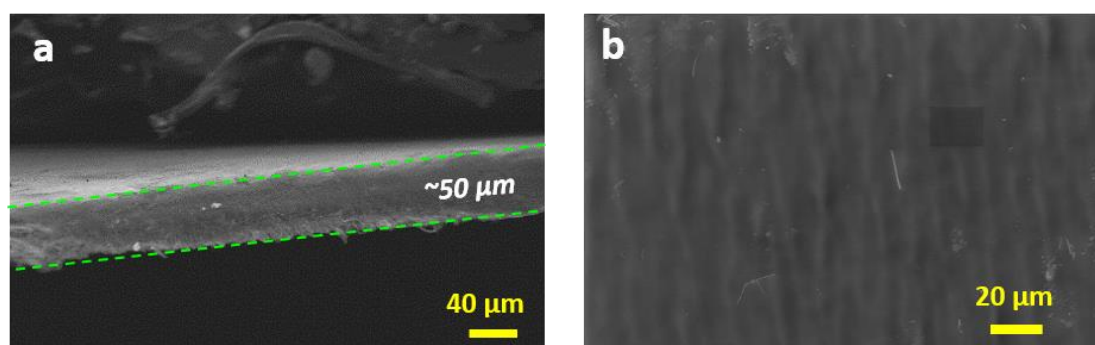


Figure 2.2 a) Cross-sectional SEM image and b) upside SEM image of the Nafion@PTFE membrane.

no cracks or holes can be observed from the surface of the membrane, indicating that the porous structure of PTFE is well filled with the lithiated Nafion. This shows the strong and dense property of the Nafion@PTFE membrane.

The FT-IR measurement is also conducted to investigate the ion form in the as prepared Nafion@PTFE membrane. We focus on the band at 1052 cm^{-1} , which is supposed to be the $-\text{SO}_3^-$ symmetric stretch in the H-form Nafion. Now, it shifts to a higher frequency, which representing the interaction between the lithium ion and the oxygen atom (Figure 2.3). This shows the result that the lithiation process of the Nafion@PTFE membrane is well completed, giving it the ability to work as a lithium ion conducting separator in the Li-ion O_2 battery.

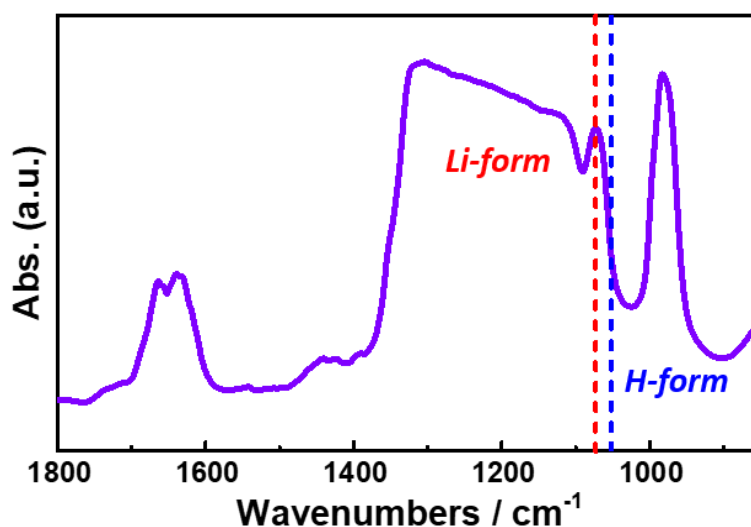


Figure 2.3 FT-IR spectrum of the Nafion@PTFE membrane

The ability of the Nafion@PTFE membrane to separate the two electrolyte systems is then confirmed through the permeation test. We set up a V-type device, in which the

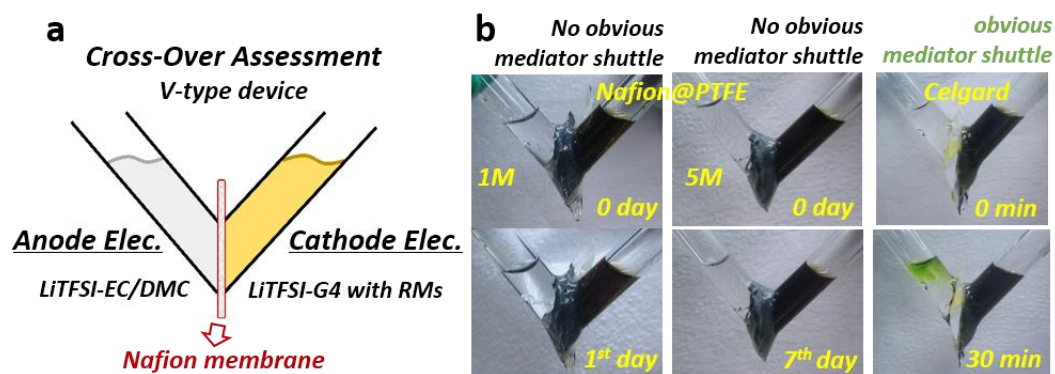


Figure 2.4 a) Schematic illustration of the permeation test. b) Images of the devices during permeation experiment.

Nafion@PTFE membrane is sandwiched between G4 based electrolyte and carbonate based electrolyte (Figure 2.4). Two kinds of RMs, the 2,5-di-tert-butyl-1,4-benzoquinone (DBBQ) as RM_R and tris[4-(diethylamino)phenyl]amine (TDPA) as RM_E , are also added in the G4 based electrolyte. DBBQ can increase the discharge capacity by promoting the formation of Li_2O_2 in a solution pathway. TDPA is reported to be a highly active RM_E with low working potential. For the anode electrolytes, two concentrations of 1M and 5M are tested respectively. As is shown in Figure 2.3b, after 1 day or 7 days, the anode electrolyte remains colorless no matter what the concentration is, confirming that no RMs in the cathode electrolyte transport the Nafion@PTFE membrane. This is in accordance with the reports that the Nafion membrane can hinder the RMs in the electrolyte.

FT-IR observation is used to trace the possible solvent permeation through the Nafion@PTFE membrane. As shown in Figure 2.5a, when the concentration of carbonate based electrolyte is 1 M, new peaks between 1750 and 1810 cm^{-1} are presented in the G4 based electrolyte after 1 day aging, which is ascribed to C=O stretching vibration of carbonate solvents.⁸⁴ This shows that the carbonate solvents of 1 M concentration transport through the Nafion@PTFE membrane to the cathode electrolyte side within 1 day. When the concentration of the anode electrolyte is increased to 5 M (Figure 2.5b), we observe no obvious permeation for both the G4

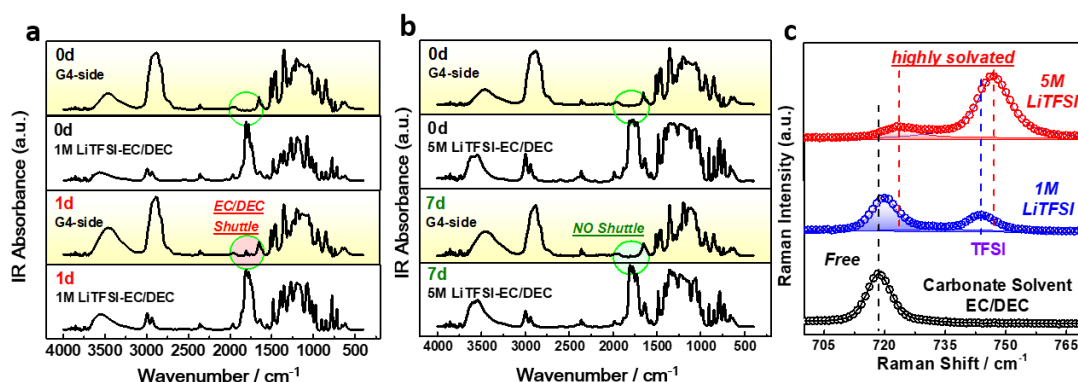


Figure 2.5 FT-IR spectrum of the permeation test. a) 1 M G4 with RMs vs 1 M EC/DEC and b) 1 M G4 with RMs vs 5 M EC/DEC. c) Raman spectrum of 1 M and 5 M LiTFSI-EC/DEC electrolytes with pure EC/DEC solvents.

based electrolyte and carbonate based electrolyte within 7 days. This indicates that the Nafion@PTFE membrane could well separate the G4 based electrolyte and a high concentration carbonate based electrolyte.

We conduct the Raman measurement on the carbonate based electrolytes to explain the reason. As is shown in Figure 2.5c, with the increase of the concentration from 1 to 5 M, the peak (blue) related to the free solvent disappears, while that for the solvated solvent (red) becomes dominated. Also, the TFSI⁻ anion band in the 740-745 cm⁻¹ region shifts to a higher wavenumber with increased concentration. Raman test results indicate that most solvents are associated with the ions and the part of free solvent turns greatly small in the high concentration carbonate based electrolyte. Consequently, the carbonate solvent in the 5 M carbonate based electrolyte is well restricted. With the combination of high concentration for the carbonate based electrolyte and effect of Nafion@PTFE membrane, the hybrid electrolyte design is thus successfully achieved.

Besides, when a normal Celgard separator is applied, RMs are observed to cross the separator within 30 minutes (Figure 2.6). The anode electrolyte begins to be colored only after 5 minutes. And within 20 hours, the anolyte turns dark green. This indicates that the Celgard separator isn't able to block the RMs crossover. The Ft-Ir spectrum

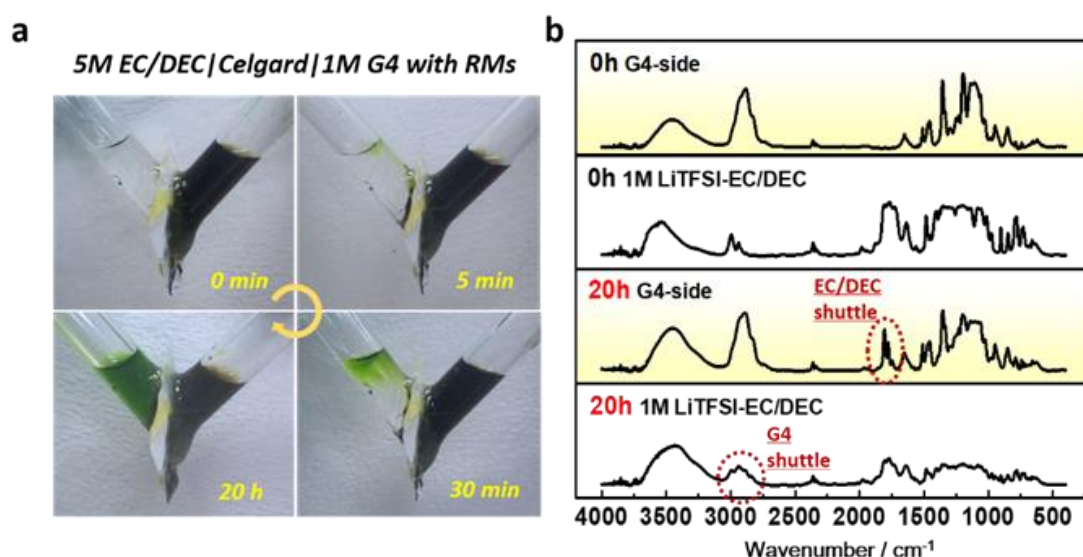


Figure 2.6 a) the images of permeation test: 5M carbonate based anode electrolyte | Celgard separator|1M G4 cathode electrolyte with RMs. b) FT-IR spectrum of electrolytes extracted during the permeation experiment within certain times.

also shows strong peaks representing for carbonate solvents at the cathode electrolyte side after 20 hours aging. Meanwhile, new peaks at 2886 cm^{-1} and 2823 cm^{-1} , which are ascribed to the G4 solvent, are observed in the anode electrolyte side. These results indicate that the crossover of the different solvents cannot be avoided solely by increasing the concentration of anolyte. These results emphasize the combination effect of Nafion@PTFE membrane and high concentration anode electrolyte to work as a RM blocker.

2.3.2 Fabrication of Silicon Alloy Anode Based Lithium Ion Oxygen Battery

After the confirmation of the Nafion@PTFE membrane for the separation of two electrolytes, we propose a Si anode based Li-ion O_2 battery with the hybrid electrolyte design (Figure 2.7). In the G4 cathode electrolyte, RMs of DBBQ and TDPA are applied to promote both ORR and OER processes on a KB porous cathode.^{47, 85} In the anode electrolyte, carbonate species would help build a strong SEI for the Si anode to function

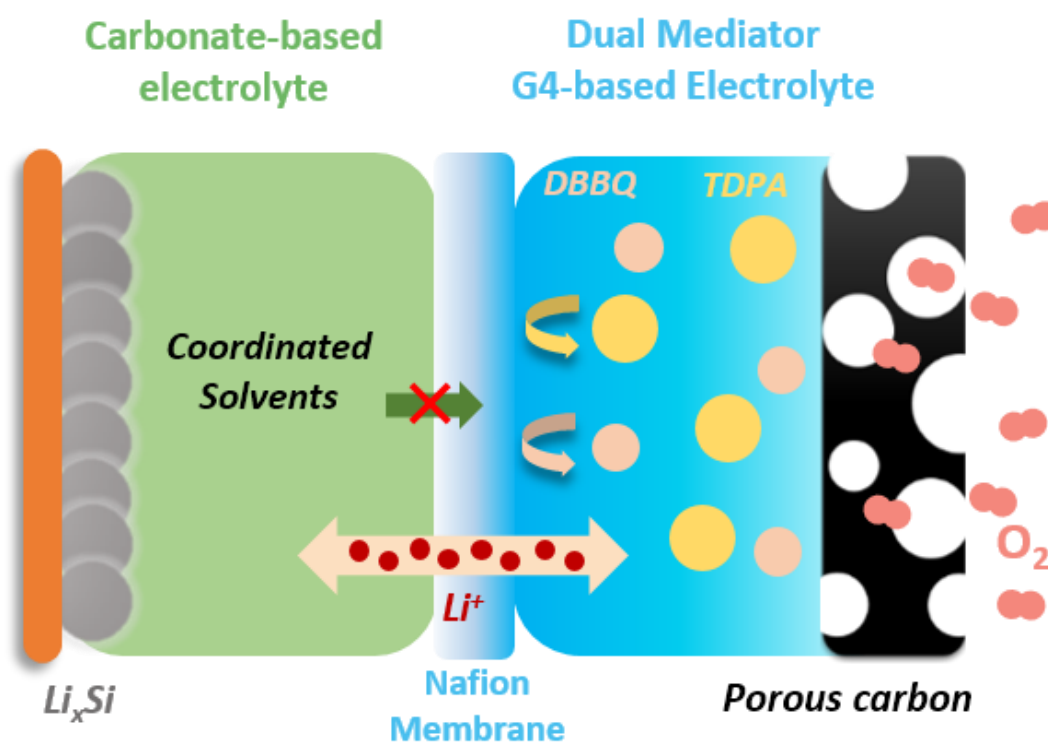


Figure 2.7 Proposed structure of hybrid electrolyte design Li-ion O_2 battery, achieved by a Nafion@PTFE membrane, with dual RMs in the cathode electrolyte and the high concentration carbonate based anode electrolyte.

stably. The Nafion@PTFE membrane is bridging the two electrolytes in the middle, conducting lithium ions and blocking the crosstalk between the cathode and anode electrolytes.

Then we fabricate a Si anode based Li-ion O₂ battery with the hybrid electrolyte design. Before the assembly of the full cell, the Si anodes are firstly lithiated by a direct contact method before assembling. As is shown in Figure 2.8, Both Si anodes chemically lithiated in carbonate based or G4 based electrolytes have a composition of Li_{3.75}Si, as their XRD patterns are in accordance with the standard patterns of Li_{3.75}Si. And both anodes lithiated in different electrolytes delivers a first cycle charge capacity of ~3200 mAh·g⁻¹, indicating the lithium source pre-stored into the Si anodes are electrochemically reactive, making them possible as the anode materials for the Li-ion O₂ battery.

The voltage profile of the first cycle deep test is presented in Figure 2.9. The discharge specific capacity of Li-ion O₂ battery with the hybrid electrolyte design is

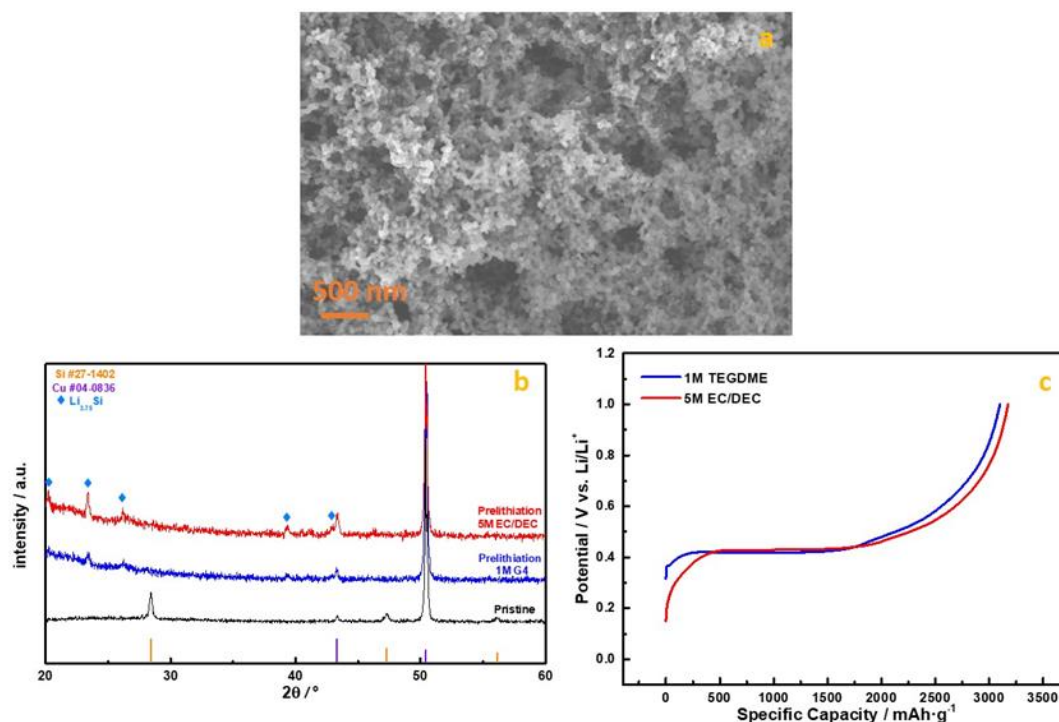


Figure 2.8 a) SEM images of the pristine Si anode. b) XRD patterns of pristine Si anode (black), Li-Si anode lithiated in 5M EC/DEC (red) and 1M G4 (blue). (c) The delithiation capacity of Li-Si anode in 5M EC/DEC (red) electrolyte and 1M G4 (blue) electrolyte.

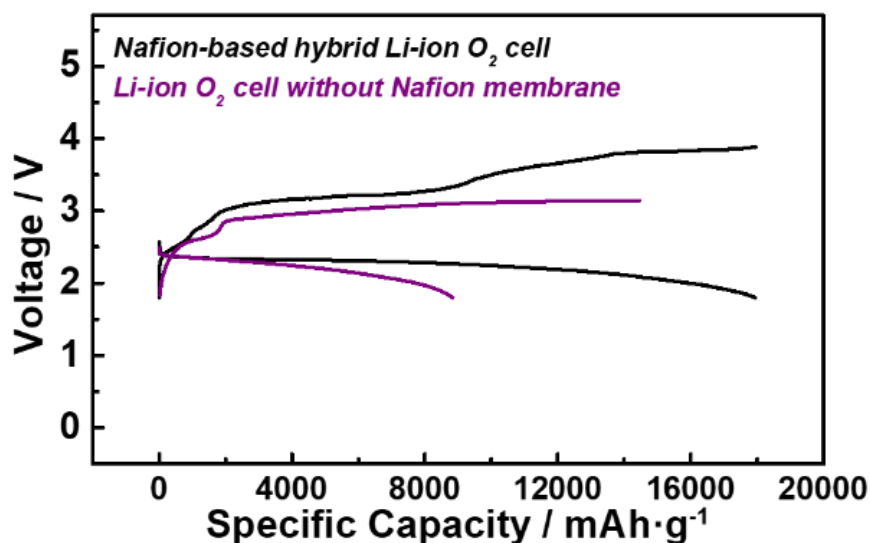


Figure 2.9 Electrochemical profile of hybrid electrolyte design Li-ion O₂ battery and normal type Li-ion O₂ battery at a current of 200 mA·g⁻¹

about 18000 mAh·g⁻¹ with a voltage plateau of near 2.3 V, which is largely increased compared with the normal type battery without the Nafion@PTFE membrane. This is a result from the blocking effect of the Nafion@PTFE membrane to DBBQ, which would crossover to the anode side and bring about side reactions in the normal type battery. During the OER process, the charge potential is reduced to about 3.3 V. The total discharge capacity is fully recharged, indicating the good reversibility of the hybrid electrolyte battery.

2.3.3 Characterization on Oxygen Cathode during Discharge/Charge

The electrochemistry at the cathode side under the effect of the dual RMs in the cathode electrolyte is confirmed through ex-situ characterizations. Figure 2.10 displays the XRD patterns of the KB cathodes in the pristine, discharged and charged states respectively. The peaks at about 33 °, 35 ° and 58 ° in the spectrum of discharged cathodes are corresponding to the crystal facets (100), (101) and (110) of Li₂O₂ respectively. This indicates the presence of Li₂O₂ as the main discharge product with the help of RM_R DBBQ. After the battery recharging, the XRD patterns of the KB

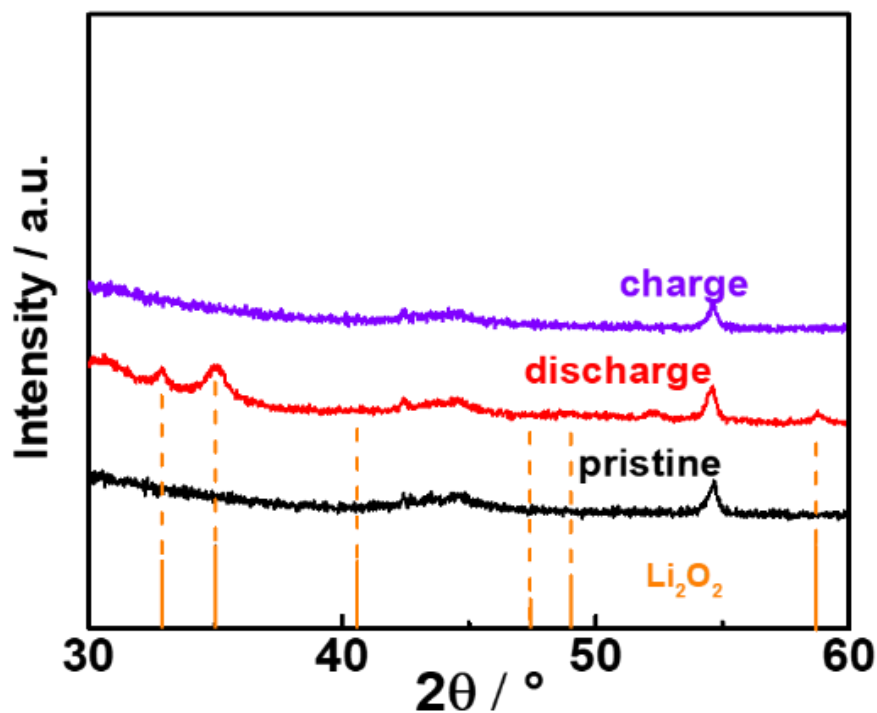


Figure 2.10 XRD patterns of the cathodes at different states.

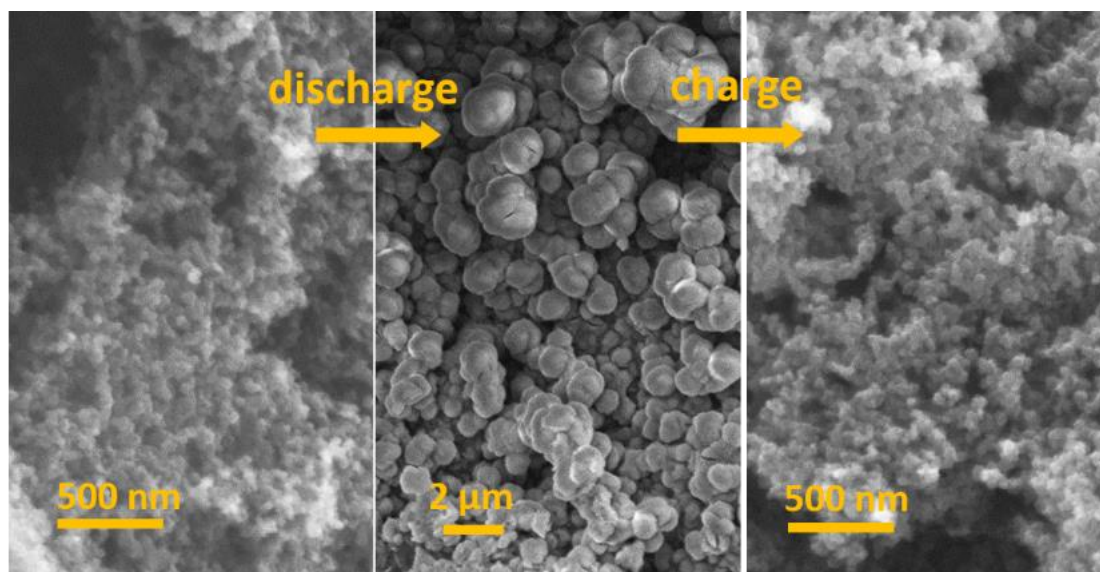


Figure 2.11 SEM images of the cathodes at different states.

cathode returns to that of the pristine cathode, indicating the decomposition of Li_2O_2 under the effect of RM_E TDPA.

To further confirm the discharge product behavior at the KB cathode, SEM measurement is conducted to observe the cathodes in different states. As is displayed in Figure 2.11, the cathode after discharging is largely occupied by particles with a

diameter of several hundred nanometers. After recharging these particles disappear, and the morphology of the charged cathode reverts back to that of the pristine cathode. These results correspond to the previous XRD results, showing that the oxygen electrochemistry at the cathode is based on the reversible formation and decomposition of Li_2O_2 under the effect of dual RMs.

2.3.4 Cycling Performances of Oxygen Batteries with Different Configurations

To investigate the improvement of cycling stability that brought by the hybrid electrolyte design, Si based Li-ion O_2 cells with three types of battery structure are fabricated and cycled at the same condition of a fixed capacity of $2500 \text{ mAh}\cdot\text{g}^{-1}$ and a current density of $1000 \text{ mA}\cdot\text{g}^{-1}$. The areal capacity ratio of anode to cathode is fixed at about 3.0, and dual RMs are added to promote the cathode electrochemistry in all cases. In the normal type battery (Figure 2.12a), the charge potential is controlled at a very low level, thanks to the effect of RM_E , TDPA. However, the battery quickly fails after only 8 cycles, showing a poor cycling stability which is the case when Si anode is directly used in replace of lithium metal in the Li O_2 battery. This is due to the Si anode

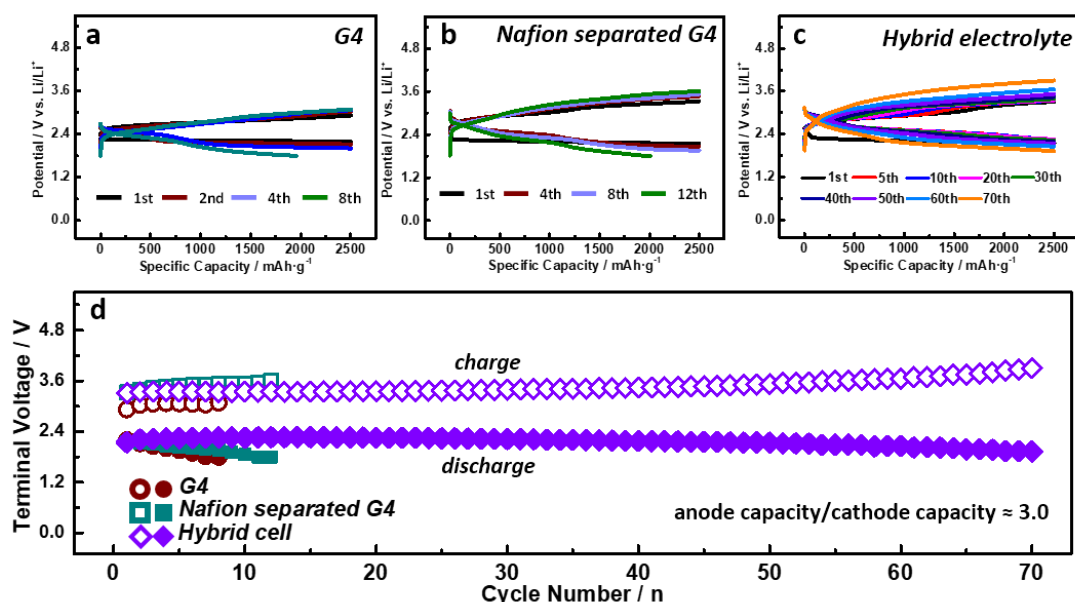


Figure 2.12 Electrochemical performance of Li-ion O_2 batteries with a) G4 based electrolyte, b) Nafion separated G4-based electrolyte, and c) hybrid electrolyte design. d) Terminal voltages of different cells with cycles.

that suffers from both the RMs crossover and poor SEI in a G4 based electrolyte. Therefore, the limited lithium source is quickly consumed. When the Nafion@PTFE membrane is employed to block the mediators, the cycle number is slightly improved to 12 cycles (Figure 2.12b). This shows that although the Si anode could be protected from the RMs during cycling, its benefit to the cycling stability is quite little. The SEI seems to play a more important role for the stable function of Si anode, and as it's still formed in a G4 based electrolyte, the poor SEI on the Si anode finally fails to support durable cycling of the battery. The hybrid electrolyte design finally brings a significant improvement to this system (Figure 2.12 c,d). The cycle number is largely increased up to 70 cycles, with the charge terminal voltages remained below 3.6 V and discharge terminal voltages staying above 2.0 V for over 50 cycles. This can be ascribed to two aspects. On the one hand, the dual RMs in the cathode electrolyte well control the charge overpotential even at a high reversible specific capacity. On the other hand, the carbonate based anode electrolyte helps build a strong and durable SEI for the Si anodes. As a result, the degradation of the Li source in the Si anode is thus well reduced, making the Si anode more durable in the Li-ion O₂ battery.

2.3.5 Characterizations on Silicon Anodes after Cycling

Si anodes in G4 and carbonate based electrolytes after cycling are then investigated. We hope to find the reasons lying under the stability difference of Si anodes in these two electrolytes. We firstly conduct SEM measurement to observe the morphology evolution of the Si anodes before and after electrochemical tests. As is shown in Figure 2.13, Si particles lithiated respectively in the electrolytes of G4 based and carbonate based display uniform particle size with diameters about 100 nm. The lithiated Si particles expand compared with the pristine silicon crystalline state, indicating that the Si anodes are successfully lithiated in the direct contact method. After cycling, Si particles in the G4 based anode electrolyte are observed embedding in thick and disorganized layers. This is in total difference with the morphology of Si anode in the carbonate based anode electrolyte. We observe a uniform layer covering the Si particles

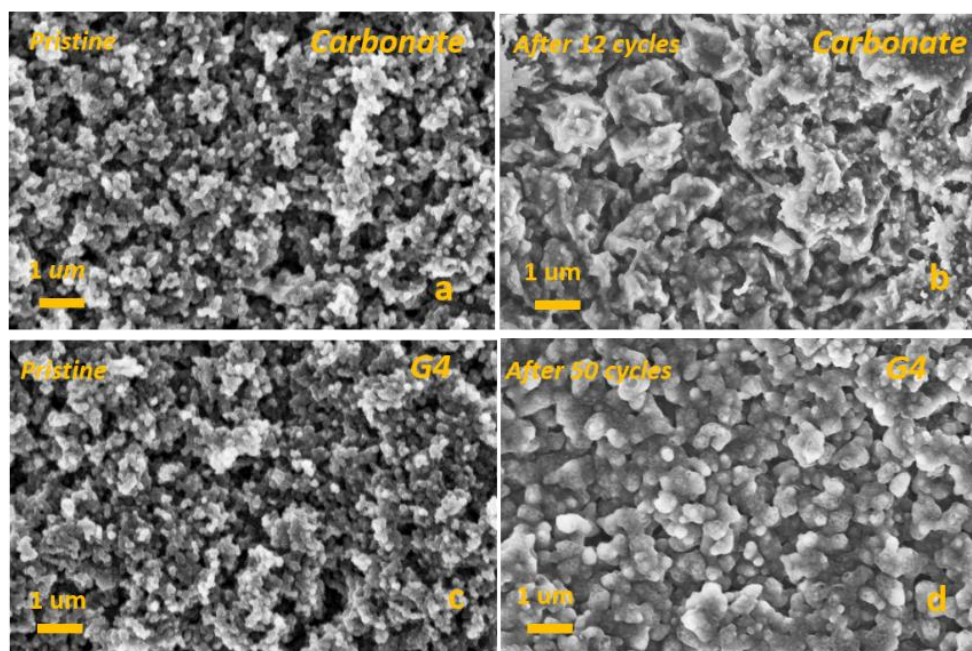


Figure 2.13 SEM images of lithiated Si anodes a) before and b) after 12 cycles in the Nafion-separated G4-based electrolyte. SEM images of lithiated Si anodes before c) and after d) 50 cycles in the hybrid electrolyte Li-ion O₂ cells.

after 50 cycles. These observations indicate the severe side reactions on the Si anodes in the G4 based electrolyte, which is thought to result in the continuous growth of the brittle and weak SEI. On the contrary, the strong and uniform SEI retard the ceaseless reaction between the electrolyte and the anode for the Si anodes in the carbonate based electrolyte, bringing in the largely improved cycling durability.

Then, XPS measurement is further carried out to characterize the composition of the observed SEI on the Si anodes (Figure 2.14). In the C 1s spectrum, the peaks between 286.0 and 288.0 eV can be attributed to the etheral and alkoxy carbon, and the peaks between 289.0 and 291.0 eV can be attributed to the carbonate species.⁸⁶ From the spectrum of Si anode cycled in the G4 based electrolyte, the etheral and the alkoxy species could be told to be dominant, which can be ascribed to the decomposition products of G4 solvent. From the SEI of the carbonate based electrolyte, carbonate species (Li₂CO₃, ROCO₂Li) are found to domain the major composition. In the F 1s spectrum, LiF is presented in the SEI composition of the carbonated based electrolyte while absent in that of the G4 based electrolyte. It's well known that Li₂CO₃ is a good

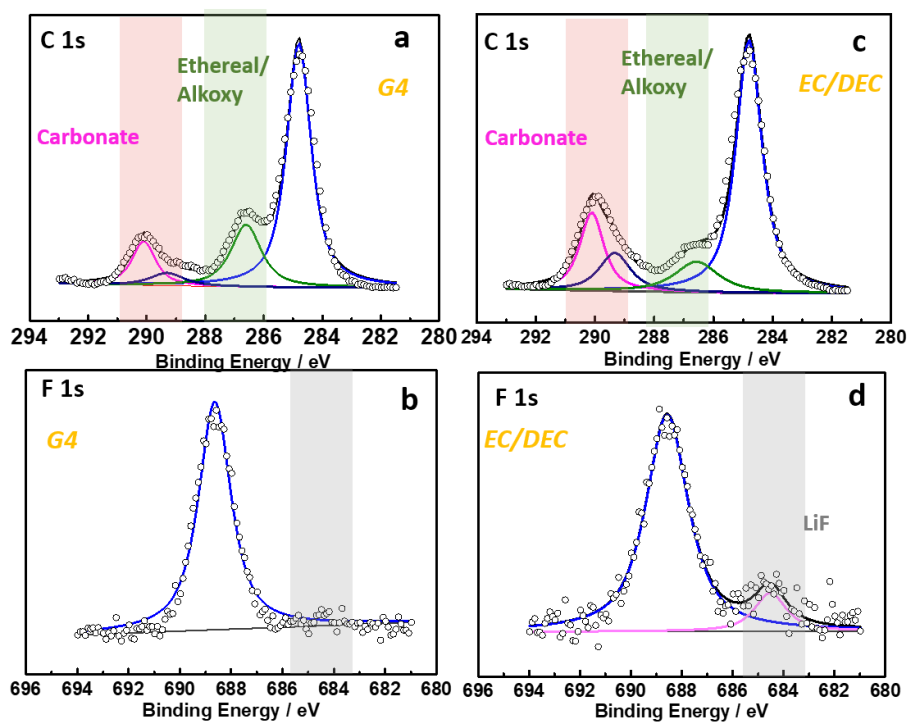


Figure 2.14 a,c) C 1s spectrum and (b, d) F 1s spectrum of Si anodes in the Nafion separated G4-based cell and the hybrid electrolyte design cell after cycling.

passivating agent due to its non-hygroscopic property and stability for the surface films of the anode. And the presence of insoluble and stable LiF may also help build a stable SEI.⁸⁷ The different compositions of SEI formed in the different electrolytes lead to different physical and chemical properties. As a result, the uniform and strong SEI in the carbonate based anode electrolyte keeps the Si particles well from continuous parasitic reaction with the electrolyte. In contrary, the ceaseless consumption of stored lithium because of the brittle and weak SEI soon fails the Li-ion O₂ battery with the Si anode in a G4 based anode electrolyte.

By now, we could say the benefits of the hybrid electrolyte design for the Si based Li-ion O₂ battery are well explored. For the cathode, the improved reversible capacity and reduced charge overpotential are achieved on the normal KB porous cathode with the help of dual RMs in the relatively stable G4 based electrolyte. For the Si anode, the carbonate based anode electrolyte promotes the formation of a strong and durable SEI, ensuring the high reversibility of limited Li sources in the Si anode. More importantly, the two electrolyte systems are well separated by the Nafion@PTFE membrane. Firstly,

the stable function time of the dual mediators is largely extended by hindering their migration to the anode side. Secondly, the different solvents are restrained in their own sides, getting rid of the unwanted electrolyte decomposition as mentioned in Scheme 2.1. Therefore, the Si based Li-ion O₂ battery with the hybrid electrolyte design exhibits long-term cycling stability with an improved energy density and reversibility.

2.4 Conclusions

To sum up, we successfully fabricate a Li-ion O₂ battery with a hybrid electrolyte design, in which the dual RMs G4 based electrolyte for the oxygen cathode and the carbonate based electrolyte for the Si anode are combined. The Nafion@PTFE membrane is prepared to bridge the two electrolytes, conducting the lithium ions while in the same time blocking the crossover of RMs and electrolyte solvents. The application of high concentration carbonate based electrolyte helps restrain the carbonate solvents thanks to the strong association between the solvent molecule and ions. Consequently, the hybrid electrolyte design Li-ion O₂ battery exhibits a high reversible capacity of near 18 000 mAh·g⁻¹ with low overpotential and long-term cycling stability (tested at a specific capacity of 2500 mAh·g⁻¹ with the anode/cathode areal capacity ratio of near 3.0, 70 cycles). The carbonate based anode electrolyte helps in the buildup of the strong SEI for Si anodes. Taking advantage of two separate systems for a better overall performance, we believe that this strategy would open up new gate for battery systems like and beyond the Li-ion O₂ battery.

Chapter 3. Hybrid Electrolyte Design for Organic Liquid Anode based Oxygen Battery

3.1 Introduction

The booming attention has been paid to the electric vehicles (EVs), considered a promising answer to the concerns for energy shortage and environmental issues growing stronger and stronger with the development of human society.⁸⁸⁻⁸⁹ Secondary battery systems with higher energy density are urgently required so as to avoid the so-called “range anxiety” feeling for the EV drivers, which is the one of the main obstacles that stop EVs from being accepted universally. Candidates to replace the state-of-the-art lithium ion batteries, aiming at providing larger energy density for better application of large electric devices like EVs, are proposed one after another in recent research booms in the energy storage devices.⁹⁰ Among them, lithium oxygen (Li-O₂) batteries stand out for the potential that they could achieve a theoretical energy density comparable to the tank-to-wheel value achieved by gasoline.¹¹ This benefits from the combination usage of oxygen from the ambient atmosphere and Li metal as the anode active material. The model anode reaction for Li-O₂ batteries are based on the highly reversible stripping/plating of the lithium metal. However, the large volume change and high reactivity of lithium metal always lead to the low lithium utilization rate. And the dendrite growth, which is resulted from the inhomogeneous distribution of current density on lithium metal surface and lithium ion in SEI, would sometimes bring about circuit shortage phenomenon.⁹¹⁻⁹² With the worry of growing into a severe hazard, this problem should be specially taken care of when the battery system is supposed to be used on devices like EVs which are related to human being’s life.

At the cathode side, the ideal electrochemistry based on reversible formation and decomposition of Li₂O₂ is always challenged by the solid-solid contact mode between the discharge product and the carbon cathode, which leads to sluggish reaction kinetics and parasitic reactions, and is responsible for the high overpotential and poor durability

of Li-O₂ batteries.⁹³ The addition of redox mediators (RMs) in the electrolyte is one of the effective strategies proposed to address the high overpotential and parasitic reaction problems. However, RMs in the electrolyte are free to diffuse, and their reactive states could move to the anode side and react with the anode material, which leads to the so-called “crossover effect” that the efficiency and durability of the battery would thus being affected. The successful application of RMs should be accompanied with the restraint of the RMs.⁹⁴⁻⁹⁵

For the lithium metal, though various strategies have been come up with, the related problems are still not fully addressed. There are several trials searching for alternative anodes for Li metal in Li-O₂ batteries. In chapter 2, we focus on the cycling stability of Si anode, one of the promising candidate for the lithium based anode with high specific capacity, and achieve to increase it by introducing the hybrid electrolyte design. However, for alloy type anode materials like Si, there are still two problems remained challenging. Firstly, the lithiated state of these materials is very reactive.^{77, 96} The direct exposure of Li-Si alloy powders to the ambient air could result in the sparks and fire. These would raise the concerning for the alloy type anode in the Li-O₂ batteries with a half open battery structure. Secondly, the rate performance of the alloy based anode is not so outstanding, due to the poor electric and ionic conductivity of the alloy anode. And strategy to overcome this like reducing the size of alloy particles,⁹⁷⁻⁹⁸ would further increase its reactivity and thus exacerbate safety problems. This would limit the power performance of EVs that would potentially load the battery system.

A kind of organic liquid is recently considered a new candidate for the high performance anode materials. It is obtained by the reaction of alkali metals with some aromatic hydrocarbons in an ether solution, and is commonly used as strong reducing agents in the field of organic synthesis.⁹⁹ Yu et al. firstly report its application in the secondary battery system.¹⁰⁰ A biphenyl-Na based organic liquid was introduced to a sulphur cathode and exhibited extremely stable cycling performance. Soon after that, Liang et al. extended the application of biphenyl-Na liquid into an oxygen battery and also obtained remarkable results.¹⁰¹ Very recently, Cong et.al reported a high rate and long life organic oxygen battery built with a biphenyl-K liquid anode.¹⁰² All these

impressive results show the potential of the alkali-biphenyl based organic liquid as a promising anode material for the energy storage system, marking their safety property and excellent conductivity. However, in spite of the advantages and potential mentioned above, the report of its application for the Li based battery is still very few.¹⁰³ One of the reasons for this could be its liquid property, which might bring about difficulty in the test.

Herein, we aim at introducing the Li based organic liquid anode with both electric and ionic conductivity, low working potential and high safety, to the oxygen cathode to build an organic oxygen battery. A hybrid electrolyte design is naturally associated, as the flowable organic liquid anode should be divided and restrained to ensure its basic function. We propose a metal organic frameworks (MOFs) based membrane to separate the liquid anode from the cathode system, which in the same time could stop the crossover of RMs in the cathode electrolyte. As a result, the fabricated organic oxygen battery shows a long durability with narrow overpotential window at several high cycling rates. Moreover, the solid electrolyte interface (SEI) like layer between the liquid anode and separator is firstly investigated, which we believe significant for the stable function of the organic liquid based battery system.

3.2 Experimental Section

3.2.1 Preparation of biphenyl-Li complex (Bp-Li) liquid anode

Biphenyl (Sigma-Aldrich) was dissolved into the 1,2-Dimethoxyethane (DME) firstly. The concentration of biphenyl is controlled to be 1.0 M or 2.0 M respectively. After dissolution, pieces of equivalent mole of Li metal were dissolved into the biphenyl-DME solution. The solution was then shaken vigorously to obtain the Bp-Li DME solution. Note that PTFE magnetic stirrer should be avoided because the Bp-Li DME solution is reactive to PTFE. The prepared solution is then stored in the glovebox and used as Bp-Li liquid anode.

3.2.2 Preparation of zeolitic imidazolate frameworks (ZIF7) particles

The preparation of ZIF7 particles were based on a previous report.¹⁰⁴ In a typical process, 0.53 g zinc acetate (TCI) and 1.18 g benzimidazole (Sigma-Aldrich) were added into 300 mL ultrapure de-ionized (DI) water (Millipore) and treated with sonication and stirring for 3 hours. The suspension was then centrifuged to get the precipitate, which was washed for several times with DI water and vacuum dried at 80 °C for several hours. Finally, the precipitate was activated by further heat treatment under vacuum at 180 °C for 72 hours to get the activated ZIF7 particles.

3.2.3 Water reaction test

Several drops of water were dropped into the prepared Bp-Li liquid anode directly. And the reaction process was recorded in digital images at different time to tell the severity of the reaction.

3.2.4 Preparation of ZIF7 membrane

In a typical procedure, 100 mg of ZIF7 powders were distributed into 5 mL acetone (Wako) uniformly by sonification for 30 minutes. Then, 50 mg of binder was dissolved into 2 mL dimethylformamide (DMF, TCI). After totally dissolved, the binder solution was transferred into the ZIF7 solution. Two kinds of binders are chosen to fabricate the membrane: poly(vinylidene fluoride-co-hexafluoropropylene) (PVDF-HFP, Sigma-Aldrich) and polyvinylidene difluoride (PVDF). The mixture was then sonicated for another 30 minutes, and heated at 100 °C to remove the acetone, and finally casted onto a glass plate. After being dried at 70 °C for several hours, the ZIF7 membrane was removed from the plate with the help of methanol, dried under vacuum and cut into pellets with a diameter of 16 mm. The ZIF7 membrane pellets were kept in air dry oven before further fabrication.

3.2.5 Permeation test

Similar to the permeation test in chapter 2, a home-made V type device was fabricated to conduct the permeation experiment. The base electrolyte for the O₂ cathode was added into the glass tube on one side. And the Bp-Li liquid anode was added into the glass tube on the other side. The base electrolyte is prepared by dissolving 1.0 M of Lithium bis(trifluoromethanesulfonyl)imide (LiTFSI, Sigma-Aldrich) into tetraethylene glycol dimethyl ether (G4, Sigma-Aldrich). The ZIF7 membrane was sandwiched in the middle of two tubes to be examined the ability of separate two electrolytes. The electrolyte on G4 side was extracted 30 μ l after a certain period for the FT-IR experiment. In the meanwhile, digital photos were taken to trace the possible transport of the Bp-Li liquid anode.

3.2.6 Conductivity measurements

The total conductivity of the Bp-Li liquid anode was measured by electrochemical impedance spectrum (EIS) on Solartron analyzer (SI 1260). The conductance cell was made by setting a tube tightly sandwiched by two copper sheets, which works as two current collectors. The cell constant was then confirmed to be 11.65 through a KCl standard solution at 25 °C with a concentration of 0.01 M. Bp-Li liquid anode of 1.0 M and 2.0 M was added in to the cell to fill the tube respectively and EIS measurement was then conducted. The total conductivity was calculated by the read resistance from the EIS data. To measure the electronic conductivity, several constant potential (1.0 ~ 5.0 V) was applied to the cell respectively. At each potential the current value was recorded when the current value finally reached stable. By fitting the current-potential points into a line, the electronic resistance could be calculated and then the electronic conductivity was also obtained.

3.2.7 Cathode preparation

The Ketjenblack (KB, EC600JD, Lion Co. Ltd.) cathodes were made by rolling the mixture paste of KB and polytetrafluoroethylene (PTFE, suspension, 14%) into a sheet at a weight ratio of 85:15. Then the sheet was removed from the plate, dried, and cut into pellets with a diameter of 7 mm. Then the pellets were pressed onto the hydrophobic carbon paper which served as the current collector. The mass loading of the cathode is 0.10~1.0 mg·cm⁻². All the cathode pellets were kept under vacuum at 90 °C before further fabrication.

3.2.8 Cell assembly

A home-made cell was designed and made to conduct the galvanostatic test of the Bp-Li liquid anode. As displayed in Figure 3.1, the main parts of the test device are described below: the Bp-Li liquid anode was stored in a vertical tube. One side of the tube was covered with the ZIF7 membrane, sealed by the liquid gasket (Type 1119, Threebond). The glass fiber saturated with 1.0 M LiTFSI-G4 electrolyte, KB cathode and cathode current collector were stacked successively at the other side of the ZIF7 membrane. The current collector was chosen to be stainless mess to allow the oxygen pass through. Like in chapter 2, dual RMs (2,5-di-tert-butyl-1,4-benzoquinone, DBBQ, for discharging process and tris[4-(diethylamino)phenyl]amine, TDPA for charging process) are added into the G4 electrolyte to improve the performance of the oxygen

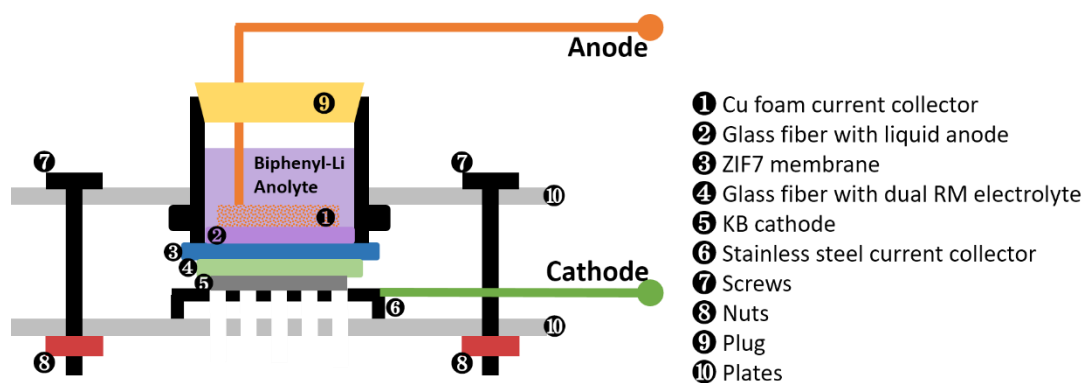


Figure 3.1 Schematic illustration of the cell structure for the electrochemical test of the Bp-Li liquid anode

cathode. The concentration is 50 mM for DBBQ, and 100 mM for TDPA. In the case of Bp-Li liquid anode half-cell with a lithium metal counter electrode, the KB cathode was replaced with Li metal electrode pressed on the stainless steel current collector. To avoid the volatilization of the DME solvent in the liquid anode, the other side of the tube was sealed with a plug. Cu foam was used as the current collector for the liquid anode, and a glassfiber was used to avoid the direct contact between the Cu foam and the ZIF7 membrane. The whole stacks were fixed between two plates with screws and nuts. The fabricated device was then transferred into a chamber (650 mL) and the chamber was continuously purged with oxygen for 1 h before electrochemical test. For the electrochemical tests with Li metal anode, the 2032-type coin cells with holes on the cathode side were used. The cell fabrication is the same with the normal type LiO₂ battery in chapter 2.

3.2.9 Electrochemical measurements

The galvanostatic electrochemical measurements were carried out on the battery tester system HJ1001SD8 (Hokuto Denko). In order to ensure enough electrolyte saturation, the organic oxygen cells were rested for 2 h before test. The cells were charged and discharged at a specific capacity of 2000 mAh·g⁻¹ and a series of current densities from 0.2 A·g⁻¹ to 4.0 A·g⁻¹ calculated by the cathode loading.

3.2.10 Characterizations

Fourier-transform infrared (FT-IR) measurements were carried out on a FT/IR-6200 spectrometer (JASCO Corp.). Grounded dry KBr powders (kept under vacuum at 90 °C) were pressed into a transparent pellet under vacuum with a pressure of 4.0 Mpa. The electrolyte samples extracted from permeation experiments were uniformly spread on the KBr pellet. The pellet with electrolyte sample was then quickly transferred into the IR chamber for the test. For the ex-situ characterization, cells after tests were disassembled in the Ar glove box. The KB cathodes were extracted and washed with DME for several times, followed by vacuum drying at room temperature for a certain

time before various characterization. The ZIF7 membrane was also extracted from the tube carefully, washed with DME for several times and dried under vacuum. The X-ray photoelectron spectroscopy (XPS) spectrum was obtained through a PHI 5000 VersaProbe. The X-ray diffraction (XRD) patterns was collected on a Bruker D8 Advanced diffractometer fitted with Cu-K α X-rays ($\lambda = 1.5406 \text{ \AA}$) radiation. A home-made cell sealed with a Kapton film window by silicone glue was used for test to avoid the affect of ambient air. The Raman spectra was collected on a JASCO microscope spectrometer (NRS-1000DT). A gas-tight sample holder was used for the test. The scanning electron microscopy (SEM) images were obtained on a LEO Gemini Supra 35 system.

3.3 Results and Discussions

3.3.1 Biphenyl based Organic Liquid

The lithium based organic liquid anode is prepared by dissolving the equal molar ratio of Li metal into the biphenyl solution in DME. After the Li metal dissolves, the

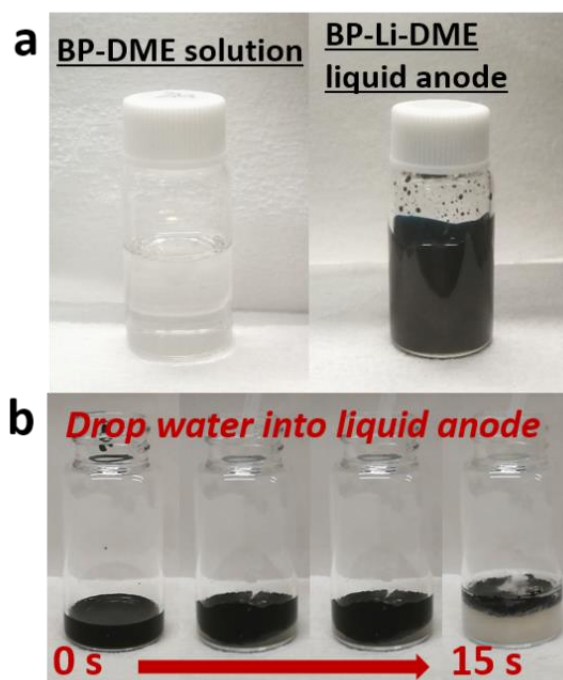


Figure 3.2 Properties of the Bp-Li liquid anode. a) Preparation of the Bp-Li liquid anode. b) Reaction of Bp-Li anode with water.

solution turns into a dark blue color (Figure 3.2a). This shows the uptake of electron from lithium atom to the biphenyl molecular and the formation of biphenyl Li complex (denoted as Bp-Li). A main worry for the anode materials is their high reactivity due to the low potential, which might result in potential safety hazard. This should be especially taken care of in the oxygen cathode battery system, where the battery structure is half open. The species from the outer atmosphere, like H₂O, could react with the lithiated anode material drastically and lead to severe accident. We explore the reactivity of Bp-Li anode by dropping H₂O into it (Figure 3.2b). As the drops of H₂O fall into Bp-Li anode, the solution turns white and cloudy, and no obvious explosion or fire is observed. The total process is milder compared with the reaction between lithium metal and hydrogen. Moreover, no bubbles are present during the reaction, indicating that the generation of hydrogen gas is avoided. This is very important to keep the battery system in a safe level. These results make the Bp-Li anode a safe candidate for the Li based battery anode.

As a liquid anode, the conductivity of Bp-Li anode would have great influence on the battery performance. We have much expect on the conductivity of this liquid anode

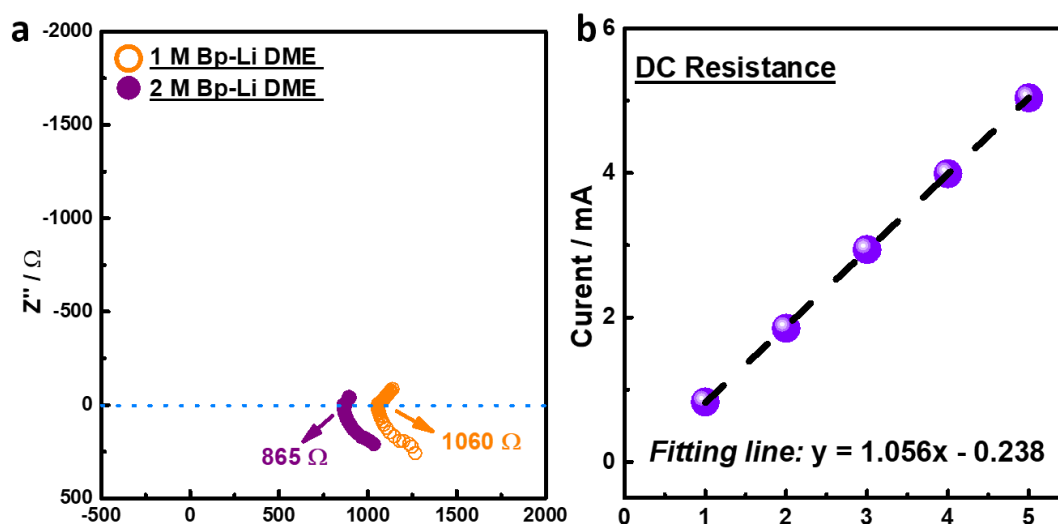


Figure 3.3 a) Measurements of conductivity of Bp-Li liquid anode through EIS methods. The calculated total conductivity $1.11 \times 10^{-2} \text{ S}\cdot\text{cm}^{-1}$ for 1 M Bp-Li liquid anode, and $1.36 \times 10^{-2} \text{ S}\cdot\text{cm}^{-1}$ for the 2 M Bp-Li liquid anode. b) Potential-current plots obtained from voltmeter ammeter method. The electrical conductivity of 2M Bp-Li anode is calculated as $1.24 \times 10^{-2} \text{ S}\cdot\text{cm}^{-1}$.

due to the previous results of its analogue. To start with, we measure the conductivity of Bp-Li anode with lithium concentrations of 1 M and 2 M, respectively. The EIS result of the each solution is displayed in Figure 3.3a. We can obtain the resistance of the measured solution in the test device when the imaginary part of impedance is zero. The observed resistance of the solution reads 1060 Ω and 865 Ω respectively for the anode with concentrations of 1 M and 2 M. The total conductivity is thus calculated to be $1.11 \times 10^{-2} \text{ S} \cdot \text{cm}^{-1}$ for the 1 M Bp-Li and $1.36 \times 10^{-2} \text{ S} \cdot \text{cm}^{-1}$ for the 2 M Bp-Li. In terms of the electronic conductivity, it's considered an interesting phenomenon for these solution ever since the first discovery in 1930s.¹⁰⁵ The DC conductivity of the 2 M Bp-Li anode is further measured through a voltmeter ammeter method. We successively apply DC voltages between the Bp-Li anode sandwiched by two copper current collectors. The current values are collected and we record the current value at each voltage when it reach stable. Then we get a graph of voltage-current plots as Figure 3.3b. The electrical conductivity of 2 M Bp-Li anode could be calculated as $1.24 \times 10^{-2} \text{ S} \cdot \text{cm}^{-1}$ according to the fitting line of the plots. These values are close to the conductivity reported for biphenyl Na complex in DME solution,¹⁰⁰ which also proves the feasibility of Bp-Li anode as a promising candidate for the Li based anode.

3.3.2 Metal Organic Frameworks based Membrane for Hybrid Electrolyte Design

As displayed in Figure 3.4a, we propose a MOFs-based membrane to replace the normally used $\beta\text{-Al}_2\text{O}_3$ SSEs to block the biphenyl-alkali liquid anode. The MOFs-based membranes recently rise as a potential ionic sieves for the rechargeable batteries because of their plentiful cavity construction and tunable pore sizes.¹⁰⁶ Wang et al. reported a MOFs-based solid state battery, with the ionic liquid electrolyte confined in the MOFs to provide improved interface stability.¹⁰⁷ Yuan et al. reported a MOFs-based separator with single ion conductivity and compatibility in various battery systems.⁵⁶ In this chapter, a kind of zeolitic imidazolate frameworks (denoted as ZIF7), which is a sub-family of MOFs, is considered as the material for separator membrane for its good thermal and chemical stability.¹⁰⁸ We hope it play a role in three aspects. Firstly,

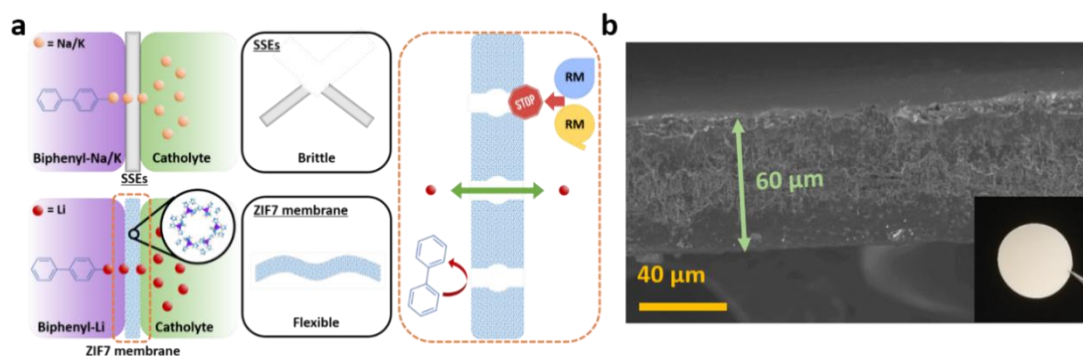


Figure 3.4 a) Schematic illustration of the difference between the previous reports of biphenyl-Na/K liquid anode with solid state electrolytes (SSEs) and this study of biphenyl-Li liquid anode with a ZIF7 membrane separator. The proposed function of the ZIF7 membrane in three aspects is also displayed. b) The cross-side SEM images of the ZIF7 membrane. Inset: the digital image of the ZIF7 membrane.

a ZIF7 membrane built with polymer binder could exhibit enough flexibility, which shows more feasibility compared with the brittle SSEs. Secondly, ZIF7 particles have a pore size of about 2.9 \AA in its structure, which is small enough to physically block the large species (biphenyl molecule in the liquid anode and RM molecule in the cathode electrolyte) in the battery system. Moreover, the unique cavity construction of ZIF7 is believed to provide significant pathways for the Li ions, optimizing their transporting. We prepare the ZIF7 membrane by casting the mixture solution of ZIF7 powders and polymer binder onto a substrate and peeling it off after drying. As shown in the inset of Figure 3.4b, the as prepared membrane shows a uniformly beige color, indicating the even distribution of ZIF7 particles in the skeleton of binder, which gives the membrane good uniformity. The cross-side image obtained by SEM further displays the membrane morphology that ZIF7 particles tightly and densely embed in the network of polymers, with a stacked thickness of about $60 \text{ }\mu\text{m}$. No cracks or voids could be observed from cross section morphology, which could ensure enough denseness for the membrane to block the liquid anode and various soluble species.

We then investigate the ability of ZIF7 membrane to separate the Bp-Li anode by the permeation test. A home-made V type device similar to the one in chapter 2 is used to conduct the test. The ZIF7 membrane is sandwiched between two leaning tubes, one

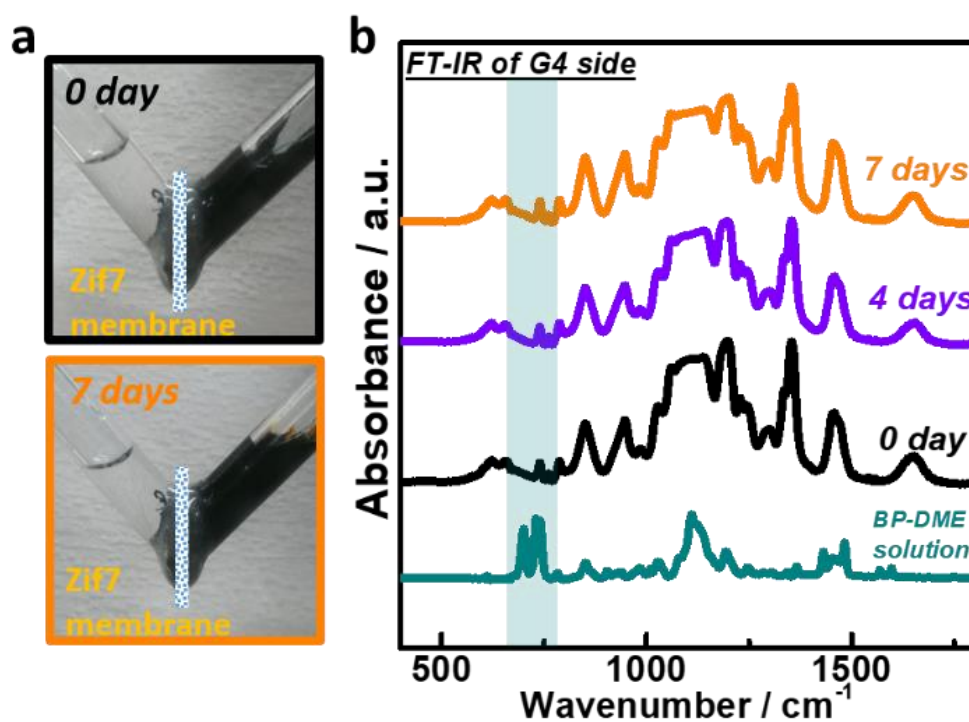


Figure 3.5 a) Digital images of the permeation device in the beginning (black) and after 7 days (orange). b) FT-IR spectrum of the electrolyte samples extracted from the G4 side at different time.

loaded with colorless base cathode electrolyte of 1 M LiTFSI in G4, and the other one loaded with dark blue Bp-Li anode. Figure 3.5a shows the digital images of the permeation test in the beginning and after 7 days. No obvious color change is observed at the cathode electrolyte side during the 7 day test, indicating the ZIF7 membrane could effectively stop the Bp-Li from moving to the cathode side. FT-IR measurement is further applied to trace the possible species crossover during the test (Figure 3.5b). We especially focus on the range of 650-750 cm⁻¹, where the biphenyl molecular exhibits two characteristic peaks due to the aromatic out-of-plane C-H bending vibrations. These peaks are also shown in the spectrum of biphenyl-DME solution.¹⁰⁹ From the spectrum of cathode electrolyte collected at different periods, no obvious additional signals or peak intensity changes can be told from the beginning spectrum. These results indicate that the biphenyl molecular could be well restrained by the ZIF7 membrane

due to the small pore size of ZIF7. In this way, the flowable active material in the liquid anode could be kept away from the cathode side.

3.3.3 Rate and Cycling Performance

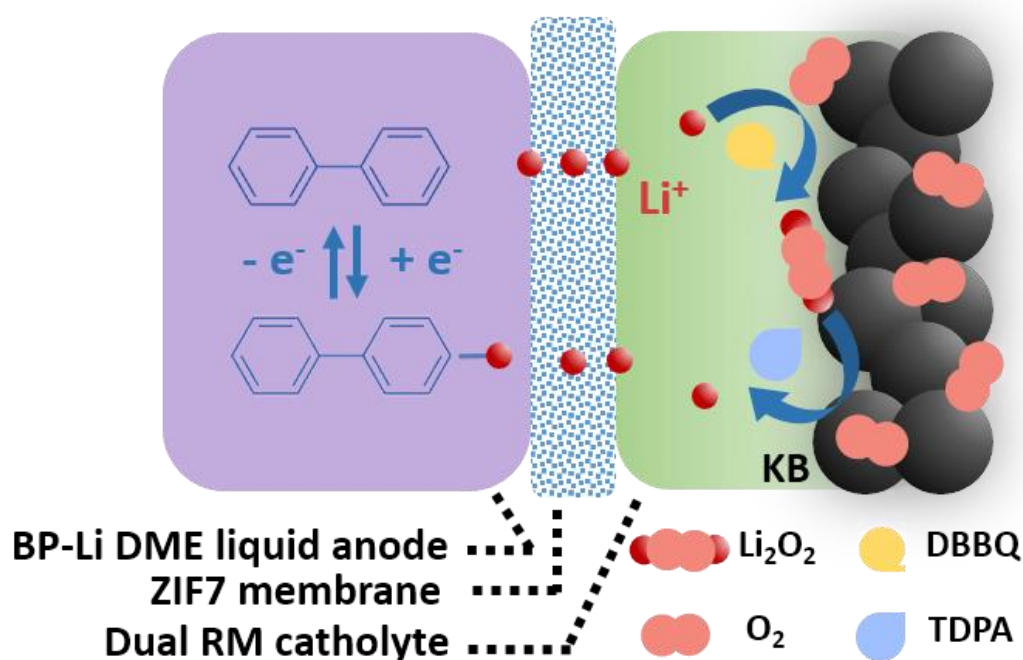


Figure 3.6 The schematic illustration of the organic oxygen battery with Bp-Li liquid anode, dual RM assisted KB cathode and ZIF7 membrane as a separator.

We then propose an organic oxygen battery with Bp-Li liquid anode and ZIF7 membrane working as a separator (Figure 3.6). We employ the KB porous carbon black as oxygen cathode, with DBBQ RM for discharging process and TDPA RM for charging process.^{47, 85} Generally, RMs are dissolved in the electrolyte. They work as the electron or hole carriers during discharging or charging process and turn the Li₂O₂ related electrochemistry into a solid-liquid contact mode, which could improve the kinetics process and suppress the unfavorable parasitic reactions. In this chapter, the dual RMs strategy based on DBBQ and TDPA in the cathode electrolyte also helps the effective and reversible formation/decomposition of Li₂O₂ in the same mechanism that we confirm in section 3.3 of Chapter 2. At the anode side, the Bp-Li serves as a safe anode material with low working potential. In the middle, the ZIF7 membrane works

as a bridge connecting the two sides in three aspects. Firstly, it could conduct the lithium ions during the cycling processes. Secondly, it prevents the BP-Li anode from transporting to the cathode side and bringing in short circuit. Moreover, it keeps RMs at the anode side to get rid of the crossover effect. The effect of a MOFs-based separator in physically blocking the RMs for Li-O₂ batteries by taking advantage of the small pore sizes of MOFs has been shown in our group's previous work.

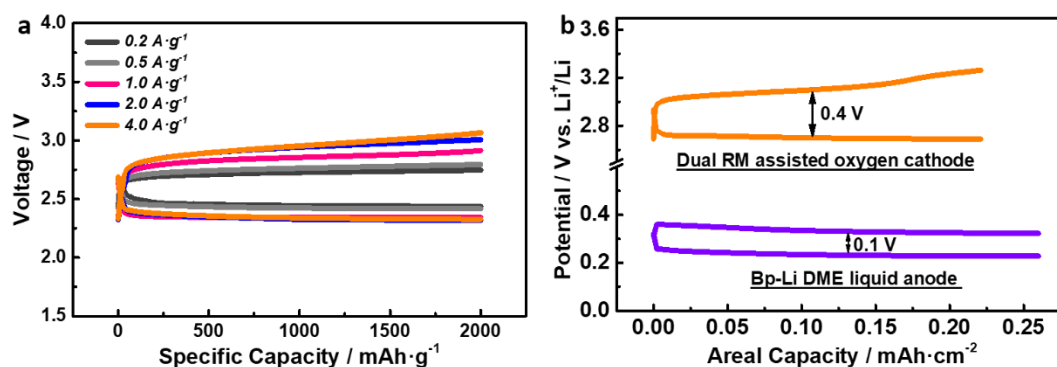


Figure 3.7 a) The electrochemical profiles of the dual RM assisted oxygen cathode and Bp-Li liquid anode half cells. b) Rate performances of the fabricated Li based organic oxygen batteries.

The electrochemical profiles of dual RMs assisted KB based oxygen cathode and Bp-Li anode half cells are presented in Figure 3.7a. The overpotential of the oxygen cathode is effectively reduced to about 0.4 V, which indicates the collaborative redox mediated effect of DBBQ and TDPA. The Bp-Li anode exhibits a low working potential about 0.3 V vs. Li⁺/Li and a narrow voltage gap about 0.1 V. This could be attributed to the high ionic and electronic conductivity of the Bp-Li anode. The electrochemical profiles of fabricated organic oxygen batteries with Bp-Li anode at different rates are presented in Figure 3.7b. At low current density, the fabricated organic O₂ battery shows a discharging plateau near 2.45 V and a recharging plateau near 2.75 V. The voltage gaps keep narrow as the applied rates increase up to 4 A·g⁻¹. The superior rate performance benefits from both the dual RMs and the Bp-Li anode with high conductivity. Simultaneously, the important role of the ZIF7 membrane is also important. The effect of ZIF7 particles with unique cavity construction in regulating the Li ion transporting helps a lot in achieving stable ion conduction at a high current density. The cycling performance of the organic oxygen batteries with Bp-Li anode is

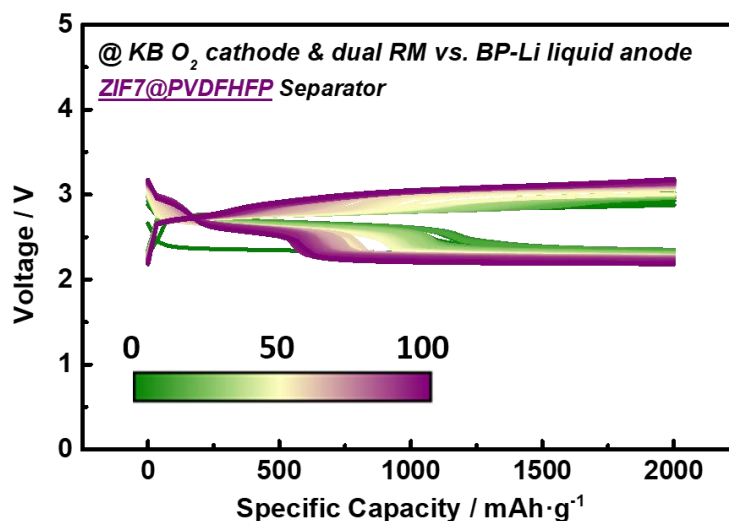


Figure 3.8 Cycling performance of the Li based organic oxygen batteries within 100 cycles.

shown in Figure 3.8. At a high current density of $4000 \text{ mA}\cdot\text{g}^{-1}$ and a high reversible specific capacity of $2000 \text{ mAh}\cdot\text{g}^{-1}$, 100 cycles can be stably achieved with an acceptable overpotential gap. The overpotentials are well controlled during the whole test, which is a key factor that ensure each part of the battery works with durability. Again, this shows the Bp-Li anode together with ZIF7 membrane could be competent as an effective combination for the anode of Li based battery.

3.3.4 Characterization of Liquid Anode/Membrane Interface

The interface behavior between the ZIF7 membrane and liquid anode raises our interest. The SEM images of the extracted ZIF7 membrane after battery cycling are presented in Figure 3.9a. The interface of ZIF7 membrane at the cathode side still exhibits the morphology of the pristine where the ZIF7 particles are embedded in polymer networks (yellow box & blue box). This illustrates that the ZIF7 membrane stays stable during restraining the RMs in the cathode electrolyte. On the other hand, a new interface is observed at the anode side (red box), which exhibits a totally different morphology of irregularly distributed small particles. FT-IR is then further applied to investigate the composition of the newly observed interface. Compared with the pristine membrane, the characteristic peak of ZIF7 at 740 cm^{-1} (ascribed to out-of-plane C-H

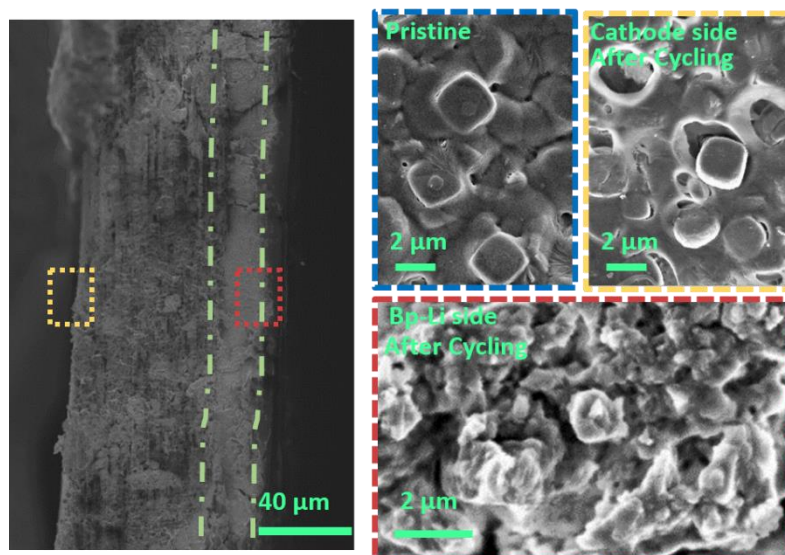


Figure 3.9 The cross-side and upside SEM images of the ZIF7 membrane. The interfaces of ZIF7 membrane facing cathode side (yellow) and anode side (red) exhibit different morphologies after cycling. The pristine morphology (blue) of ZIF7 membrane is also displayed to be compared with.

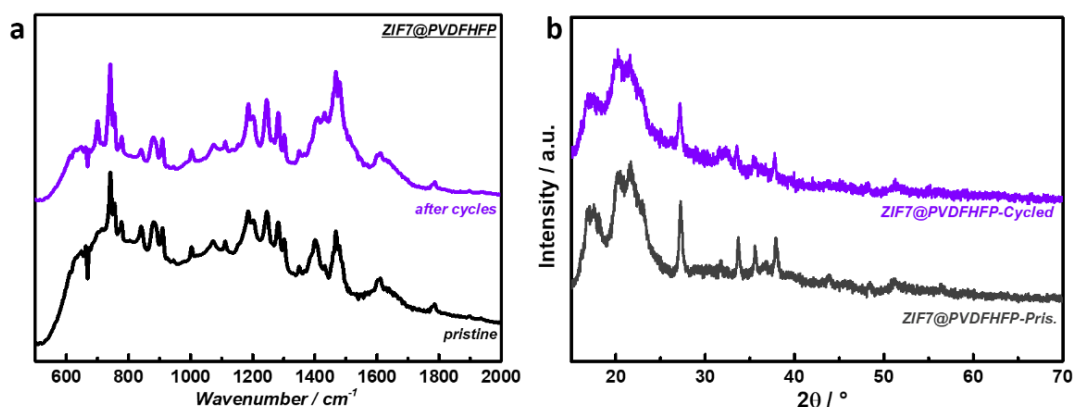


Figure 3.10 a) The FT-IR spectrum of ZIF7 membranes before and after cycles. b) The XRD patterns of the ZIF7 membrane before and after electrochemical cycles in the organic O_2 battery.

bending vibration of ortho-disubstituted benzene) remains well after cycling (Figure 3.10a). This is in accordance with the XRD results (Figure 3.10b), that the XRD patterns remain of ZIF7 membrane remain well after cycling test.¹¹⁰ This confirms the stable structures of ZIF7 particles during the electrochemical test. Signals of Li_2CO_3 species ($1400\sim 1550\text{ cm}^{-1}$) and some residual biphenyl ($650\sim 750\text{ cm}^{-1}$) appear in the FT-IR after cycling, indicating the composition of the new interface mainly consists of

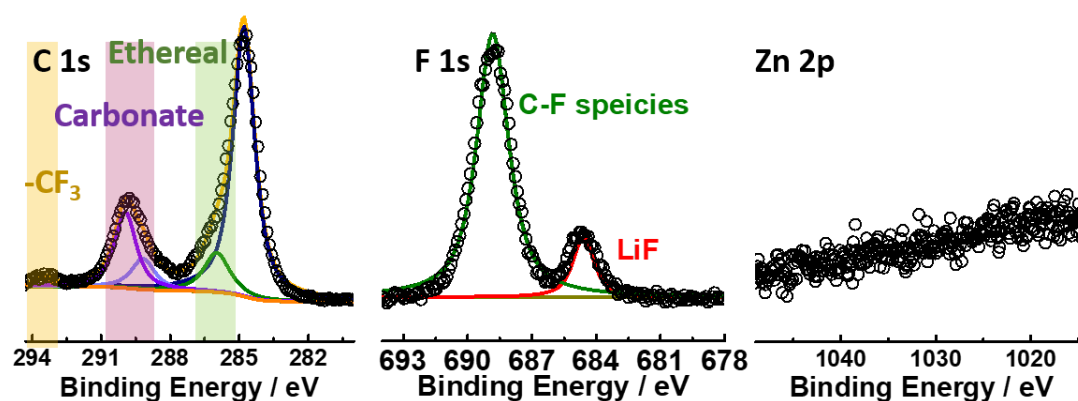


Figure 3.11 XPS C 1s, F 1s and Zn 2p spectrum of the ZIF7/Bp-Li interface after cycles.

Li_2CO_3 and undissolved biphenyl.⁷⁸

To further investigate the composition of the new interface, XPS measurement is then carried out (Figure 3.11). Carbonate species at around 289~291 eV are significantly presented in the interface after cycling. And the C-F species are also presented which might come from the decomposition of the LiTFSI salt trapped in the ZIF7 membrane from the cathode side electrolyte. LiF is also detected presented in the interface, which could originate from the decomposition of the binder and/or LiTFSI salt from the confined electrolyte in the ZIF7 membrane. No ZnO or $\text{Zn}(\text{OH})_2$ signals are presented.¹¹¹ These results prove the stability of the ZIF7 membrane supported with PVDF-HFP binder.

We note that the binder is of vital importance for the durability of the ZIF7 membrane. When PVDF is chosen as the binder for the membrane, the fabricated battery suffers from short circuit after only 41 cycles (Figure 3.12 a). Although a new interface is still observed at the liquid anode side, obvious cracks are also presented through the extracted membrane, which is speculated the reason of the short circuit (Figure 3.12b). In the FT-IR results, besides the undissolved biphenyl and Li_2CO_3 which are also detected in the interface of PVDF-HFP based ZIF7 membrane, an obvious signal between $950 \sim 1150 \text{ cm}^{-1}$ is observed in PVDF based ZIF7 membrane. This could be attributed to the C-O species, which might be caused by the decomposition of the ether solvent from the liquid anode or cathode electrolyte (Figure 3.12c). Moreover, the XPS

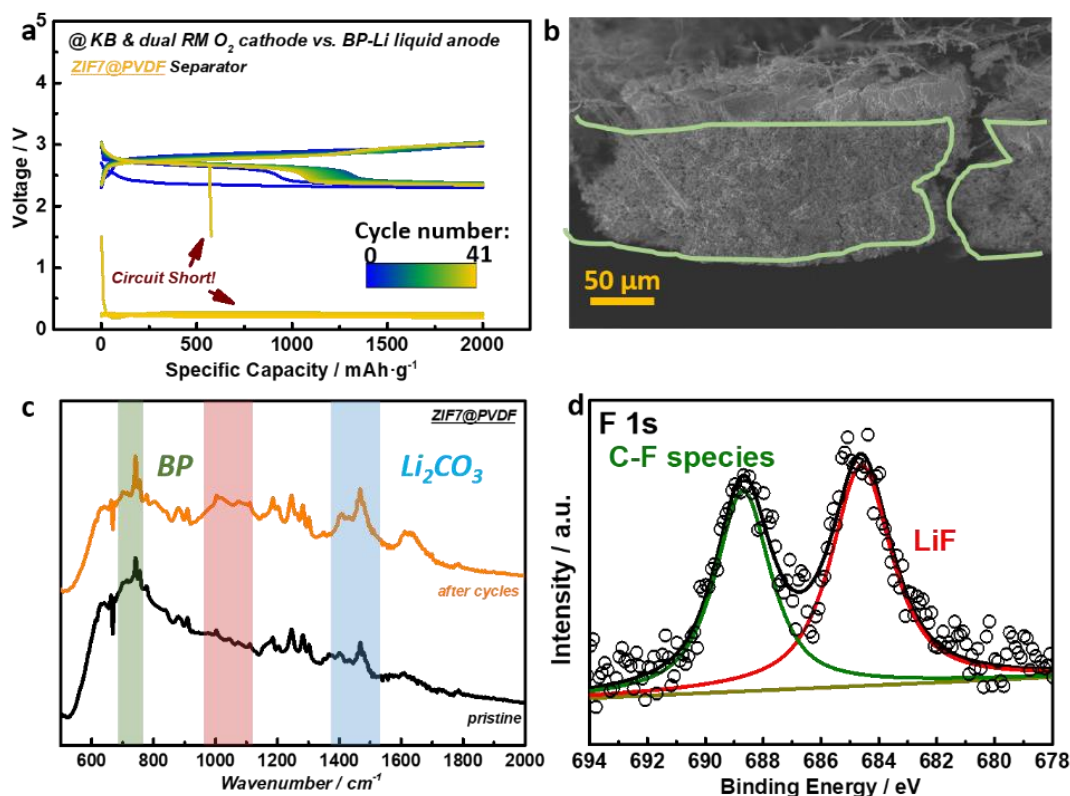


Figure 3.12 a) The electrochemical profiles of the organic oxygen batteries with a PVDF based ZIF7 membrane. b) The cross-side SEM images, c) FT-IR spectrum and d) XPS F1s spectrum of the PVDF based ZIF7 membrane after cycles.

results of the PVDF based ZIF7 membrane after cycling exhibits reduced signals for C-F species and increased signal for LiF (Figure 3.12d), suggesting the decomposition of the PVDF binder during cycling, which finally leads to the membrane failure to separate the two electrodes (Figure 3.12b).

In a typical process, the SEI on the electrode plays an important role for the stable work of the battery system. It forms between the electrolyte and electrode, with the ability to conduct Li ions and resist electrons so that the continuous decomposition of the electrolyte is prohibited.¹⁵ The interface between the ZIF7 membrane and Bp-Li anode locates in a similar position, where the Li ions should be allowed to pass and the electrons available from the electronically conductive Bp-Li anode should be stopped. As is shown in Figure 3.13, we propose the formation of a new SEI-like interface between a ZIF7 separator and a liquid anode. The interface is made up of carbonate species like Li_2CO_3 , LiF, C-F species and some undissolved biphenyl. Note that Li_2CO_3

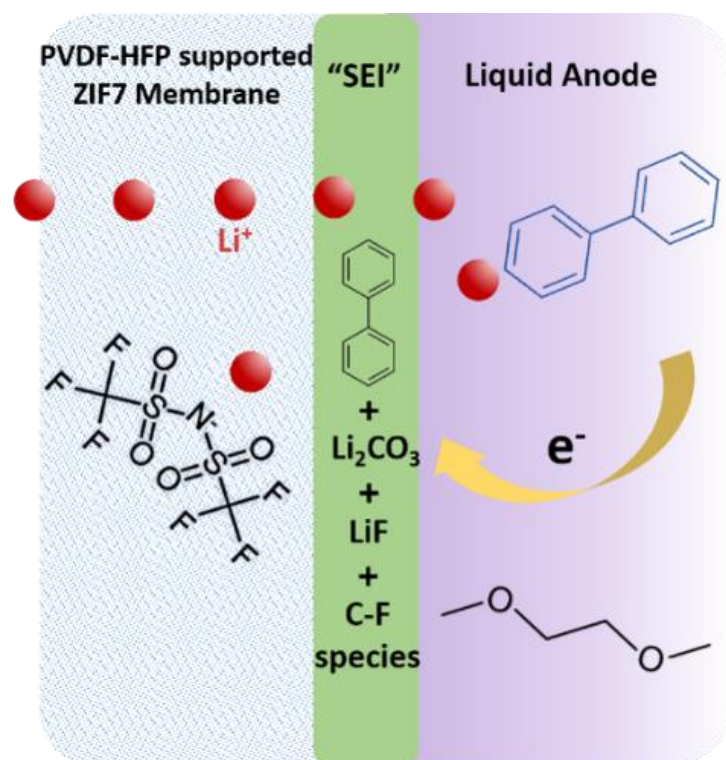


Figure 3.13 The schematic illustration of the formation of SEI-like ZIF7/Bp-Li interface.

and LiF are classically beneficial components for the SEI of anode materials, which is believed helpful for stable function of the Bp-Li liquid anode. The possible formation pathways of this layer are discussed as below, though we argue that further work is needed to clarify the mechanism. The carbonate species like Li_2CO_3 are likely the decomposition products of ether solvents, mainly DME solvent, considering the G4 solvent is hard to transport to this side. The presence of oxygen in a Li O_2 battery environment would promote this pathway. The LiF comes from two origins, one is the decomposition of the PVDF-HFP binder, and other one is the decomposition of the LiTFSI in the ZIF7 membrane. And we think the LiTFSI decomposition accounts for the main part. As for the undissolved biphenyl, we suspect that part of solvents (DME) from the biphenyl-Li liquid anode are trapped in the ZIF7 particles to provide the Li ion conductivity. As a result, with some DME solvents diffuse into the ZIF7 membrane, some biphenyl deposits onto the surface of the ZIF7 membrane. In the meanwhile, Li atom on the biphenyl molecule might induce a series of reactions leading to the presence of decomposition products like Li_2CO_3 and LiF. The polymer binders are also important for the stability of ZIF7 membrane. It should provide strong and stable

support for the ZIF7 particles, in order to ensure the intensity of the ZIF7 membrane and the formed interface on the membrane. As a result, the membrane of ZIF7 particles connected by PVDF-HFP binder possesses enough mechanical strength and stable SEI-like interface, successfully bridging the Bp-Li anode and oxygen cathode side to achieve stable cycling.

3.4 Conclusions

To conclude, we successfully fabricate a lithium based organic oxygen battery with a non SSEs separator. A ZIF7 membrane is introduced to work as a bridge connecting the Bp-Li liquid anode and oxygen cathode by conducting lithium ions while simultaneously separating the Bp-Li at the anode side and RMs at the cathode side. Thanks to the high electrical and ionic conductivity of Bp-Li anode and ZIF7 particles with unique cavity construction benefitting fast ion transporting, the fabricated organic oxygen battery shows superior rate performance up to $4 \text{ A}\cdot\text{g}^{-1}$ and stable discharging/charging performances up to 100 cycles. Furthermore, we firstly study the SEI-like layer formed in the liquid anode on the ZIF7 membrane separator. Li_2CO_3 , LiF, C-F species and some undissolved biphenyl are found in the compositions of the SEI-like interface. With the strong supportive networks of the PVDF-HFP binder, these species help build a stable interface for cycling of Bp-Li liquid anode. This work would not only bring about new choices of anode materials for Li based battery, but also provide deeper understanding for the better application of alkali metal based liquid anode.

Chapter 4. A Practical Lithium Oxygen Cell Based on Hybrid Electrolyte Design

4.1 Introduction

Lithium oxygen (Li-O₂) batteries receive a lot of research attention recently, as they hold the potential to boost the universal application of electric vehicles (EVs) with their theoretical energy density equaling to that of the gasoline used for internal combustion engine cars.¹¹² Nevertheless, this battery system, proposed for over 20 years and extensively studied during the last 10 years, is still in its infant stage. Problems are found in all the components of the battery. Parasitic reactions at the cathode and electrolyte would influence the efficiency and durability of the battery.⁹⁵ The ideal application of lithium metal as anode, is challenged by the intrinsic problems of lithium metal like low utilization rate and dendrite growth. Affected by all these obstacles, most of the researches on Li-O₂ batteries are usually confined in a small scale, that in most cases tiny coin cells are applied to conduct the experiments.¹¹³⁻¹¹⁴ However, to fully understand the potential of the Li-O₂ batteries, a larger size cell is never avoidable. It would either show the potential of Li-O₂ batteries in a more practical way, or magnify the shortcomings of this battery system to a more obvious level. No matter what, there are only a few reports on the scale-up performances of Li-O₂ batteries.¹¹⁵⁻¹¹⁷

Pouch type cells are a good choice in the magnification of Li-O₂ batteries. Wang et al. reported a pouch type Li-O₂ battery and discussed its structure design dating back to 2010, achieving an energy density of 344 Wh·kg⁻¹ based on a carbonate based electrolyte.¹¹⁶ However, as we state in Chapter 1 and 2, the carbonate based electrolyte are found vulnerable and inappropriate for the oxygen cathode. Shin et al. also reported the trial for a pouch type Li-O₂ battery, claiming that lithium metal anode would collapse more severely in an enlarged battery scale.¹¹⁷ However, there are still new challenges that appear along with the magnification of research scale of Li-O₂ battery.

We go back to the discussion on the cathode issue. In order to suppress the blocking

of the porous structure in the cathode to obtain a large discharging capacity, redox mediator (RM) for the oxygen reduction reaction (ORR) process, is proposed as an additive in the electrolyte for the cathode electrolyte. 2,5-di-tert-butyl-1,4-benzoquinone, denoted as DBBQ, is one of the typical RM for ORR. According to the proposed mechanism of DBBQ by Bruce et al., it firstly receives an electron from the cathode during ORR process, and then interacts with the soluble oxygen to give the discharge product of Li-O₂ battery, Li₂O₂. There is no problem for this procedure in the scale of coin cell, as the cathode is exposed in the oxygen atmosphere sufficiently and the soluble oxygen in the electrolyte is to some extent abundant.⁴⁷ However, things might turn different when pouch type cell is applied for research. This is due to the fact that structure design of the cell, in which as a subjective result not all the electrode areas could have enough contact with the oxygen. As a result, the key step for this procedure, that soluble oxygen interacts with the reduced DBBQ, might be affected, leading to the function of DBBQ in a scale up pouch type cell less effective. In other words, it's more important to improve the oxygen solubility, or oxygen transportation in the cathode electrolyte if we want to take advantages of the effect from DBBQ to obtain high discharging capacity.

Herein, aiming at improving the oxygen solubility of cathode electrolyte in a pouch type Li-O₂ battery, we propose a kind of per fluorinated chemical, denoted as HFE, as a co-solvent for the cathode electrolyte. Per fluorinated chemicals have been reported to have a high oxygen solubility and are widely used in artificial blood. Taking advantages of its ability to dissolve oxygen, we'd like to promote the effect of DBBQ which might be limited due to the poor oxygen supply. Moreover, a hybrid electrolyte design is also applied, mainly to separate anode from the added species, like RMs and HFE in the cathode electrolyte. Benefitting from the synergetic effect of DBBQ and HFE, the fabricated pouch type Li-O₂ battery exhibits an improved energy density, showing the practical potent of Li-O₂ battery with the hybrid electrolyte design.

4.2 Experimental Section

4.2.1 Preparation of cathodes for Li-O₂ cells

A commercial carbon fiber material was used as a carbon based cathode material for the electrochemical test in coin cells. Carbon fiber sheet was pouched into pellets of 10 mm, and dried under vacuum at 90 °C overnight before transferred into the glovebox for further fabrication. For the fabrication of pouch type Li-O₂ battery, the Ketjenblack (KB, EC600JD, Lion Co. Ltd.) cathodes were prepared by heat rolling the paste of KB and Polytetrafluoroethylene (suspension, 14%) at a weight ratio of 80:20, and pressing into a sheet with a KB mass loading of 5 mg·cm⁻². Then, the KB sheet was cut into small sheets with a size of 3 cm * 3.5 cm and pressed onto a carbon paper current collector with the same size. An aluminum tap was attached to the carbon paper to conduct with the outer circuit. The fabricated KB cathode was also dried under vacuum at 90 °C overnight before transferred into the glovebox for further fabrication.

4.2.2 Preparation of metal organic frameworks (MOFs) based separator

The preparation of the MOFs based separator was based on the previous report.¹¹⁸ In a typical process, a mixture solution of copper (II) nitrate trihydrate and 1,3,5-benzenetricarboxylic acid was vigorously stirred for 30 minutes. Crystalline nanoparticles were synthesized and self-assembled during the procedure. Then, the solution was vacuum filtrated through a commercial Celgard separator, and the formed MOFs particles were then attached onto the Celgard separator. 5 mL of PVDF-HFP solution in acetone was spread onto the Celgard to strengthen the attachment of MOFs particles and Celgard separator. Finally, the MOFs based separator was obtained after drying treatment. The MOFs based separator is cut in to pellets of 16 mm for the coin cell test and sheets of 3.7 cm* 4 cm for the pouch type cell fabrication.

4.2.3 Preparation of electrolytes

Two kinds of cathode electrolytes were prepared. The base electrolyte is prepared by

dissolving 1.0 M of Lithium bis(trifluoromethanesulfonyl)imide (LiTFSI, Sigma-Aldrich) into tetraethylene glycol dimethyl ether (G4, Sigma-Aldrich). RM contained cathode electrolyte was prepared by adding 50 mM DBBQ into the base electrolyte. HFE contained cathode electrolyte was prepared by adding 30% volume ratio of HFE into the cathode electrolytes. During cycling test, 150 mM of 2,2,6,6-tetramethylpiperidinyloxy (TEMPO) was added as RM for OER.

4.2.4 Fabrication of coin type Li-O₂ cells

The coin cell assembly was conducted in a glove box filled with Ar. 2032-type coin cells with holes on the cathode side were used. Typically, the Li-O₂ cell was fabricated by successively stacking a Li metal anode, a glassy fiber separator saturated with certain electrolyte and a KB cathode. For the discharging test, MOFs based separator was added, separating two glass fibers with electrolytes respectively for cathode and anode. The prepared cells were sealed in a chamber (650 mL) and the chamber was continuously purged with oxygen for 1 h.

4.2.5 Fabrication of pouch type Li-O₂ cells

The pouch type Li-O₂ cells are fabricated by sandwiching a sheet of lithium metal anode between two oxygen cathode sheets. At each side, the Celgard separator with base electrolyte, the MOFs based separator and the glass fiber with cathode electrolyte were successively stacked from anode to cathode. The lithium metal was rolled into a sheet with thickness of about 0.1 mm, attached to the both sides of copper foil to serve as the anode. A nickel tap was attached to the copper foil to conduct current with the outer circuit. Each membrane was cut into appropriate size to avoid the short circuit. The whole cell core was then packed with an aluminum plastic film and fixed with two plastic plates. Then, the fabricated cells were sealed in a chamber (650 mL) and the chamber was continuously purged with oxygen for 1 h.

4.2.6 Electrochemical measurements

The galvanostatic electrochemical measurements were conducted on the battery tester system HJ1001SD8 (Hokuto Denko). For the discharging test, both coin type and pouch type cells were discharged at various current densities based on the cathode area with a cutting potential of 2.4 V vs Li⁺/Li. Cyclic voltammetry (CV) was measured on a Solartron analyzer (SI 1260) at various scan rates from 2.0 to 3.6 V vs Li⁺/Li. The pouch type cells were also discharged and charged at different fixed areal capacity and current density for the cycling test.

4.2.7 Characterizations

The X-ray diffraction (XRD) patterns was collected on a Bruker D8 Advanced diffractometer fitted with Cu-K α X-rays ($\lambda = 1.5406 \text{ \AA}$) radiation. A home-made cell sealed with a Kapton film window by silicone glue was used for test to avoid the affect of ambient air. The scanning electron microscopy (SEM) images were obtained on a LEO Gemini Supra 35 system.

4.3 Results and Discussions

4.3.1 Perfluoro Solvents for Oxygen Solubility Improvement

The perfluoro solvents were found with strong capability to dissolve oxygen, and considered for in vivo oxygen delivery in human body due to its chemical and biological inertness.¹¹⁹⁻¹²² Inspired by these properties, we take advantage of it as a co-solvent for the oxygen cathode electrolyte, in order to improve the oxygen solubility and synergetic effect with DBBQ during ORR process.¹²³⁻¹²⁴ We firstly conduct the galvanostatic discharge test to investigate the effect of DBBQ RM and HFE co-solvent for the discharging capacity of the coin type Li-O₂ cells. The discharge load curves at a low current density of 0.1 mA·cm⁻² are presented in Figure 4.1a. In absence of DBBQ in the electrolyte, the discharge potentials drop rapidly, exhibiting very small capacities of less than 0.5 mAh·cm⁻², in accordance with previous observations. In this case, the

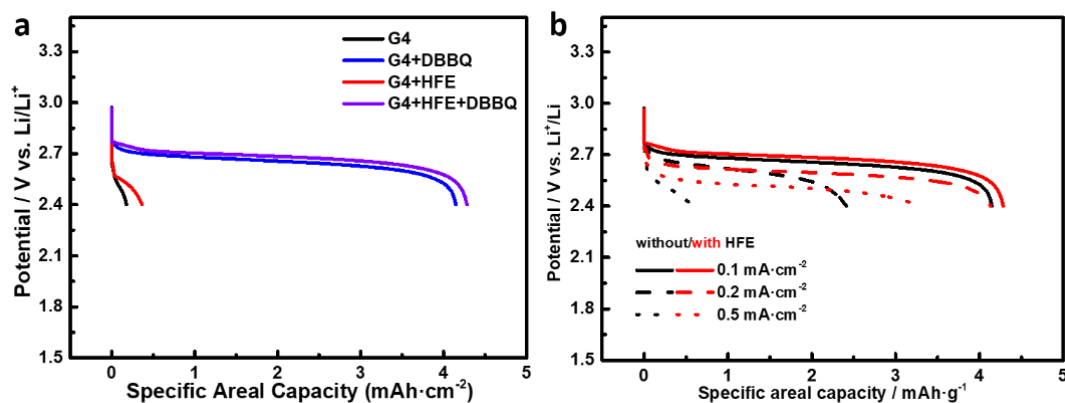


Figure 4.1 a) Discharge load curves of coin type Li-O₂ cells in various condition at 0.1 mA·cm⁻². b) Discharge load curves of DBBQ contained coin type Li-O₂ cells with and without HFE at different current densities.

presence of HFE would to some extent help increase the discharge capacity by increasing the oxygen solubility in the electrolyte. However, the effect is limited, as the ORR pathway is still a surface pathway, leading to quickly covered cathode surface and early death of the cells. With the addition of DBBQ, the ORR process turns into a solution pathway. As a result, the discharge capacity largely increases to over 4.0 mAh·cm⁻². The capacity of cell with HFE is a little larger than that of the cell without HFE, indicating that the improvement of oxygen solubility would benefit the ORR process, though at a low current density it's not so obvious. At high current densities,

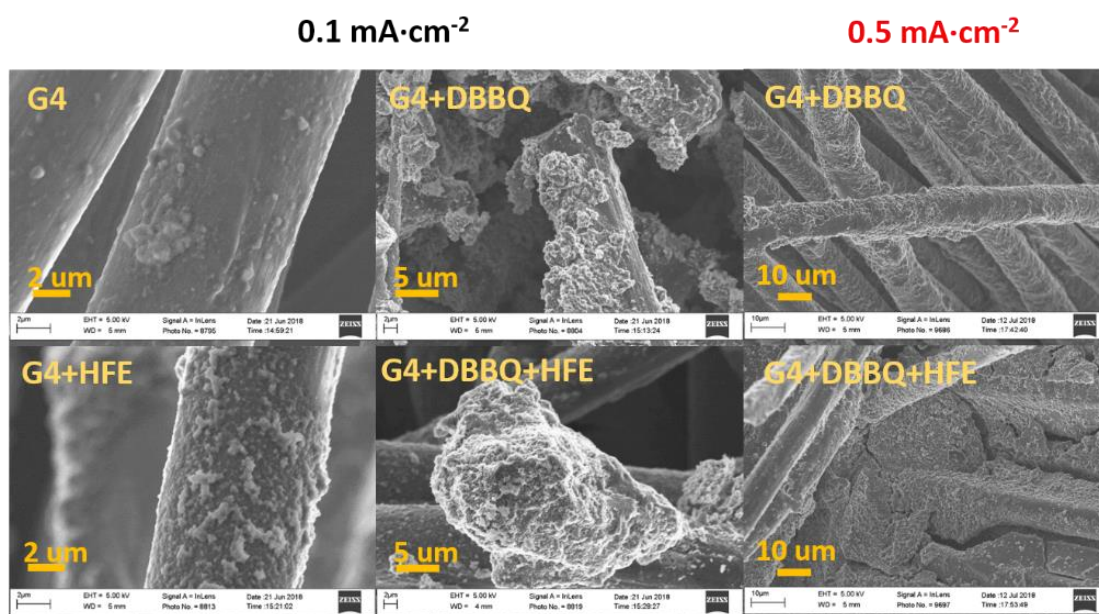


Figure 4.2 Oxygen cathodes in various electrolytes after discharging.

the cells with both DBBQ and HFE exhibit much better performances compared with cells with only DBBQ. At each current, higher capacity and working potential are achieved. These results show that the significant role of synergetic effect of HFE and DBBQ. During ORR process, HFE provides more soluble oxygen for the DBBQ to conduct the mediation process, and they together boost the oxygen transport in the ORR of solution pathway, resulting in improved capacity and rate performances.

The discharged cathodes were then extracted out and observed through SEM. As is with the discharge capacity, at a low current density of $0.1 \text{ mA}\cdot\text{cm}^{-2}$, there is very few small product particles observed on the carbon fiber for the cell in base electrolyte, and in presence of HFE the particles grow a little bit more. In the case of ORR with the presence of DBBQ, the large product particles domain the carbon fiber, indicating the outstanding effect of DBBQ for benefiting the growth of Li_2O_2 particles. When the current density is increased to $0.5 \text{ mA}\cdot\text{cm}^{-2}$, the morphology of the cathode discharged in the electrolyte without HFE exhibits film-like discharge product, while in the cathode discharged with HFE and DBBQ large and dense product particles are still observed. These results are in accordance with the galvanostatic discharge results, showing the synergetic effect of HFE and DBBQ for the ORR process.

The synergetic effect of HFE and DBBQ for ORR process is also confirmed by the CV measurements. The CV curves of oxygen cathode in the electrolyte of only DBBQ are presented in Figure 4.3a. In Ar atmosphere, DBBQ shows two reductive peaks

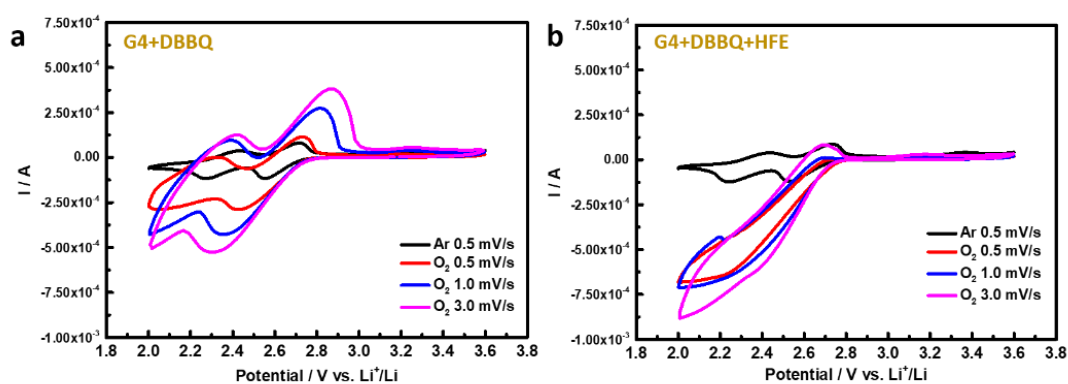


Figure 4.3 CV curves of KB cathode under Ar and oxygen atmosphere at various scanning rates in the electrolyte of a) only DBBQ and b) DBBQ and HFE.

during the negative scanning and two anodic peaks during in positive scanning in both electrolytes. The redox are considered to play a role in the ORR process. In the oxygen atmosphere, the intensity of reductive peaks increased largely compared with the case in Ar atmosphere, indicating the function of DBBQ in boosting the ORR process. The differences between the cells with and without HFE appear during the positive scanning process. For the cell with only DBBQ, there are obvious anodic peaks present, while in the cell with both DBBQ and HFE the anodic peaks are very weak (Figure 4.3b). The presence of HFE increases the amount of oxygen in the electrolyte, making more reduced DBBQ react with them and revert back to DBBQ. As a result, there are weaker anodic peaks during the positive scanning process. These results correspond with the discharging test, showing that HFE co-solvent helps provide enough oxygen for the reduced DBBQ to continue its reaction. There, the combination of both DBBQ and HFE further boost the discharge process in the for the Li-O₂ battery.

4.3.2 Pouch-type Cell Fabrication

The structure design is of vital importance to obtain a high energy density pouch type Li-O₂ cells. For the oxygen cathode, there must be pathways for the oxygen to transport

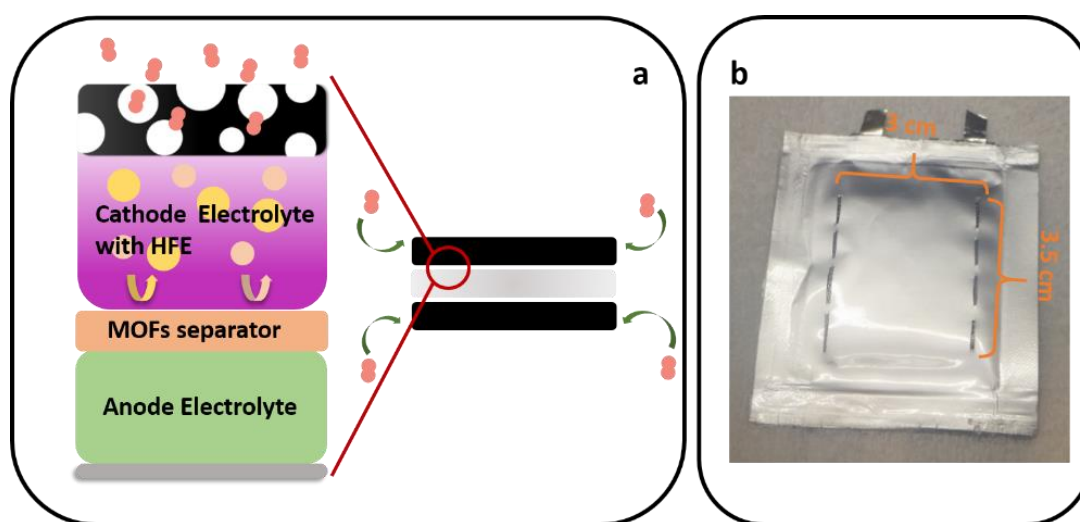


Figure 4.4 a) Schematic illustration of the pouch type Li-O₂ cells with oxygen windows at the cell side in a hybrid electrolyte design. b) Digital image of the fabricated pouch type Li-O₂ cells.

through. Previous reports of pouch type Li-O₂ cells usually apply a one side or double side cell design, so that the cathode could be open to the ambient oxygen atmosphere. In this design, for the electrode stack with over two cathode layers, it would be difficult for the cathode layers in the middle to get contact with the oxygen. This would limit the improvement of the energy density of the cell, as it's well known that the more electrodes packed in the cell, the higher the energy density there could be. However, with more cathodes in the middle but in a situation out of oxygen, the improvement would not be obvious and even be doubted. In this work, we try to get over this problem by a cell structure that the oxygen windows are arranged at the side of the cathode. In this way, the transport of oxygen is ensured with the help of the gas diffusion layer carbon paper and the HFE modified cathode electrolyte with improved oxygen solubility. Inside the cell stack, the hybrid electrolyte design is also applied for the better performance of the Li-O₂ cell. In the cathode electrolyte, RMs are applied to help the ORR and OER processes by turning them into a more effective solution pathway. Moreover, HFE is added as the co-solvent in the cathode electrolyte, so as to improve the solubility and mobility of oxygen in the electrolyte, which collaborate with the DBBQ and further boost the ORR process in a pouch type Li-O₂ cell. The MOFs based separator is applied to separate the RMs from transferring to the anode side and resulting in parasitic reactions. In this work, we applied this Cu based MOFs separator, as our previous study has proved its ability in blocking RMs in a Li-O₂ battery.⁶³ Moreover, its effect in facilitating the homogeneous lithium ion flux by “caging” the electrolyte with its unique natural pores is also considered beneficial for the lithium metal anode. As a primary study focusing on the discharge capacity in the pouch type Li-O₂ cell, we use the lithium metal as the anode in spite of its intrinsic problems. We argue that the application of lithium metal doesn't bother the goal to study the effect of HFE with a hybrid electrolyte for the high energy density pouch type Li-O₂ cell.

The fabricated pouch type Li-O₂ cell is presented in Figure 4.4b. A square of aluminum plastic film covered pouch type cell is prepared. In the middle, an area of 3 cm * 3.5 cm is set, under which the cell core for the electrochemistry is placed, and the oxygen window is set at the longer side of the area to let in/out the oxygen during

discharge and charge process. The cell is then transferred in to a bottle filled with oxygen, and rested for 12 hours so that the electrolyte and oxygen could get fully immersed. The rest time is longer than the case for the coin type Li-O₂ cells, as the open window for the oxygen in the pouch type cells is smaller and need more time for the electrolyte get well saturated in the cathode with soluble oxygen. During the test, two plastic plates are applied to sandwich the cell to provide enough contact for the cell. The aluminum plastic film is heat sealed in the glove box, so that the components in the cell are well fixed. This design is could set up a good reference, as the increase in number of electrode layers would not add any influences to the function environment of each cell component. This would make the evaluation of the energy density for the pouch type Li-O₂ cells in below more meaningful.

4.3.3 Discharging Energy Density

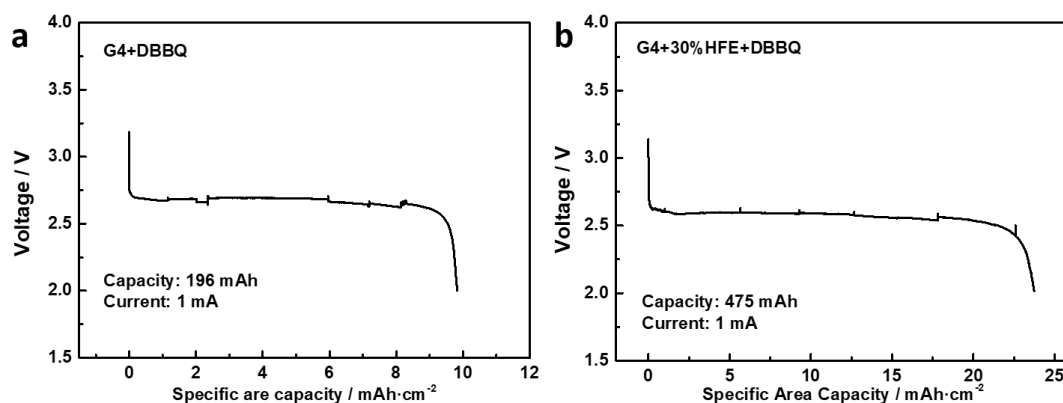


Figure 4.5 Discharge load curves of pouch type Li-O₂ battery in a hybrid electrolyte design with a) DBBQ only and b) DBBQ and HFE contained cathode electrolyte.

The discharge performances of the pouch type Li-O₂ cells with different cathode electrolytes are presented in Figure 4.5, respectively. For the cell with cathode electrolyte containing only DBBQ, a discharge plateau of near 2.69 V vs. Li⁺/Li is obtained, with a total discharge capacity of 196 mAh, equaling to a specific areal density of 9.83 mAh·cm⁻². The areal density is much higher than the state-of-the-art LIBs, which usually possess an areal density of near 2 mAh·cm⁻². This result indicating the promising benefits of Li-O₂ battery in delivering high energy density. For the cell

with cathode electrolyte containing both HFE and DBBQ, the discharge capacity is largely increased to 475 mAh, equaling to a specific areal density of 23.74 mAh·cm⁻². The potential of energy density implied in the Li-O₂ battery is further developed, thanks to the synergetic collaboration of HFE and DBBQ. These results show that the limitation of oxygen transportation in the cathode electrolyte could be largely broken through. With the help of improved oxygen solubility by the HFE, the function of DBBQ could be more effective, leading to a prolonged discharge capacity and enlarged energy density. The discharge plateau for the cell with both HFE and DBBQ decreased a little bit to 2.60 V vs. Li⁺/Li, this due to the addition of HFE, which lowers the ion conductivity of the cathode electrolyte because of the dilution of the electrolyte. Nevertheless, the little sacrifice in the discharge potential is largely offset by the increase in the discharge capacity. As the result, the output energy density achieved in the cell with HFE and DBBQ is still overwhelming.

The cell parameters of the two fabricated pouch type Li-O₂ cells are presented in Table 4.1. The two cells are with a total mass of near 3.30 g. The slight difference in the total mass is mainly resulted from the types of aluminum plastic film used to package the cells. And the calculated energy density based on the total mass is 153.2 Wh·kg⁻¹ for the cell with only DBBQ and 385.7 Wh·kg⁻¹ for the cell with both HFE and DBBQ. It should be noted that this evaluation is very rough as the packaging materials take a large part in the total mass, more than 1.0 g over the total mass. And even in this case, the energy density of the cell with both HFE and DBBQ exhibits a level better than the state-of-the-art LIBs. Moreover, the packaging materials vary with times and still have much potential to be optimized. In order to avoid the interference of the aluminum plastic film, we define the components except the aluminum plastic film and conducting tabs as the core cell. And we argue that the energy density of core cell is more valuable as the reference, as the core cell could be copied into multiple layers and the energy density could still be estimated as the working parts in the cell don't change. As is shown in Table 4.1, the core energy density of the cell with only DBBQ is 308.2 Wh·kg⁻¹, and the value for the cell with both DBBQ and HFE reaches as high as 633.1 Wh·kg⁻¹, which is far beyond the conventional energy density for the

	Total Mass / g	Core Cell Mass / g	Specific Area Capacity / mAh·cm ⁻²	Energy Density / Wh·kg ⁻¹	Core Energy Density / Wh·kg ⁻¹
G4+DBBQ	3.40	1.69	9.83	153.2	308.2
G4+DBBQ+HFE	3.20	1.95	23.74	385.7	633.1

Table 4.1 Cell parameters of the pouch type Li-O₂ cells with two kinds of cathode electrolyte respectively.

LIBs, indicating the potential of Li-O₂ battery could be realized with the help of modified cathode electrolyte in a hybrid electrolyte design.

The discharge products in the cathode of pouch type Li-O₂ cells are also confirmed by the XRD measurements (Figure 4.6). After discharge, both cathodes in the electrolytes of only DBBQ or DBBQ and HFE exhibit characteristic peaks of Li₂O₂ at near 33 ° and 35 ° respectively. The two peaks are corresponding to the crystal facets

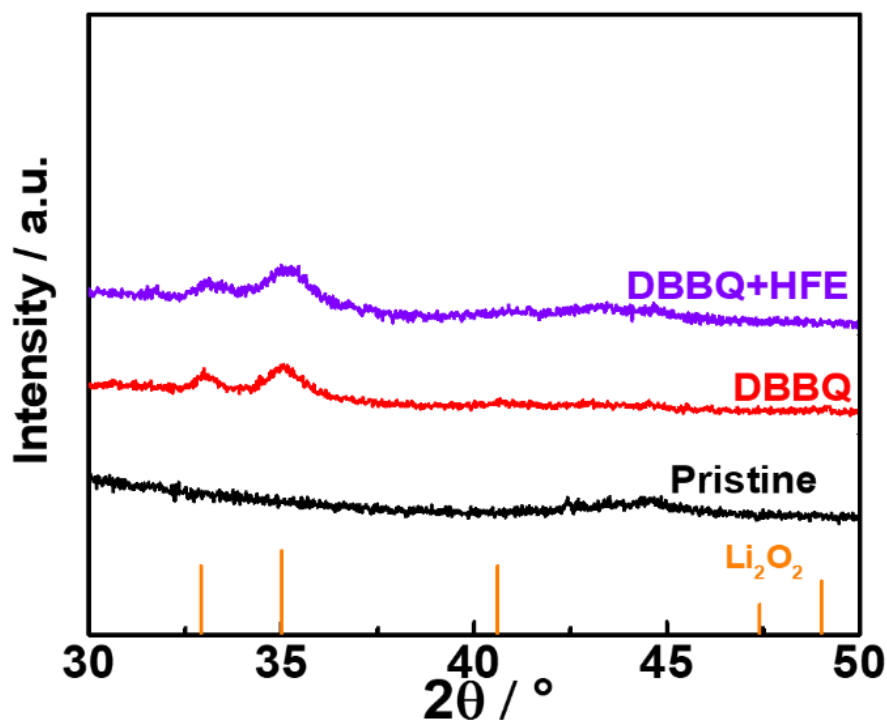


Figure 4.6 XRD patterns of the cathodes in the pouch type Li-O₂ cells with two kinds of cathode electrolyte respectively.

(100), (101) of the Li_2O_2 crystalline respectively. These results show that in both cases, Li_2O_2 still forms as the main discharge products. Under the function of DBBQ, the formation of Li_2O_2 is turned into a solution pathway from the surface pathway that is supposed for the G4 based electrolyte. Besides, the addition of HFE would help increase the supply of soluble oxygen in the cathode electrolyte, and it would not affect the formation mechanism of Li_2O_2 with the scale up of the cell into a pouch type. As a result, high energy density pouch type Li-O₂ cells based on the Li_2O_2 electrochemistry in the cathode are achieved for both pouch type Li-O₂ cells with the cathode electrolytes containing only DBBQ or both DBBQ and HFE.

4.3.4 Cycling Performance

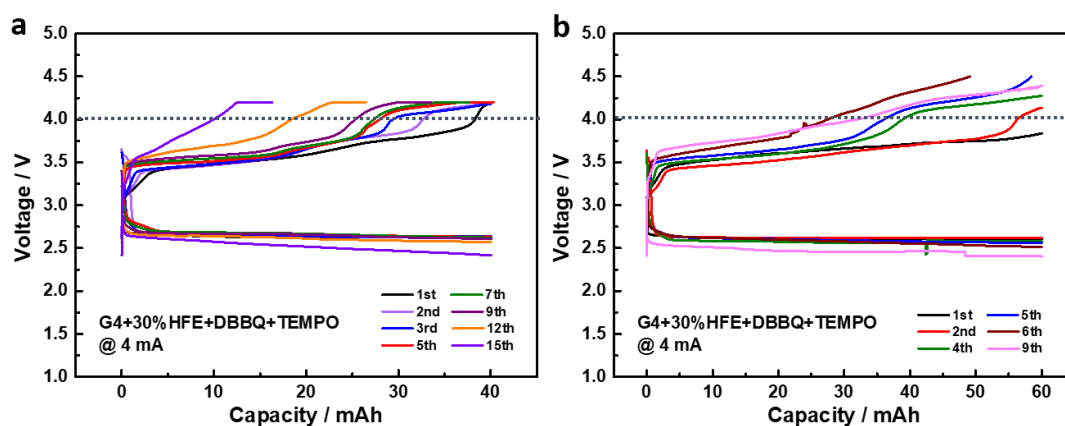


Figure 4.7 Cycling tests of pouch type Li-O₂ cells in hybrid electrolyte design with dual RMs and HFE in the cathode electrolyte. The fixed capacity is a) 40 mAh and b) 60 mAh respectively.

Finally, the cycling performances of the pouch type Li-O₂ cells with HFE are investigated. A typical RM for the OER process, 2,2,6,6-tetramethylpiperidinyloxy, denoted as TEMPO, is added in the cathode electrolyte to facilitate the charge process. The cycling tests were fixed at capacities of 40 mAh and 60 mAh respectively, equaling to a specific areal capacity of 2 and 3 mAh·cm⁻², respectively. As is shown in Figure 4.7, both cells shows a stable discharge plateau o near 2.7 V in the first cycle, and the charge potential is controlled to near 3.7 V thanks to the effective function of TEMPO. However, as the cycles go on, the charging potential gradually increases, with the

capacity failing to be fully recharged at the last several cycles, indicating the gradual invalid of TEMPO. It's suggested that charging potential below 4.0 V vs. Li^+/Li for the cathode is relatively safe to keep stable. As the failure of the TEMPO, the charge potential higher than 4.0 V vs. Li^+/Li becomes longer and longer, which further accelerates the instability of the cycling performance. Consequently, the fabricated pouch type Li-O₂ cell with the hybrid electrolyte design could exhibit stable discharge output within 15 cycles for the cell of 40 mAh fixed capacity, and 9 cycles for the cell of 60 mAh fixed capacity.

As we mention in the introduction section, the scale up of Li-O₂ battery would be difficult as the shortcomings of the battery are also magnified.¹²⁵⁻¹²⁶ The poor cycling performances of the pouch type Li-O₂ cells could be an exact example for us to see the difficulty and complex of Li-O₂ battery. And it could be understood in the following two aspects.

On the one hand, the reactive species generated at the cathode side during cycling are very complicated. Besides the superoxide species, recent researches have shown that singlet oxygen, one kind of very reactive oxygen gas is also generated during cycling and is responsible for many parasitic reactions.¹²⁷⁻¹²⁹ It could be partially avoided by the control of the charge overpotential by RMs, but there is still a lot generated during discharge process.¹³⁰ Though the superoxide species during the ORR process could be suppressed by RM like DBBQ, but the singlet oxygen cannot be removed in this way. And with the scale up of the battery, the damage of the reactive singlet oxygen to the cathode and electrolyte will also become severe and be responsible for the poor cycling performances.

On the other hand, at the anode side the lithium metal is still applied in this study. As we mainly focus on the cathode discharge capacity, we don't apply many specific strategies to address the intrinsic problems of lithium metal. A normal ether base electrolyte is used for the lithium metal. And we control the amount of the lithium in order to achieve a higher energy density. As a result, the lithium metal quickly fails during the plating and stripping process, also leading to the poor durability of the pouch type Li-O₂ battery. The failure of lithium metal in a pouch type Li-O₂ battery has also

been reported by other researchers, and is considered a main reason for the battery failure.¹¹⁷ Therefore, it's of vital importance to further optimize the anode side for the pouch type Li-O₂ battery. Nevertheless, the main goal in this study is to investigate the synergetic effect of HFE and DBBQ for achieving a high discharge energy density in the hybrid electrolyte design pouch type Li-O₂ battery, and we argue that the lithium metal would not affect the purpose of our present study. However, the upgrade of the anode side is still urgently needed if we really want to realize a practical lithium based oxygen battery, no matter by the modification of lithium metal with kinds of unique strategies, or by searching for alternatives of lithium metal as we conduct in Chapter 2 and Chapter 3.

4.4 Conclusions

In conclusion, we successfully fabricate a pouch type Li-O₂ battery in a hybrid electrolyte design with a special modified cathode electrolyte to achieve high energy density. By introducing the per fluorinated chemical HFE as a co-solvent for the cathode electrolyte, the oxygen solubility is largely increased, boosting the function of DBBQ RM for ORR process. As a result, the synergetic effect of HFE and DBBQ not only increase the rate performance of the coin type Li-O₂ battery, but also help build a pouch type Li-O₂ battery with a high core energy density of more than 600 Wh·kg⁻¹. Although the cycling performances of the pouch type Li-O₂ battery need further optimization, this work exhibits the real potential of the lithium based oxygen electrochemistry for achieving energy storage devices with high energy density.

Chapter 5. General Conclusions and Perspectives

5.1 General Conclusions

In this dissertation, we have intensively investigated the hybrid electrolyte design for the improvement of the aprotic Li-O₂ battery. With the help of this design, we are able to build proper electrolytes for both cathode and anode respectively, broadening the strategies to solve the problems of Li-O₂ battery including cycling stability, rate and safety property and practical potential. For the problem of cycling stability, it relates to the silicon anode which is chosen as an alternative of lithium metal. And we address the key issue by providing silicon anode with a suitable electrolyte in the hybrid electrolyte design. For the problem of rate and safety concerning, we introduce an organic liquid anode with outstanding electronic and ionic conductivity for the oxygen cathode, and realized the hybrid electrolyte design with a MOFs based separator. Finally, for the practical potential of the aprotic Li-O₂ battery, we succeed in build a hybrid electrolyte design pouch type Li-O₂ battery, able to realize a high energy density with the help of a modified cathode electrolyte. The specific conclusion on each work is summarized as follows:

In Chapter 2, the purpose of improving the cycling stability of a Si anode based Li-ion O₂ battery is achieved in a hybrid electrolyte design. A Nafion@PTFE membrane is fabricated to separate the two electrolytes, with lithium ion conductivity and blocking effect of RMs and electrolyte solvents confirmed by permeation test (Chapter 2.3.1). The hybrid electrolyte design Li-ion O₂ battery delivers a high reversible capacity of near 18 000 mAh·g⁻¹ with low overpotential based on the Li₂O₂ electrochemistry at the cathode (Chapter 2.3.2 and Chapter 2.3.3). The cycling performance of the Li-ion O₂ battery with hybrid electrolyte design keeps stable for over 70 cycles, much improved compared with a normal type cell (Chapter 2.3.4). The SEI built in the carbonate based anode electrolyte is found uniform with beneficial compositions like LiF and Li₂CO₃, and helpful for the long duration of Si anode in the Li-ion O₂ battery (Chapter 2.3.5).

In Chapter 3, the purpose of building a high rate performance lithium based oxygen

battery with improved safety is realized. To achieve this, a biphenyl lithium liquid anode is proposed as a promising anode material for its impressive electronic and ionic conductivity and mild reaction with reactive species (Chapter 3.3.1). A MOFs based separator is fabricated and confirmed with the ability to serve as the separator to achieve the hybrid electrolyte design (Chapter 3.3.2). The fabricated organic oxygen battery exhibits superior rate performance and stable cycling performance up to 100 cycles (Chapter 3.3.3). In the characterization after the electrochemical test, a SEI-like interface formed in the liquid anode on the separator is observed and found consisted of Li_2CO_3 , LiF , C-F species and some undissolved biphenyl (Chapter 3.3.4). Together with the mechanical support of the PVDF-HFP binder, these species benefits a durable interface for the function of liquid anode.

In Chapter 4, the purpose of exploring the practical potential of a pouch type Li-O₂ battery in hybrid electrolyte design is implemented. A kind of per fluorinated chemical, HFE, is introduced as a co-solvent to increase the oxygen solubility for the cathode electrolyte, thus facilitating the function of DBBQ RM for ORR process (Chapter 4.3.1). A double layer structure pouch type Li-O₂ battery with side oxygen window in a hybrid electrolyte design is fabricated (Chapter 4.3.2). The fabricated pouch type Li-O₂ cell delivers a high core energy density of over 600 Wh·kg⁻¹ (Chapter 4.3.3), showing the real potential of the lithium based oxygen electrochemistry for achieving energy storage devices with high energy density.

Generally speaking, the hybrid electrolyte design could bring about wider strategies in dealing with the complicated issues related to the aprotic Li-O₂ battery. For the issues at the anode side, the application of hybrid electrolyte provides more promising alternatives in replace of the lithium metal, by stabilizing the Si anode to support a durable Li-ion O₂ battery, or introducing an organic liquid anode with high conductivity to build a lithium based oxygen battery with high rate performance and safety. At cathode side, the oxygen solubility and transport are optimized for the scale up of Li-O₂ battery in a pouch type cell, and realized also by the hybrid electrolyte design. The concept of hybrid electrolyte design is usual for the aqueous Li-O₂ battery, and to some degree it's a must as the anode side should be kept from the aqueous cathode side. But

its application for the aprotic Li-O₂ battery is quite few, and most of them just take a shallow try on the purpose of blocking RMs. The researches in this dissertation aims at exploring the deep possibility of hybrid electrolyte design for the aprotic Li-O₂ battery. And we hope our results would contribute to the development of the Li-O₂ battery with high energy density, superior power performance, long durability and improved safety for the next generation energy storage devices.

5.2 Perspectives

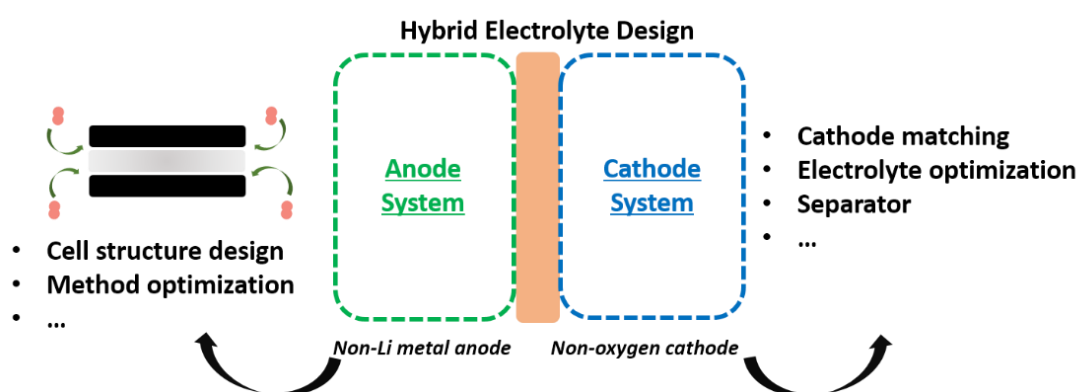


Figure 5.1 Schematic illustration of the potential of hybrid electrolyte design for the energy storage devices.

The application of hybrid electrolyte design for the energy storage devices could be further developed in many aspects. As is shown in Figure 5.1, on the one hand, for the lithium based oxygen battery, exploration for other more anode materials should be continued considering the poor performance of lithium metal, especially in a large scale application. Therefore, the scale up of the non-lithium metal anode based oxygen battery should be considered and further explored. And thus many issues should be studied including the design of the cell structure to ensure the function of anode with unique property (like liquid anode), the optimization of functional separator to realize the hybrid electrolyte design, and so on. On the other hand, the hybrid electrolyte design can be extended to other electrochemistry beyond the oxygen related one.¹³¹ In this case, much should be done including the material screening to find the proper cathode,

electrolyte optimization to address the cathode problem and separator design. In total, the hybrid electrolyte design could provide a wider view for the battery researchers to develop energy storage devices in a more flexible way.

List of Publications

1. **Deng Han**, Chang zhi, Qiu Feilong, Qiao Yu, Yang Huijun, He ping and Zhou Haoshen. A Safe Organic Oxygen Battery Built with Li-Based Liquid Anode and MOFs Separator. *Advanced Energy Materials*, 2020, 10, 12, 1903953.
2. **Deng Han**, Qiao Yu, Wu Shichao, Qiu Feilong, Zhang Na, He Ping and Zhou Haoshen. NonAqueous, Metal-Free, and Hybrid Electrolyte Li-Ion O₂ Battery with a Single-Ion-Conducting Separator. *ACS Applied Materials & Interfaces*, 2019, 11, 5, 4908-4914.
3. **Deng Han**, Qiao Yu, Zhang Xueping, Qiu Feilong, Chang Zhi, He ping and Zhou Haoshen. Killing Two Birds with One Stone: a Cu Ion Redox Mediator for a Non-aqueous Li–O₂ Battery. *Journal of Materials Chemistry A*, 2019, 7, 17261.

(The first two papers are related to this dissertation)

Acknowledgement

To study in a foreign country is a dream I always have kept that could date back to the start of my primary school. I'm so pleased and proud that I now make my dream come true at the last stage of my identity as a student. Time has passed so fast before I can realize it, and now I am given the chance to apply for the doctoral degree with this dissertation. But without the help and support from many people, I would never make it today. Please allow me express my deepest and sincerest gratitude to them.

Firstly, I'd like to show my heartfelt thanks to my supervisor Prof. Haoshen Zhou (University of Tsukuba, National Institute of Advanced Industrial Science and Technology/AIST) for his excellent guidance and constructive advices on my research work. He is a man of integrity, honor and diligence, and his attitude and methodology towards his work would be an inspiration for my entire career. He shares not only his research ideas but also his life experiences with us, enlightening my path in the future. I still feel touched during this challenging time of COVID-19 pandemic, he showed his philanthropy to us by offering us his masks. I really learnt a lot from him.

Secondly, I'd like to appreciate my vice-supervisors at University of Tsukuba, Prof. Masayoshi Ishida, and Associate Prof. Hirohisa Aki. They provide help with my school procedures and suggestions on school life to me, which makes me able to adapt to the research life in this new country quickly.

Thirdly, many thanks will go to all my group members at AIST. Dr. Hirofumi Matsuda, Dr. Eunjoo Yoo, Dr. Hirokazu Kitaura and Mr. Jun Okagaki give me a hand while I have trouble with the experiment machines. I learn a lot from their professional attitude towards work. Dr. Yu Qiao, who is proficient in the field of lithium oxygen battery and all other secondary battery systems, give me lots of advices and help in doing experiments and writing papers. I will always cherish the time when we eat sashimi at the fresh fish market near AIST together. Dr. Shichao Wu also helps me with the experiments when I just began my research. Dr. Qi Li, Dr. Xiang Li and Dr. Yibo He who share with us their experiences more than research, make my life in Tsukuba

more convenient and colorful. I also want to thank Dr. Feilong Qiu, Dr. Linlin Wang, Mr. Xin Cao, Mr. Huijun Yang and Mr. Xingyu Zhu for the joyful time we spend together, making the experiment and dinner time more pleasant. I'd also like to express my appreciation to Mr. Zhi Chang and Mrs. Min Jia. As classmates of the same grade, we flew the same flight to Japan, bought the bicycles on the same day and spent lots of unforgettable time on our way to and back from the AIST office. With all the achievements we made here, I wish us a bright future.

Furthermore, I owe many thanks to the financial support provided by the China Scholarship Council, without which I cannot focus on my research work so easily and freely.

Last but not the least, I'd like to appreciate my parents for supporting me spiritually throughout my study in the distant foreign country and my life in general. Specially, I show my deepest thanks to my girlfriend, Yitian Dong. She has been supportive for my study and beyond study, and we've had a lot of wonderful time in Japan. I know you will be behind my back, always!

References

- (1) GhaffarianHoseini, A.; Dahlan, N. D.; Berardi, U.; GhaffarianHoseini, A.; Makaremi, N.; GhaffarianHoseini, M. Sustainable Energy Performances of Green Buildings: A Review of Current Theories, Implementations and Challenges. *Renewable and Sustainable Energy Reviews* **2013**, *25*, 1-17.
- (2) Chu, S.; Cui, Y.; Liu, N. The Path Towards Sustainable Energy. *Nat Mater* **2016**, *16*, 16-22.
- (3) Mwasilu, F.; Justo, J. J.; Kim, E.-K.; Do, T. D.; Jung, J.-W. Electric Vehicles and Smart Grid Interaction: A Review on Vehicle to Grid and Renewable Energy Sources Integration. *Renewable and Sustainable Energy Reviews* **2014**, *34*, 501-516.
- (4) Bruce, D.; Haresh, K.; Jean-Marie, T. Electrical Energy Storage for the Grid: A Battery of Choices. *Science* **2011**, *334*, 928.
- (5) IEA Global Ev Outlook 2019. <https://www.iea.org/reports/global-ev-outlook-2019>.
- (6) Nitta, N.; Wu, F.; Lee, J. T.; Yushin, G. Li-Ion Battery Materials: Present and Future. *Materials Today* **2015**, *18*, 252-264.
- (7) J.-M., T.; M., A. Issues and Challenges Facing Rechargeable Lithium Batteries. **2011**, *414*, 359.
- (8) Armstrong, G. The Li-Ions Share. *Nat Chem* **2019**, *11*, 1076.
- (9) A Long-Expected Party. *Nat Mater* **2019**, *18*, 1265.
- (10) Li, M.; Lu, J.; Chen, Z.; Amine, K. 30 Years of Lithium-Ion Batteries. *Adv Mater* **2018**, e1800561.
- (11) Grande, L.; Paillard, E.; Hassoun, J.; Park, J. B.; Lee, Y. J.; Sun, Y. K.; Passerini, S.; Scrosati, B. The Lithium/Air Battery: Still an Emerging System or a Practical Reality? *Adv Mater* **2015**, *27*, 784-800.
- (12) Abraham, K. M. Prospects and Limits of Energy Storage in Batteries. *J Phys Chem*

Lett **2015**, *6*, 830-44.

(13) Vinodkumar, E.; Rotem, M.; Ran, E.; Gregory, S.; Doron, A. Challenges in the Development of Advanced Li-Ion Batteries: A Review *Energy & Environmental Science* **2011**, *4*, 3243.

(14) Akira, Y. The Birth of the Lithium-Ion Battery. *Angewandte Chemie International Edition* **2012**, *51*, 5798.

(15) Peled, E.; Menkin, S. Review—Sei: Past, Present and Future. *Journal of The Electrochemical Society* **2017**, *164*, A1703-A1719.

(16) Keith, F. B.; Anthony, F. S. Metal/Air Batteries: Their Status and Potential —a Review. *Journal of Power Sources* **1979**, *4*, 263.

(17) K., M. A.; Z., J. A Polymer Electrolyte-Based Rechargeable Lithium/Oxygen Battery. *Journal of The Electrochemical Society* **1996**, *143*, 1951.

(18) Takeshi, O.; Aurélie, D.; Michael, H.; Petr, N.; Peter, G. B. Rechargeable Li₂O₂ Electrode for Lithium Batteries. *Journal of the American Chemical Society* **2006**, *128*, 1390.

(19) Kwak, W. J.; Rosy; Sharon, D.; Xia, C.; Kim, H.; Johnson, L. R.; Bruce, P. G.; Nazar, L. F.; Sun, Y. K.; Frimer, A. A., *et al.* Lithium-Oxygen Batteries and Related Systems: Potential, Status, and Future. *Chem Rev* **2020**.

(20) Liu, T.; Vivek, J. P.; Zhao, E. W.; Lei, J.; Garcia-Araez, N.; Grey, C. P. Current Challenges and Routes Forward for Nonaqueous Lithium-Air Batteries. *Chem Rev* **2020**.

(21) He, P.; Zhang, T.; Jiang, J.; Zhou, H. Lithium-Air Batteries with Hybrid Electrolytes. *J Phys Chem Lett* **2016**, *7*, 1267-80.

(22) Zhou, H.; Wang, Y.; Li, H.; He, P. The Development of a New Type of Rechargeable Batteries Based on Hybrid Electrolytes. *ChemSusChem* **2010**, *3*, 1009-19.

- (23) Wang, Y.; Zhou, H. A Lithium-Air Battery with a Potential to Continuously Reduce O₂ from Air for Delivering Energy. *Journal of Power Sources* **2010**, *195*, 358-361.
- (24) Johnson, L.; Li, C.; Liu, Z.; Chen, Y.; Freunberger, S. A.; Ashok, P. C.; Praveen, B. B.; Dholakia, K.; Tarascon, J. M.; Bruce, P. G. The Role of Li₂O₂ Solubility in O₂ Reduction in Aprotic Solvents and Its Consequences for Li-O₂ Batteries. *Nat Chem* **2014**, *6*, 1091-9.
- (25) Aetukuri, N. B.; McCloskey, B. D.; Garcia, J. M.; Krupp, L. E.; Viswanathan, V.; Luntz, A. C. Solvating Additives Drive Solution-Mediated Electrochemistry and Enhance Toroid Growth in Non-Aqueous Li-O₂ Batteries. *Nat Chem* **2015**, *7*, 50-6.
- (26) Lu, Y.; Tong, S.; Qiu, F.; Jiang, J.; Feng, N.; Zhang, X.; He, P.; Zhou, H. Exploration of Li₂O₂ by the Method of Electrochemical Quartz Crystal Microbalance in TEGDME Based Li-O₂ Battery. *Journal of Power Sources* **2016**, *329*, 525-529.
- (27) Aurbach, D.; McCloskey, B. D.; Nazar, L. F.; Bruce, P. G. Advances in Understanding Mechanisms Underpinning Lithium-Air Batteries. *Nature Energy* **2016**, *1*.
- (28) Birger, H.; Betar, G.; Robert, M.; Wolfgang, G. B.; Yang, S.-H.; Martin, Z. B. Rate-Dependent Morphology of Li₂O₂ Growth in Li-O₂ Batteries. *The Journal of Physical Chemistry Letters* **2013**, *4*, 4217.
- (29) Adams, B. D.; Radtke, C.; Black, R.; Trudeau, M. L.; Zaghbi, K.; Nazar, L. F. Current Density Dependence of Peroxide Formation in the Li-O₂ Battery and Its Effect on Charge. *Energy & Environmental Science* **2013**, *6*, 1772.
- (30) Gerbig, O.; Merkle, R.; Maier, J. Electron and Ion Transport in Li₂O₂. *Adv Mater* **2013**, *25*, 3129-33.
- (31) Stefano, M.; Michele, P.; Nikolaos, T.; Arnd, G.; Hubert, A. G. The Effect of Water on the Discharge Capacity of a Non-Catalyzed Carbon Cathode for Li-O₂ Batteries. *Electrochemical and Solid State Letters* **2012**, *15*, A45.
- (32) Oh, S. H.; Adams, B.; Lee, B.; Nazar, L. F. Soft Chemical Route to Mesoporous

Metallic Lead Ruthenium Pyrochlore and Exploration of Its Electrochemical Properties. *Chem. Mater.* **2015**, *27*, 2322.

(33) Hummelshoj, J. S.; Luntz, A. C.; Norskov, J. K. Theoretical Evidence for Low Kinetic Overpotentials in Li-O₂ Electrochemistry. *J Chem Phys* **2013**, *138*, 034703.

(34) Ganapathy, S.; Adams, B. D.; Stenou, G.; Anastasaki, M. S.; Goubitz, K.; Miao, X. F.; Nazar, L. F.; Wagemaker, M. Nature of Li₂O₂ Oxidation in a Li-O₂ Battery Revealed by Operando X-Ray Diffraction. *J Am Chem Soc* **2014**, *136*, 16335-44.

(35) Lu, J.; Lee, Y. J.; Luo, X.; Lau, K. C.; Asadi, M.; Wang, H. H.; Brombosz, S.; Wen, J.; Zhai, D.; Chen, Z., *et al.* A Lithium-Oxygen Battery Based on Lithium Superoxide. *Nature* **2016**, *529*, 377-82.

(36) Yang, S.; He, P.; Zhou, H. Research Progresses on Materials and Electrode Design Towards Key Challenges of Li-Air Batteries. *Energy Storage Materials* **2018**, *13*, 29-48.

(37) Kwak, W.-J.; Park, J.-B.; Jung, H.-G.; Sun, Y.-K. Controversial Topics on Lithium Superoxide in Li-O₂ Batteries. *ACS Energy Letters* **2017**, *2*, 2756-2760.

(38) Li, F.; Tang, D.-M.; Zhang, T.; Liao, K.; He, P.; Golberg, D.; Yamada, A.; Zhou, H. Superior Performance of a Li-O₂ battery with Metallic RuO₂ hollow Spheres as the Carbon-Free Cathode. *Advanced Energy Materials* **2015**, *5*, 1500294.

(39) Tong, S.; Zheng, M.; Lu, Y.; Lin, Z.; Li, J.; Zhang, X.; Shi, Y.; He, P.; Zhou, H. Mesoporous NiO with a Single-Crystalline Structure Utilized as a Noble Metal-Free Catalyst for Non-Aqueous Li-O₂ Batteries. *Journal of Materials Chemistry A* **2015**, *3*, 16177-16182.

(40) Xie, J.; Yao, X.; Cheng, Q.; Madden, I. P.; Dornath, P.; Chang, C. C.; Fan, W.; Wang, D. Three Dimensionally Ordered Mesoporous Carbon as a Stable, High-Performance Li-O₂ Battery Cathode. *Angew Chem Int Ed Engl* **2015**, *54*, 4299-303.

(41) Jian, Z.; Liu, P.; Li, F.; He, P.; Guo, X.; Chen, M.; Zhou, H. Core-Shell-Structured Cnt@RuO₂ Composite as a High-Performance Cathode Catalyst for Rechargeable Li-

- O(2) Batteries. *Angew Chem Int Ed Engl* **2014**, *53*, 442-6.
- (42) Xu, J. J.; Chang, Z. W.; Wang, Y.; Liu, D. P.; Zhang, Y.; Zhang, X. B. Cathode Surface-Induced, Solvation-Mediated, Micrometer-Sized Li₂O₂ Cycling for Li-O₂ Batteries. *Adv Mater* **2016**, *28*, 9620-9628.
- (43) Wang, K. X.; Zhu, Q. C.; Chen, J. S. Strategies toward High-Performance Cathode Materials for Lithium-Oxygen Batteries. *Small* **2018**, *14*, e1800078.
- (44) Cheng, F.; Chen, J. Metal-Air Batteries: From Oxygen Reduction Electrochemistry to Cathode Catalysts. *Chem Soc Rev* **2012**, *41*, 2172-92.
- (45) McCloskey, B. D.; Addison, D. A Viewpoint on Heterogeneous Electrocatalysis and Redox Mediation in Nonaqueous Li-O₂ Batteries. *ACS Catalysis* **2016**, *7*, 772-778.
- (46) Gao, X.; Chen, Y.; Johnson, L. R.; Jovanov, Z. P.; Bruce, P. G. A Rechargeable Lithium–Oxygen Battery with Dual Mediators Stabilizing the Carbon Cathode. *Nature Energy* **2017**, *2*, 17118.
- (47) Gao, X.; Chen, Y.; Johnson, L.; Bruce, P. G. Promoting Solution Phase Discharge in Li-O₂ Batteries Containing Weakly Solvating Electrolyte Solutions. *Nat Mater* **2016**, *15*, 882-8.
- (48) Homewood, T.; Frith, J. T.; Vivek, J. P.; Casan-Pastor, N.; Tonti, D.; Owen, J. R.; Garcia-Araez, N. Using Polyoxometalates to Enhance the Capacity of Lithium-Oxygen Batteries. *Chem Commun (Camb)* **2018**, *54*, 9599-9602.
- (49) Zhang, Y.; Wang, L.; Zhang, X.; Guo, L.; Wang, Y.; Peng, Z. High-Capacity and High-Rate Discharging of a Coenzyme Q₁₀-Catalyzed Li-O₂ Battery. *Adv Mater* **2018**, *30*.
- (50) Xu, W.; Wang, J.; Ding, F.; Chen, X.; Nasybulin, E.; Zhang, Y.; Zhang, J.-G. Lithium Metal Anodes for Rechargeable Batteries. *Energy Environ. Sci.* **2014**, *7*, 513-537.
- (51) Wood, K. N.; Noked, M.; Dasgupta, N. P. Lithium Metal Anodes: Toward an

Improved Understanding of Coupled Morphological, Electrochemical, and Mechanical Behavior. *ACS Energy Letters* **2017**, *2*, 664-672.

(52) Lin, D.; Liu, Y.; Cui, Y. Reviving the Lithium Metal Anode for High-Energy Batteries. *Nat Nanotechnol* **2017**, *12*, 194-206.

(53) Cheng, X. B.; Zhang, R.; Zhao, C. Z.; Wei, F.; Zhang, J. G.; Zhang, Q. A Review of Solid Electrolyte Interphases on Lithium Metal Anode. *Adv Sci (Weinh)* **2016**, *3*, 1500213.

(54) Qiu, F.; Li, X.; Deng, H.; Wang, D.; Mu, X.; He, P.; Zhou, H. A Concentrated Ternary-Salts Electrolyte for High Reversible Li Metal Battery with Slight Excess Li. *Advanced Energy Materials* **2018**, *9*, 1803372.

(55) Suo, L.; Hu, Y. S.; Li, H.; Armand, M.; Chen, L. A New Class of Solvent-in-Salt Electrolyte for High-Energy Rechargeable Metallic Lithium Batteries. *Nat Commun* **2013**, *4*, 1481.

(56) Yuan, S.; Bao, J. L.; Wei, J.; Xia, Y.; Truhlar, D. G.; Wang, Y. A Versatile Single-Ion Electrolyte with a Grotthuss-Like Li Conduction Mechanism for Dendrite-Free Li Metal Batteries. *Energy & Environmental Science* **2019**, *12*, 2741-2750.

(57) Lee, H.; Lee, D. J.; Kim, Y.-J.; Park, J.-K.; Kim, H.-T. A Simple Composite Protective Layer Coating That Enhances the Cycling Stability of Lithium Metal Batteries. *Journal of Power Sources* **2015**, *284*, 103-108.

(58) Lin, D.; Liu, Y.; Liang, Z.; Lee, H. W.; Sun, J.; Wang, H.; Yan, K.; Xie, J.; Cui, Y. Layered Reduced Graphene Oxide with Nanoscale Interlayer Gaps as a Stable Host for Lithium Metal Anodes. *Nat Nanotechnol* **2016**, *11*, 626-32.

(59) Liu, Y.; Lin, D.; Liang, Z.; Zhao, J.; Yan, K.; Cui, Y. Lithium-Coated Polymeric Matrix as a Minimum Volume-Change and Dendrite-Free Lithium Metal Anode. *Nat Commun* **2016**, *7*, 10992.

(60) Park, J. B.; Lee, S. H.; Jung, H. G.; Aurbach, D.; Sun, Y. K. Redox Mediators for Li-O₂ Batteries: Status and Perspectives. *Adv Mater* **2018**, *30*.

- (61) Lim, H. D.; Song, H.; Kim, J.; Gwon, H.; Bae, Y.; Park, K. Y.; Hong, J.; Kim, H.; Kim, T.; Kim, Y. H., *et al.* Superior Rechargeability and Efficiency of Lithium-Oxygen Batteries: Hierarchical Air Electrode Architecture Combined with a Soluble Catalyst. *Angew Chem Int Ed Engl* **2014**, *53*, 3926-31.
- (62) Kwak, W.-J.; Park, S.-J.; Jung, H.-G.; Sun, Y.-K. Optimized Concentration of Redox Mediator and Surface Protection of Li Metal for Maintenance of High Energy Efficiency in Li-O₂ Batteries. *Advanced Energy Materials* **2018**, *8*, 1702258.
- (63) Qiao, Y.; He, Y.; Wu, S.; Jiang, K.; Li, X.; Guo, S.; He, P.; Zhou, H. Mof-Based Separator in an Li-O₂ Battery: An Effective Strategy to Restrain the Shuttling of Dual Redox Mediators. *ACS Energy Letters* **2018**, *3*, 463-468.
- (64) Hassoun, J.; Jung, H. G.; Lee, D. J.; Park, J. B.; Amine, K.; Sun, Y. K.; Scrosati, B. A Metal-Free, Lithium-Ion Oxygen Battery: A Step Forward to Safety in Lithium-Air Batteries. *Nano Lett* **2012**, *12*, 5775-9.
- (65) Guo, Z.; Dong, X.; Wang, Y.; Xia, Y. A Lithium Air Battery with a Lithiated Al-Carbon Anode. *Chem Commun (Camb)* **2015**, *51*, 676-8.
- (66) Elia, G. A.; Bernhard, R.; Hassoun, J. A Lithium-Ion Oxygen Battery Using a Polyethylene Glyme Electrolyte Mixed with an Ionic Liquid. *RSC Advances* **2015**, *5*, 21360-21365.
- (67) Elia, G. A.; Hassoun, J. A Gel Polymer Membrane for Lithium-Ion Oxygen Battery. *Solid State Ionics* **2016**, *287*, 22-27.
- (68) McDowell, M. T.; Lee, S. W.; Nix, W. D.; Cui, Y. 25th Anniversary Article: Understanding the Lithiation of Silicon and Other Alloying Anodes for Lithium-Ion Batteries. *Adv Mater* **2013**, *25*, 4966-85.
- (69) Luntz, A. C.; McCloskey, B. D. Nonaqueous Li-Air Batteries: A Status Report. *Chem Rev* **2014**, *114*, 11721-50.

- (70) Li, F.; Zhang, T.; Zhou, H. Challenges of Non-Aqueous Li–O₂ Batteries: Electrolytes, Catalysts, and Anodes. *Energy & Environmental Science* **2013**, *6*, 1125.
- (71) Ottakam Thotiyl, M. M.; Freunberger, S. A.; Peng, Z.; Bruce, P. G. The Carbon Electrode in Nonaqueous Li–O₂ Cells. *J Am Chem Soc* **2013**, *135*, 494–500.
- (72) Kwak, W.-J.; Jung, H.-G.; Aurbach, D.; Sun, Y.-K. Optimized Bicompartiment Two Solution Cells for Effective and Stable Operation of Li–O₂ Batteries. *Advanced Energy Materials* **2017**, *7*, 1701232.
- (73) Chen, Y.; Freunberger, S. A.; Peng, Z.; Fontaine, O.; Bruce, P. G. Charging a Li–O(2) Battery Using a Redox Mediator. *Nat Chem* **2013**, *5*, 489–94.
- (74) Bergner, B. J.; Busche, M. R.; Pinedo, R.; Berkes, B. B.; Schroder, D.; Janek, J. How to Improve Capacity and Cycling Stability for Next Generation Li–O₂ Batteries: Approach with a Solid Electrolyte and Elevated Redox Mediator Concentrations. *ACS Appl Mater Interfaces* **2016**, *8*, 7756–65.
- (75) Wu, S.; Qiao, Y.; Deng, H.; Zhou, H. A Single Ion Conducting Separator and Dual Mediator-Based Electrolyte for High-Performance Lithium–Oxygen Batteries with Non-Carbon Cathodes. *Journal of Materials Chemistry A* **2018**, *6*, 9816–9822.
- (76) Deng, H.; Qiu, F.; Li, X.; Qin, H.; Zhao, S.; He, P.; Zhou, H. A Li-Ion Oxygen Battery with Li–Si Alloy Anode Prepared by a Mechanical Method. *Electrochemistry Communications* **2017**, *78*, 11–15.
- (77) Cloud, J. E.; Wang, Y.; Li, X.; Yoder, T. S.; Yang, Y.; Yang, Y. Lithium Silicide Nanocrystals: Synthesis, Chemical Stability, Thermal Stability, and Carbon Encapsulation. *Inorg Chem* **2014**, *53*, 11289–97.
- (78) Freunberger, S. A.; Chen, Y.; Drewett, N. E.; Hardwick, L. J.; Barde, F.; Bruce, P. G. The Lithium–Oxygen Battery with Ether-Based Electrolytes. *Angew Chem Int Ed Engl* **2011**, *50*, 8609–13.
- (79) Wu, S.; Zhu, K.; Tang, J.; Liao, K.; Bai, S.; Yi, J.; Yamauchi, Y.; Ishida, M.; Zhou,

H. A Long-Life Lithium Ion Oxygen Battery Based on Commercial Silicon Particles as the Anode. *Energy & Environmental Science* **2016**, *9*, 3262-3271.

(80) Freunberger, S. A.; Chen, Y.; Peng, Z.; Griffin, J. M.; Hardwick, L. J.; Barde, F.; Novak, P.; Bruce, P. G. Reactions in the Rechargeable Lithium-O₂ Battery with Alkyl Carbonate Electrolytes. *J Am Chem Soc* **2011**, *133*, 8040-7.

(81) Shi, Y.; Wu, C.; Li, L.; Yang, J. A Lithiated Perfluorinated Sulfonic Acid Polymer Electrolyte for Lithium-Oxygen Batteries. *Journal of The Electrochemical Society* **2017**, *164*, A2031-A2037.

(82) Bai, S.; Liu, X.; Zhu, K.; Wu, S.; Zhou, H. Metal–Organic Framework-Based Separator for Lithium–Sulfur Batteries. *Nature Energy* **2016**, *1*.

(83) Zhang, L.; Zhang, L.; Chai, L.; Xue, P.; Hao, W.; Zheng, H. A Coordinatively Cross-Linked Polymeric Network as a Functional Binder for High-Performance Silicon Submicro-Particle Anodes in Lithium-Ion Batteries. *J. Mater. Chem. A* **2014**, *2*, 19036-19045.

(84) Shi, F.; Ross, P. N.; Zhao, H.; Liu, G.; Somorjai, G. A.; Komvopoulos, K. A Catalytic Path for Electrolyte Reduction in Lithium-Ion Cells Revealed by in Situ Attenuated Total Reflection-Fourier Transform Infrared Spectroscopy. *J Am Chem Soc* **2015**, *137*, 3181-4.

(85) Kundu, D.; Black, R.; Adams, B.; Nazar, L. F. A Highly Active Low Voltage Redox Mediator for Enhanced Rechargeability of Lithium-Oxygen Batteries. *ACS Cent Sci* **2015**, *1*, 510-5.

(86) Etacheri, V.; Haik, O.; Goffer, Y.; Roberts, G. A.; Stefan, I. C.; Fasching, R.; Aurbach, D. Effect of Fluoroethylene Carbonate (Fec) on the Performance and Surface Chemistry of Si-Nanowire Li-Ion Battery Anodes. *Langmuir* **2012**, *28*, 965-76.

(87) Doron, A.; Eran, G. The Study of Electrolyte Solutions Based on Solvents from the “Glyme” Family (Linear Polyethers) for Secondary Li Battery Systems. *Electrochimica Acta* **1997**, *42*, 697.

- (88) Cano, Z. P.; Banham, D.; Ye, S.; Hintennach, A.; Lu, J.; Fowler, M.; Chen, Z. Batteries and Fuel Cells for Emerging Electric Vehicle Markets. *Nature Energy* **2018**, *3*, 279-289.
- (89) Kwade, A.; Haselrieder, W.; Leithoff, R.; Modlinger, A.; Dietrich, F.; Droeder, K. Current Status and Challenges for Automotive Battery Production Technologies. *Nature Energy* **2018**, *3*, 290-300.
- (90) Bruce, P. G.; Freunberger, S. A.; Hardwick, L. J.; Tarascon, J. M. Li-O₂ and Li-S Batteries with High Energy Storage. *Nat Mater* **2011**, *11*, 19-29.
- (91) Cheng, X. B.; Zhang, R.; Zhao, C. Z.; Zhang, Q. Toward Safe Lithium Metal Anode in Rechargeable Batteries: A Review. *Chem Rev* **2017**, *117*, 10403-10473.
- (92) Liu, H.; Cheng, X. B.; Xu, R.; Zhang, X. Q.; Yan, C.; Huang, J. Q.; Zhang, Q. Plating/Stripping Behavior of Actual Lithium Metal Anode. *Advanced Energy Materials* **2019**, 1902254.
- (93) Lyu, Z.; Zhou, Y.; Dai, W.; Cui, X.; Lai, M.; Wang, L.; Huo, F.; Huang, W.; Hu, Z.; Chen, W. Recent Advances in Understanding of the Mechanism and Control of Li₂O₂ Formation in Aprotic Li-O₂ Batteries. *Chem Soc Rev* **2017**, *46*, 6046-6072.
- (94) Feng, N.; Mu, X.; Zhang, X.; He, P.; Zhou, H. Intensive Study on the Catalytic Behavior of N-Methylphenothiazine as a Soluble Mediator to Oxidize the Li₂O₂ Cathode of the Li-O₂ Battery. *ACS Applied Materials & Interfaces* **2017**, *9*, 3733-3739.
- (95) Pande, V.; Viswanathan, V. Criteria and Considerations for the Selection of Redox Mediators in Nonaqueous Li-O₂ Batteries. *ACS Energy Letters* **2016**, *2*, 60-63.
- (96) Zhao, J.; Lu, Z.; Liu, N.; Lee, H.-W.; McDowell, M. T.; Cui, Y. Dry-Air-Stable Lithium Silicide-Lithium Oxide Core-Shell Nanoparticles as High-Capacity Prelithiation Reagents. *Nature Communications* **2014**, *5*.
- (97) Chan, C. K.; Peng, H.; Liu, G.; McIlwrath, K.; Zhang, X. F.; Huggins, R. A.; Cui, Y. High-Performance Lithium Battery Anodes Using Silicon Nanowires. *Nat Nanotechnol* **2008**, *3*, 31-5.

- (98) Wu, H.; Chan, G.; Choi, J. W.; Ryu, I.; Yao, Y.; McDowell, M. T.; Lee, S. W.; Jackson, A.; Yang, Y.; Hu, L., *et al.* Stable Cycling of Double-Walled Silicon Nanotube Battery Anodes through Solid-Electrolyte Interphase Control. *Nat Nanotechnol* **2012**, *7*, 310-5.
- (99) N., L. H. Reactions of the Radical Anions and Dianions of Aromatic Hydrocarbons. *Chemical Reviews* **1974**, *74*, 243.
- (100) Yu, J.; Hu, Y. S.; Pan, F.; Zhang, Z.; Wang, Q.; Li, H.; Huang, X.; Chen, L. A Class of Liquid Anode for Rechargeable Batteries with Ultralong Cycle Life. *Nat Commun* **2017**, *8*, 14629.
- (101) Liang, F.; Qiu, X.; Zhang, Q.; Kang, Y.; Koo, A.; Hayashi, K.; Chen, K.; Xue, D.; Hui, K. N.; Yadegari, H., *et al.* A Liquid Anode for Rechargeable Sodium-Air Batteries with Low Voltage Gap and High Safety. *Nano Energy* **2018**, *49*, 574-579.
- (102) Cong, G.; Wang, W.; Lai, N. C.; Liang, Z.; Lu, Y. C. A High-Rate and Long-Life Organic-Oxygen Battery. *Nat Mater* **2019**, *18*, 390-396.
- (103) Pan, F.; Yang, J.; Jia, C.; Li, H.; Wang, Q. Biphenyl-Lithium-Tegdme Solution as Anolyte for High Energy Density Non-Aqueous Redox Flow Lithium Battery. *Journal of Energy Chemistry* **2018**, *27*, 1362-1368.
- (104) Chang, Z.; Qiao, Y.; Wang, J.; Deng, H.; He, P.; Zhou, H. Fabricating Better Metal-Organic Frameworks Separators for Li-S Batteries: Pore Sizes Effects Inspired Channel Modification Strategy. *Energy Storage Materials* **2019**.
- (105) J., F. W.; N., D. S. Sodium Naphthalene. Ii. Preparation and Properties of Dihydronaphthalene Dicarboxylic Acids. *Journal of the American Chemical Society* **1938**, *60*, 951.
- (106) He, Y.; Qiao, Y.; Chang, Z.; Zhou, H. The Potential of Electrolyte Filled Mof Membranes as Ionic Sieves in Rechargeable Batteries. *Energy & Environmental Science* **2019**, *12*, 2327-2344.
- (107) Wang, Z.; Tan, R.; Wang, H.; Yang, L.; Hu, J.; Chen, H.; Pan, F. A Metal-Organic-

Framework-Based Electrolyte with Nanowetted Interfaces for High-Energy-Density Solid-State Lithium Battery. *Adv Mater* **2018**, *30*.

(108) Li, Y.; Liang, F.; Bux, H.; Yang, W.; Caro, J. Zeolitic Imidazolate Framework Zif-7 Based Molecular Sieve Membrane for Hydrogen Separation. *Journal of Membrane Science* **2010**, *354*, 48-54.

(109) Kumar Trivedi, M. Characterization of Physical, Spectroscopic and Thermal Properties of Biofield Treated Biphenyl. *American Journal of Chemical Engineering* **2015**, *3*, 58.

(110) Tu, M.; Wiktor, C.; Rosler, C.; Fischer, R. A. Rapid Room Temperature Syntheses of Zeolitic-Imidazolate Framework (Zif) Nanocrystals. *Chem Commun (Camb)* **2014**, *50*, 13258-60.

(111) Biesinger, M. C.; Lau, L. W. M.; Gerson, A. R.; Smart, R. S. C. Resolving Surface Chemical States in Xps Analysis of First Row Transition Metals, Oxides and Hydroxides: Sc, Ti, V, Cu and Zn. *Applied Surface Science* **2010**, *257*, 887-898.

(112) Geng, D.; Ding, N.; Hor, T. S. A.; Chien, S. W.; Liu, Z.; Wu, D.; Sun, X.; Zong, Y. From Lithium-Oxygen to Lithium-Air Batteries: Challenges and Opportunities. *Advanced Energy Materials* **2016**, *6*, 1502164.

(113) Tao, L.; Michal, L.; Wanjing, Y.; Amy, J. M.; Lina, Z.; Paul, M. B.; Gunwoo, K.; Clare, P. G. Cycling Li-O₂ Batteries Via Lioh Formation and Decomposition. *Science* **2015**, *350*, 530.

(114) Li, F.; Wu, S.; Li, D.; Zhang, T.; He, P.; Yamada, A.; Zhou, H. The Water Catalysis at Oxygen Cathodes of Lithium-Oxygen Cells. *Nat Commun* **2015**, *6*, 7843.

(115) Zhang, J.-G.; Wang, D.; Xu, W.; Xiao, J.; Williford, R. E. Ambient Operation of Li/Air Batteries. *Journal of Power Sources* **2010**, *195*, 4332-4337.

(116) Wang, D.; Xiao, J.; Xu, W.; Zhang, J.-G. High Capacity Pouch-Type Li-Air Batteries. *Journal of The Electrochemical Society* **2010**, *157*, A760.

- (117) Shin, H.-J.; Kwak, W.-J.; Aurbach, D.; Sun, Y.-K. Large-Scale Li O₂pouch Type Cells for Practical Evaluation and Applications. *Advanced Functional Materials* **2017**, *27*, 1605500.
- (118) Yibo, H.; Zhi, C.; Shichao, W.; Yu, Q.; Songyan, B.; Kezhu, J.; Ping, H.; Haoshen, Z. Simultaneously Inhibiting Lithium Dendrites Growth and Polysulfides Shuttle by a Flexible Mof-Based Membrane in Li-S Batteries. *Advanced Energy Materials* **2018**, *8*, 1802130.
- (119) Jean, G. R. Oxygen Carriers (“Blood Substitutes”) Raison D'etre, Chemistry, and Some Physiology *Chemical Reviews* **2001**, *101*, 2797.
- (120) Zhang, S. S.; Read, J. Partially Fluorinated Solvent as a Co-Solvent for the Non-Aqueous Electrolyte of Li/Air Battery. *Journal of Power Sources* **2011**, *196*, 2867-2870.
- (121) Wang, Y.; Zheng, D.; Yang, X.-Q.; Qu, D. High Rate Oxygen Reduction in Non-Aqueous Electrolytes with the Addition of Perfluorinated Additives. *Energy & Environmental Science* **2011**, *4*, 3697.
- (122) Wan, H.; Mao, Y.; Liu, Z.; Bai, Q.; Peng, Z.; Bao, J.; Wu, G.; Liu, Y.; Wang, D.; Xie, J. Influence of Enhanced O₂ Provision on the Discharge Performance of Li-Air Batteries by Incorporating Fluoroether. *ChemSusChem* **2017**, *10*, 1385-1389.
- (123) Read, J.; Mutolo, K.; Ervin, M.; Behl, W.; Wolfenstine, J.; Driedger, A.; Foster, D. Oxygen Transport Properties of Organic Electrolytes and Performance of Lithium/Oxygen Battery. *Journal of The Electrochemical Society* **2003**, *150*, A1351.
- (124) Balaish, M.; Gao, X.; Bruce, P. G.; Ein-Eli, Y. Enhanced Li-O₂ Battery Performance in a Binary “Liquid Teflon” and Dual Redox Mediators. *Advanced Materials Technologies* **2019**, *4*, 1800645.
- (125) Shui, J. L.; Okasinski, J. S.; Kenesei, P.; Dobbs, H. A.; Zhao, D.; Almer, J. D.; Liu, D. J. Reversibility of Anodic Lithium in Rechargeable Lithium-Oxygen Batteries. *Nat Commun* **2013**, *4*, 2255.

- (126) Assary, R. S.; Lu, J.; Du, P.; Luo, X.; Zhang, X.; Ren, Y.; Curtiss, L. A.; Amine, K. The Effect of Oxygen Crossover on the Anode of a Li-O₂ Battery Using an Ether-Based Solvent: Insights from Experimental and Computational Studies. *ChemSusChem* **2013**, *6*, 51-5.
- (127) Mahne, N.; Schafzahl, B.; Leypold, C.; Leypold, M.; Grumm, S.; Leitgeb, A.; Strohmeier, Gernot A.; Wilkening, M.; Fontaine, O.; Kramer, D., *et al.* Singlet Oxygen Generation as a Major Cause for Parasitic Reactions During Cycling of Aprotic Lithium–Oxygen Batteries. *Nature Energy* **2017**, *2*.
- (128) Kwak, W. J.; Kim, H.; Petit, Y. K.; Leypold, C.; Nguyen, T. T.; Mahne, N.; Redfern, P.; Curtiss, L. A.; Jung, H. G.; Borisov, S. M., *et al.* Deactivation of Redox Mediators in Lithium-Oxygen Batteries by Singlet Oxygen. *Nat Commun* **2019**, *10*, 1380.
- (129) Schafzahl, L.; Mahne, N.; Schafzahl, B.; Wilkening, M.; Slugovc, C.; Borisov, S. M.; Freunberger, S. A. Singlet Oxygen During Cycling of the Aprotic Sodium-O₂ Battery. *Angew Chem Int Ed Engl* **2017**, *56*, 15728-15732.
- (130) Kwak, W.-J.; Freunberger, S. A.; Kim, H.; Park, J.; Nguyen, T. T.; Jung, H.-G.; Byon, H. R.; Sun, Y.-K. Mutual Conservation of Redox Mediator and Singlet Oxygen Quencher in Lithium–Oxygen Batteries. *ACS Catalysis* **2019**, *9*, 9914-9922.
- (131) Qiao, Y.; Jiang, K.; Li, X.; Deng, H.; He, Y.; Chang, Z.; Wu, S.; Guo, S.; Zhou, H. A Hybrid Electrolytes Design for Capacity-Equivalent Dual-Graphite Battery with Superior Long-Term Cycle Life. *Advanced Energy Materials* **2018**, *8*, 1801120.